



2015.  
GODINA  
LVIII



# GRAĐEVINSKI MATERIJALI I KONSTRUKCIJE

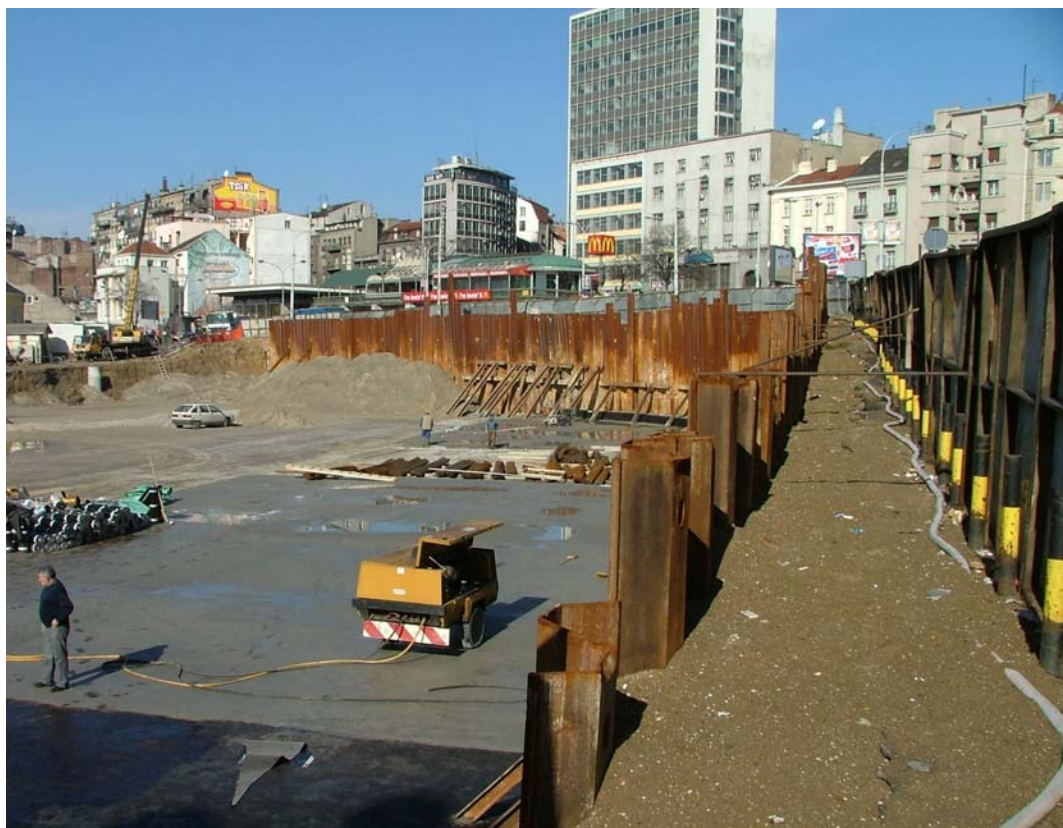
# 4

# BUILDING MATERIALS AND STRUCTURES

---

ČASOPIS ZA ISTRAŽIVANJA U OBLASTI MATERIJALA I KONSTRUKCIJA  
JOURNAL FOR RESEARCH OF MATERIALS AND STRUCTURES

---



---

DRUŠTVO ZA ISPITIVANJE I ISTRAŽIVANJE MATERIJALA I KONSTRUKCIJA SRBIJE  
SOCIETY FOR MATERIALS AND STRUCTURES TESTING OF SERBIA

---



# GRAĐEVINSKI MATERIJALI I KONSTRUKCIJE

# BUILDING MATERIALS AND STRUCTURES

ČASOPIS ZA ISTRAŽIVANJA U OBLASTI MATERIJALA I KONSTRUKCIJA  
JOURNAL FOR RESEARCH IN THE FIELD OF MATERIALS AND STRUCTURES

---

## INTERNATIONAL EDITORIAL BOARD

Professor **Radomir Folić**, Editor in-Chief  
Faculty of Technical Sciences, University of Novi Sad, Serbia  
Fakultet tehničkih nauka, Univerzitet u Novom Sadu, Srbija  
e-mail: [folic@uns.ac.rs](mailto:folic@uns.ac.rs)

Professor **Mirjana Malešev**, Deputy editor  
Faculty of Technical Sciences, University of Novi Sad,  
Serbia - Fakultet tehničkih nauka, Univerzitet u Novom  
Sadu, Srbija, e-mail: [miram@uns.ac.rs](mailto:miram@uns.ac.rs)

Dr **Ksenija Janković**  
Institute for Testing Materials, Belgrade, Serbia  
Institut za ispitivanje materijala, Beograd, Srbija

Dr **Jose Adam, ICITECH**  
Department of Construction Engineering, Valencia,  
Spain.

Professor **Radu Banchila**  
Dep. of Civil Eng. „Politehnica“ University of  
Temesoara, Romania

Professor **Dubravka Bjegović**  
University of Zagreb, Faculty of Civil Engineering,  
Department of Materials, Zagreb, Croatia

Assoc. professor **Meri Cvetkovska**  
Faculty of Civil Eng. University "St Kiril and Metodij",  
Skopje, Macedonia

Professor **Michael Forde**  
University of Edinburgh, Dep. of Environmental Eng.  
UK

Dr **Vladimir Gocevski**  
Hydro-Quebec, Montreal, Canada

Lektori za srpski jezik: Dr **Miloš Zubac**, profesor  
**Aleksandra Borojev**, profesor  
Proofreader: Prof. **Jelisaveta Šafranjić**, Ph D  
Technical editor: Stoja Todorovic, e-mail: [saska@imk.grf.bg.ac.rs](mailto:saska@imk.grf.bg.ac.rs)

Acad. Professor **Yachko Ivanov**  
Bulgarian Academy of Sciences, Sofia, Bulgaria

Dr. Habil. **Miklos M. Ivanyi**  
UVATERV, Budapest, Hungary

Professor **Asterios Liolios**  
Democritus University of Thrace, Faculty of Civil  
Eng., Greece

Professor **Doncho Partov**  
University of Construction and Architecture - VSU  
"LJ.Karavelov" Sofia, Bulgaria

**Predrag Popović**  
Wiss, Janney, Elstner Associates, Northbrook,  
Illinois, USA.

Professor **Tom Schanz**  
Ruhr University of Bochum, Germany

Professor **Valeriu Stoin**  
Dep. of Civil Eng. „Poloitehnica“ University of  
Temesoara, Romania

Acad. Professor **Miha Tomažević**, SNB and CEI,  
Slovenian Academy of Sciences and Arts,

Professor **Mihailo Trifunac**, Civil Eng.  
Department University of Southern California, Los  
Angeles, USA

## PUBLISHER

Society for Materials and Structures Testing of Serbia, 11000 Belgrade, Kneza Milosa 9  
Telephone: 381 11/3242-589; e-mail: [dimk@ptt.rs](mailto:dimk@ptt.rs), veb sajt: [www.dimk.rs](http://www.dimk.rs)

REVIEWERS: All papers were reviewed

KORICE: Izgradnja podzemne etaže pijace Zeleni Venac u Beogradu (foto: prof. dr M. Maksimović)  
COVER: "Zeleni Venac" Market in Belgrade - Construction of subsurface level dig (photo: prof. dr M. Maksimović)

Financial supports: Ministry of Scientific and Technological Development of the Republic of Serbia

DRUŠTVO ZA ISPITIVANJE I ISTRAŽIVANJE MATERIJALA I KONSTRUKCIJA SRBIJE  
SOCIETY FOR MATERIALS AND STRUCTURES TESTING OF SERBIA

# GRAĐEVINSKI MATERIJALI I KONSTRUKCIJE

# BUILDING MATERIALS AND STRUCTURES

ČASOPIS ZA ISTRAŽIVANJA U OBLASTI MATERIJALA I KONSTRUKCIJA  
JOURNAL FOR RESEARCH IN THE FIELD OF MATERIALS AND STRUCTURES

## SADRŽAJ

<b>Iva DESPOTOVIĆ</b> SVOJSTVA SAMOUGRAĐUJUĆEG BETONA SPRAVLJENOG S RECIKLIRANIM AGREGATOM I RAZLIČITIM MINERALNIM DODACIMA <b>Originalni naučni rad</b> .....	3
<b>Vojkan JOVIČIĆ</b> <b>Jasmin BUČO</b> <b>Nermin ŠEHAGIĆ</b> <b>Alaga HUSIĆ</b> KORISNI KONCEPTI U PRIMENI NOVE AUSTRIJSKE METODE ZA GRADNJU TUNELA <b>Pregledni rad</b> .....	21
<b>Selimir V. LELOVIĆ</b> KRITERIJUM STABILNOSTI DEFORMACIJE ELASTOPLASTIČNIH MATERIJALA <b>Originalni naučni rad</b> .....	37
<b>Ljiljana KOZARIĆ</b> <b>Aleksandar PROKIV</b> <b>Miroslav BEŠEVIĆ</b> UNAKRSNO LAMELIRANI DRVENI ELEMENTI U SAVREMENIM DRVENIM KONSTRUKCIJAMA ZGRADA - primena i proračun <b>Stručni rad</b> .....	51
<b>Uputstvo autorima</b> .....	70

## CONTENTS

<b>Iva DESPOTOVIC</b> PROPERTIES OF SELF-COMPACTING CONCRETE MADE OF RECYCLED AGGREGATES AND VARIOUS MINERAL ADDITIVES <b>Original scientific paper</b> .....	3
<b>Vojkan JOVICIC</b> <b>Jasmin BUCO</b> <b>Nermin SEHAGIC</b> <b>Alaga HUSIC</b> USEFUL CONCEPTS FOR APPLICATION OF NEW AUSTRIAN TUNNELLING METHOD IN TUNNEL CONSTRUCTION <b>Review paper</b> .....	21
<b>Selimir V. LELOVIC</b> CONDITIONS FOR STABILITY OF DEFORMATION IN ELASTO-PLASTIC MATERIALS <b>Original scientific paper</b> .....	37
<b>Ljiljana KOZARIC</b> <b>Aleksandar PROKIV</b> <b>Miroslav BESEVIC</b> CROSS LAMINATED TIMBER ELEMENTS IN CONTEMPORARY TIMBER STRUCTURES OF BUILDINGS - application and design <b>Professional paper</b> .....	51
<b>Preview report</b> .....	70

CIP - Каталогизacija u publikaciji  
Народна библиотека Србије, Београд

620.1

**GRAĐEVINSKI materijali i konstrukcije :**  
časopis za istraživanja u oblasti materijala  
i konstrukcija = Building Materials and  
Structures : journal for research of  
materials and structures / editor-in-chief  
Radomir Folić. - God. 54, br. 1 (2011)-  
- Beograd (Kneza Miloša 9) : Društvo za  
ispitivanje i istraživanje materijala i  
konstrukcija Srbije, 2011- (Novi Beograd :  
Hektor print). - 30 cm

Tromesečno. - Je nastavak: Materijali i  
konstrukcije = ISSN 0543-0798  
ISSN 2217-8139 = Građevinski materijali i  
konstrukcije  
COBISS.SR-ID 188695820



# SVOJSTVA SAMOUGRAĐUJUĆEG BETONA SPRAVLJENOG S RECIKLIRANIM AGREGATOM I RAZLIČITIM MINERALNIM DODACIMA

## PROPERTIES OF SELF-COMPACTING CONCRETE MADE OF RECYCLED AGGREGATES AND VARIOUS MINERAL ADDITIVES

Iva DESPOTOVIĆ

ORIGINALNI NAUČNI RAD  
ORIGINAL SCIENTIFIC PAPER  
UDK: 666.972.1  
doi: 10.5937/grmk1504003D

### 1 UVOD

Građevinska industrija koristi ogromne količine prirodnih resursa, istovremeno proizvodeći značajne količine građevinskog otpada, tako da ima veliki uticaj na prirodnu sredinu. Godišnja proizvodnja betona u svetu dostigla je deset milijardi tona, svrstavajući beton u daleko najkorišćeniji građevinski materijal. Ako se ima u vidu činjenica da je oko 70% betona agregat, jasno je kolika je količina prirodnog i drobljenog agregata potrebna. Nekonrolisana eksploatacija agregata iz reka ozbiljno narušava vodene ekosisteme i staništa, dok proizvodnja drobljenog prirodnog agregata povećava emisiju štetnih gasova, prvenstveno CO<sub>2</sub>, odgovornih za efekat staklene bašte. Ovi gasovi nastaju u toku miniranja stena i tokom transporta agregata do često udaljenih gradskih sredina.

S druge strane, količina građevinskog otpada koji nastaje tokom gradnje i rušenja objekata rapidno raste, produbljujući problem odlaganja ovog otpada, koji se najčešće rešava predviđenim deponijama (zauzimaju velike površine zemljišta, a odlaganje je skupo) ili „divljim”, nelegalnim deponijama.

Jedno od rešenja navedenih problema jeste recikliranje deponovanih građevinskih materijala, prvenstveno betona. Ova ideja nije nova i razvijene zemlje poput Japana, Holandije, Belgije i Danske ostvaruju visok procenat reciklaže građevinskog otpada. Reciklirani betonski agregat najviše se koristi u putarstvu, za različite ispune i izradu nekonstruktivnih elemenata (ivičnjaka, ograda i sličnog). Zbog neujednačenog kvaliteta, mogućnosti ostatka različitih primesa prilikom reciklaže,

---

Dr Iva Despotović, profesor, Visoka građevinsko-geodetska škola, Beograd, email: ivickad@gmail.com

### 1 INTRODUCTION

Construction industry uses vast amounts of natural resources, simultaneously producing significant amounts of construction waste, so that it has a great impact on the environment. Annual production of concrete in the world has reached 10 billion tons, classifying concrete in the most widely used building material. Having in mind the fact that 70 % of concrete is aggregate, it is clear what the quantity of natural and crushed aggregates requires. Uncontrolled exploitation of aggregates from rivers seriously disrupts aquatic ecosystems and habitats, while the production of crushed natural aggregates increases harmful gas emissions, primarily of CO<sub>2</sub>, which are responsible for the greenhouse effect. These gases are formed during blasting rocks and during the transportation of aggregates to the usually distant urban areas.

On the other hand, the amount of construction waste generated during the construction and demolition of buildings is growing rapidly, deepening the problem of disposing this waste, which is usually solved by making planned landfills (which occupy large areas of land and disposal is costly) or illegal dumps.

One of the solutions of the mentioned problems is recycling deposited building materials, primarily concrete. This idea is not new and developed countries, like Japan, the Netherlands, Belgium and Denmark achieve a high percentage of recycling of construction waste. Recycled concrete aggregates are mostly used in road engineering, for different fillings and making non-structural elements (curbs, fences, etc). Because of the

---

Iva Despotovic PhD, professor, University of Belgrade, College of Applied Studies in Civil Engineering and Geodesy, Hajduk Stankova 2, Belgrade

većeg upijanja vode i niže zapreminske mase u odnosu na prirodni agregat, reciklirani agregat zahteva niz ispitivanja i posebnu tehnologiju spravljanja betona.

Samougrađujući beton, i sama inovacija u području tehnologije betona, sadrži određenu količinu praškastog materijala – filera. Postoje različite mogućnosti odabira ove komponente. Ukoliko bi se upotrebio neki od industrijskih nusproizvoda, poput letećeg pepela ili silikatne prašine, rešio bi se problem deponovanja ovih materijala, a ovako spravljen beton svakako bi se mogao uvrstiti u ekološke materijale.

Predmet istraživanja u ovom radu jesu svojstva i tehnologija samougrađujućeg betona koji je spravljen s različitim mineralnim dodacima: mlevenim krečnjakom, letećim pepelom i silikatnom prašinom, pri čemu su, kao agregat, korišćeni i prirodni i reciklirani agregat, dobijen rušenjem potpornog zida, čija je količina u betonu varirana.

## 2 SAMOUGRAĐUJUĆI BETON

Samougrađujući beton (engl. Self-Compacting Concrete - SCC), po mnogim autorima „najrevolucionarnije otkriće industrije betona XX veka”, ne zahteva vibriranje prilikom ugrađivanja i zbijanja. Pod dejstvom sopstvene težine u potpunosti ispunjava sve delove oplata čak i u prisustvu gusto postavljene armature. Njegove prednosti su: brža gradnja, smanjenje broja potrebnih radnika, bolje finalne površine, lakše ugrađivanje, poboljšana trajnost, veća sloboda oblikovanja elemenata, smanjenje buke, odsustvo vibracija, i samim tim, zdravije radno okruženje. Procena je da se prilikom upotrebe samougrađujućeg betona umesto vibriranog, potrebe za radnom snagom smanjuju za oko 10%; kod primene prefabrikovanih elemenata, vreme gradnje je kraće za oko 5%, a potreba za radnicima manja za oko 20%; prilikom primene sendvič-elemenata (čelik–beton) ušteda u vremenu je 20%, a u radnoj snazi 50%. Glavni nedostaci upotrebe samougrađujućeg betona jesu veća cena materijala, stroži zahtevi kvaliteta i veći pritisak na oplatu u odnosu na vibrirani beton [13].

Kod samougrađujućeg betona najvažnije su njegove karakteristike u svežem stanju. Prilikom projektovanja mešavine, akcenat se stavlja na sposobnost betona da se razliva samo pod dejstvom sopstvene težine i da u potpunosti ispunji oplatu ma kog oblika i dimenzija bez ostavljanja šupljina, da prođe kroz gusto postavljenu armaturu bez zaglavljivanja, da zadrži homogenu strukturu bez izdvajanja agregata iz paste ili vode od čvrste faze, kao i bez tendencije krupnog agregata da „propadne” kroz betonsku masu pod dejstvom gravitacije (segregacija). Dakle, ključne karakteristike svežeg SCC-a jesu: sposobnost tečenja, viskoznost (izražena brzinom tečenja), sposobnost prolaza i otpornost na segregaciju [2]. Betonska mešavina će biti klasifikovana kao SCC jedino ako su sva navedena svojstva u potpunosti ostvarena, pri čemu se svako od njih može testirati na više načina.

Osnovne komponente mešavina kod vibriranog i samougrađujućeg betona jesu iste, ali se razlikuju odnosi mešanja i SCC sadrži više sitnog agregata i sitnih čestica, kao i aditive najnovije generacije (modifikatore viskoziteta i visoke sposobnosti redukcije vode) u odnosu na vibrirani beton. Propisno projektovan i ugrađen, SCC se odlikuje većom kompaktnošću i

uneven quality, the possibility of various impurities to rest during recycling, larger water absorption and lower bulk density, compared to natural aggregates, recycled aggregates require a series of tests and special technology of concrete making.

Self-compacting concrete, being innovation in the field of concrete technology, contains a certain amount of powdered materials – fillers. There are various possibilities of selecting this component. If we used any of the industrial by-products, such as fly ash or silica fume, we would solve the problem of depositing these materials, and thus made concrete ecological material.

The research subject presented in this paper are properties and technology of self-compacting concrete made with various mineral additives: lime, fly ash, and silica fume, wherein the aggregates used, are both natural and recycled aggregates, obtained by demolition of retaining wall, whose amount is varied in the concrete.

## 2 SELF - COMPACTING CONCRETE

Self - compacting concrete (SCC), according to many authors “the most revolutionary discovery of concrete industry of the 20<sup>th</sup> century”, does not need vibrating when placing and compacting. Under the influence of its own weight, it completely fills all parts of the formwork, even in the presence of dense reinforcement. Its advantages are fast construction, a reduced number of required workers, better final surface, easier placement, and increased durability, greater freedom in designing elements, noise reduction, vibration absence, and therefore healthier work environment. It is estimated that when using self-compacting concrete instead of vibrated concrete, the need for workers is reduced by about 10%; when using prefabricated elements, construction time is shorter by about 5%, and demand for workers decreased by about 20%; when applying sandwich elements (steel - concrete) time saving is 20%, and savings in the labour force 50%. The main disadvantages of the use of self - compacting concrete are higher material prices, stricter quality requirements and increasing pressure on the formwork compared to vibrated concrete [13].

With self-compacting concrete, its most important characteristics are in its fresh state. When designing mixes, emphasis is placed on the ability of concrete to be levelled out only under the influence of its own weight and to fully fill the formwork of any shape and dimensions without leaving voids, to pass through dense reinforcement without blocking, to retain a homogenous structure without separating aggregate from paste or water from the solid phase, as well as without the tendency of coarse aggregates to “fall” through the concrete mass under the influence of gravity (segregation). Therefore, the key characteristics of fresh SCC are floating, viscosity (expressed by floating rate), passing ability and resistance to segregation [2]. Concrete mix will be classified as SCC only if all the above properties are fully achieved, wherein each of them can be tested in a number of ways.

The basic components of the mixes in vibrated and self - compacting concrete are the same, but ratios differ, so that SCC contains more fine aggregate and fine particles, as well as additives of the latest generation (modifiers of viscosity and high capacity water

homogenošću u odnosu na vibrirani beton, pri čemu se svojstva očvrstlog samougrađujućeg betona ispituju na isti način kao odgovarajuća svojstva vibriranog betona.

### 3 MINERALNI DODACI

#### 3.1 Leteći pepeo

Začetnici ideje o primeni letećeg pepela, dobijenog sagorevanjem uglja u betonu, bili su McMillan i Powers 1934. godine. Krajem 40-tih godina izvršena ispitivanja u Britaniji (Fulton i Marshall) dovela su do gradnje brana Lednock, Clatworthy i Lubreoch, s letećim pepelom kao cementnim dodatkom. Sve ove konstrukcije su i posle šezdeset godina u odličnom stanju [10].

Prilikom sagorevanja uglja u peći na temperaturi između 1250°C i 1600°C, nesagorive čestice se spajaju, formirajući sferične staklaste kapljice silikata ( $\text{SiO}_2$ ), aluminata ( $\text{Al}_2\text{O}_3$ ), oksida gvožđa ( $\text{Fe}_2\text{O}_3$ ) i drugih, manje važnih konstituenata. Kada se leteći pepeo doda betonu, počinje pucolanska reakcija između silicijum-dioksida ( $\text{SiO}_2$ ) i kalcijum-hidroksida ( $\text{Ca(OH)}_2$ ) ili kreča, koji je nusprodukt hidratacije Portland cementa. Nastali produkti hidratacije popunjavaju pore, smanjujući poroznost matrice. Ovi produkti se razlikuju od produkata nastalih u betonima, koji sadrže samo Portland cement. U reakcijama Portland cementa i vode nastaje najpre hidratisan kreč ( $\text{Ca(OH)}_2$ ), koji se zbog svoje ograničene rastvorljivosti formira u međuprostoru čestica. U prisustvu vode, kreč pucolanski reaguje s letećim pepelom, pri čemu nastaju novi produkti hidratacije fine strukture pora.

Čestice sitnije od 50µm uglavnom su sferične (slika 1) dok krupnije čestice mogu da budu nepravilnijeg oblika. Sferične čestice daju značajan doprinos fluidnosti betona u plastičnom stanju, optimizujući upakovanost čestica [1].

#### 3.2 Silikatna prašina

Silikatna prašina (slika 2) veoma je fin prah sledećih osobina:

- 1) sadržaj silicijum-dioksida,  $\text{SiO}_2$ , najmanje 85%;
- 2) prosečna veličina čestica između 0.1 i 0.2 mikrona;
- 3) minimalna specifična površina 15000 m<sup>2</sup>/kg;
- 4) sferni oblik čestica.

Silikatna prašina nastaje prilikom topljenja kvarca na visokoj temperaturi u peći sa električnim lukom, pri čemu nastaje silicijum ili ferossilicijum. Zbog ogromne količine potrebne električne energije, ove peći se nalaze u zemljama sa značajnim elektropotencijalom poput skandinavskih zemalja, Sjedinjenih Država, Kanade, Južne Afrike i Australije. Kvarc visoke čistoće zagreva se do 2000°C, gde se kao gorivo koriste ugalj, koks i drvena piljevina, a zatim uvodi električni luk da bi se izdvojili metali. Topljenjem kvarca oslobađa se silicijum-oksidi u gasovitom stanju, koji se meša s kiseonikom u višim delovima peći, gde oksidira, prelazeći u sićušne čestice amorfno silicijum-dioksida. Čestice se izvode iz

redukcijom) compared to vibrated concrete. Properly designed and placed, SCC is characterized by a greater compactness and homogeneity compared with the vibrated concrete, wherein the properties of the hardened self-compacting concrete are tested in the same way as the corresponding properties of the vibrated concrete.

### 3 MINERAL ADDITIVES

#### 3.1 Fly Ash

The initiators of the idea of applying fly ash, resulted from coal burning, in concrete were McMillan and Powers (1934). At the end of 40s the experiments carried out in the UK (Fulton and Marshall) led to the construction of dams Lednock, Clatworthy and Lubreoch, with fly ash as a cement additive. All these structures are after 60 years in excellent condition [10].

During the combustion of coal in a furnace at temperatures between 1250°C and 1600°C, non-combustible particles combine to form spherical glassy droplets of silicate ( $\text{SiO}_2$ ), aluminate ( $\text{Al}_2\text{O}_3$ ), iron oxide ( $\text{Fe}_2\text{O}_3$ ) and other less important constituents. When fly ash is added to concrete, pozzollanic reaction starts between silicon dioxide ( $\text{SiO}_2$ ) and calcium hydroxide ( $\text{Ca(OH)}_2$ ) or lime, which is a by-product of hydration of Portland cement. The resulting products of hydration fill pores reducing the porosity of the matrix. These products differ from the products formed in concrete containing only Portland cement. In the reactions of Portland cement and water, hydrated lime ( $\text{Ca(OH)}_2$ ) is formed first, in the space between particles, because of its limited solubility. In the presence of water, lime reacts pozzollanic with fly ash to form new hydration products with fine pore structures.

Particles smaller than 50µm are generally spherical (Figure 1), while larger particles may be irregularly shaped. Spherical particles provide a significant contribution to the fluidity of concrete in the plastic state, optimizing the packing of particles [1].

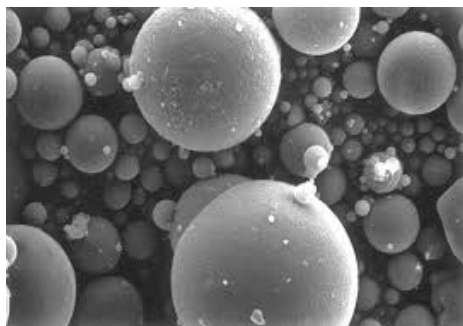
#### 3.2 Silica Fume

Silica fume (Figure 2) is very fine powder with the following characteristics:

- 1) the silica,  $\text{SiO}_2$ , content of at least 85%
- 2) average particle size between 0.1 and 0.2 microns
- 3) minimum specific area 15 000 m<sup>2</sup>/kg
- 4) spherical shape of particles.

Silica fume is formed during melting quartz at high temperature in an electric arc furnace, wherein silicon or ferrosilicon occurs. Because of the huge amount of electricity needed, these furnaces are located in the countries with significant electrical potential, such as Scandinavian countries, USA, Canada, South Africa and Australia. High purity quartz is heated to 2000°C using coal, coke or wood chips as fuel and then electric arc is introduced in order to remove metals. By melting quartz, silicon oxide is released in gaseous state, and it is mixed with oxygen in the upper parts of the furnace, where it oxidizes turning into tiny particles of amorphous silicon dioxide. Particles are carried out from the furnace

peći kroz kolektor i obrtni deo u kojima se odstranjuju nesagoreli delovi uglja, a onda „uduvavaju” u posebne filter- vreće.



Slika 1. Čestica letećeg pepela (SEM slika) [10]  
Figure 1. Fly ash particle (SEM picture) [10]

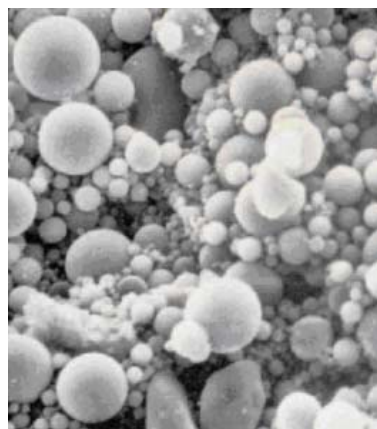
Zahvaljujući svojoj prirodi, i mali dodatak silikatne prašine znatno menja fizičko- hemijske osobine betona. Uobičajeno doziranje od 8 do 10% težine cementa znači između 50000 i 100000 mikrosfera prašine po zrnju cementa, što direktno povećava koheziju betona. Ukoliko se koristi silikatna prašina u praškastoj formi, javiće se potreba za većom količinom vode da bi se omogućili mešanje i ugradnja, pa je nužna primena plastifikatora ili superplastifikatora.

Iz aspekta ugradljivosti, treba pomenuti da svež beton sa silikatnom prašinom zbog veće kohezije ima manje rasprostiranje (slump vrednosti). Veoma fine čestice prašine obezbediće znatno veću kontaktnu površinu svežeg betona i armature i na taj način stvoriti bolju vezu očvrstlog betona sa armaturom. Osim odsustva segregacije i popunjavanja glavnih šupljina, tipično za betone sa silikatnom prašinom jeste da nema izdvajanja vode. Zbog toga se odmah po ugrađivanju mora otpočeti sa odgovarajućom negom. Takođe se i završna obrada, poput perdašenja, radi znatno ranije nego kod običnih betona.

Bez obzira na manje rasprostiranje, odsustvo izdvojene vode i „želiranje” (zgušnjavanje kada se ne meša) ne ukazuju na ubrzano očvršćavanje. Silikatna prašina je pucolan i za njeno aktiviranje neophodno je prisustvo kalcijum-hidroksida. On nastaje u procesu hidratacije cementa tako da silikatna prašina može da se aktivira tek kada cement počne da reaguje. Vreme vezivanja kod betona sa silikatnom prašinom isto je kao i kod običnih betona. Kako beton počinje da vezuje i očvršćava, pucolanska aktivnost silikatne prašine postaje dominantna reakcija. Silikatna prašina reaguje sa slobodnim kalcijum-hidroksidom, gradeći kalcijum-silikat i hidrate aluminijuma. Ova jedinjenja povećavaju čvrstoću i smanjuju propusnost, proglašujući cementnu matricu.

Zbog veće specifične površine i višeg sadržaja silicijum-dioksida, silikatna prašina je mnogo reaktivnija od letećeg pepela ili granulisanog zgušćiva. Ova pojačana reaktivnost prvobitno će znatno pojačati brzinu hidratacije  $C_3S$  minerala cementa, ali se nakon dva dana proces normalizuje.

through the collector and cyclone, where the unburned parts of coal are removed, and then “blown” into the special filter bags.



Slika 2. Silikatna prašina (SEM slika) [14]  
Figure 2. Silica fume (SEM picture) [14]

Due to its nature, even a small addition of silica fume significantly changes physical and chemical properties of concrete. The customary dosage of 8- 10% by weight of cement means between 50 000 and 100 000 microspheres of dust per cement grain, which directly increases the cohesion of concrete. If silica fume is used in the powder form, there will be a need for a greater amount of water to allow mixing and placement of concrete so it is necessary to apply plasticizers and superplasticizers.

In terms of placeability, it should be noted that fresh concrete with silica fume has less spreading (slump values) because of greater cohesion. Very fine silica fume particles will provide considerably larger contact area of fresh concrete and reinforcement and thus make better bonding of hardened concrete with reinforcement. Besides the lack of segregation and filling the main cavities, in concrete with silica fume, there is no separation of water. That is why, immediately after placement, it is necessary to begin with appropriate curing. Finishing, such as pargeing, is also done much earlier than in ordinary concrete.

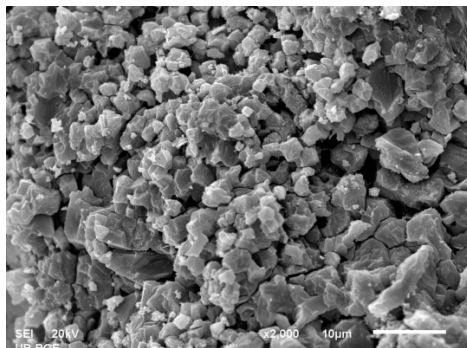
Regardless of less spreading, the absence of free water and “gelling” (jellification when not stirred) do not indicate rapid hardening. Silica fume is pozzolan and it requires the presence of calcium hydroxide to be activated. Calcium hydroxide is formed in the cement hydration process, so that silica fume can be activated only when the cement begins to react. Setting time of concrete with silica fume is the same as in plain concrete. As concrete begins to set and harden, pozzolanic activity of silica fume becomes dominant reaction. Silica fume reacts with free calcium hydroxide, thus forming calcium silicate and hydrates of aluminium. These compounds increase the strength and reduce permeability, thickening the cement matrix.

Because of higher specific area and higher content of silicon dioxide, silica fume is much more reactive than fly ash or granulated slag. This increased reactivity initially increases hydration rate of  $C_3S$  cement mineral, but after two days the process becomes normal.



### 3.3 Mleveni krečnjak

Mleveni krečnjak (slika 3) više se koristi kao dodatak cementu nego betonu. Evropska norma EN197 – 1 predviđa dve klase Portland cementa s krečnjakom čije su oznake CEM II/A-L (ili L-L umesto A-L) i CEM II/B-L (ili L-L umesto B-L). Prvi sadrži između 6 i 20% krečnjaka, a drugi 21–35%.



Slika 3. Mleveni krečnjak (SEM slika)  
Figure 3. Lime (SEM picture)

Zahtevi koje krečnjak za cement treba da ispuni jesu sledeći: sadržaj  $\text{CaCO}_3$  mora da bude veći od 75%, sadržaj gline određen metilenskim plavim testom ne sme da pređe 1.20g /100 g, ukupni sadržaj organskog ugljenika ne sme da pređe 0.20% za LL krečnjak i 0.50% za L krečnjak.

Prisustvo krečnjaka izaziva ubrzanje hidratacionog procesa i hidratacionog skupljanja betona već u prvih nekoliko sati, zbog toga što čestice krečnjaka služe kao dodatna jezgra za hidrataciju.

### 4 RECIKLIRANI AGREGAT

Kao održivo rešenje za probleme građevinskog otpada i iscrpljivanje nalazišta prirodnih agregata, nametnuo se postupak recikliranja deponovanih građevinskih materijala, u prvom redu betona. Recikliranje i očuvanje prirodnih resursa bezrezervno su prihvaćeni od strane građevinske industrije, ali pozitivni efekti takvog pristupa donekle su ograničeni, zato što nisu obezbeđeni svi uslovi za primenu. To se prvenstveno odnosi na nedostatak: prostora i opreme za sortiranje građevinskog šuta, iskustva u postupcima recikliranja otpadnih materijala, obučanih radnika i kontrolora, znanja o tržištu sekundarnih materijala, zakonske regulative u oblasti zaštite životne sredine, i tako dalje [7].

Upotreba recikliranog agregata u konstrukcijama još je relativno nova priča. Njen početak Bak (Buck, 1977) smešta u period neposredno nakon Drugog svetskog rata, kada je postojala ogromna potreba da se grade novi objekti i infrastruktura i istovremeno raščišćavaju postojeće ruševine. Nakon toga, reciklirani agregat prestaje da se upotrebljava, da bi tokom sedamdesetih godina, Sjedinjene Države počele ponovo da koriste reciklirani agregat u nekonstrukcijske svrhe, mahom kao materijal za ispunu i različita nasipanja u putarstvu [8]. Zbog razloga koji su napred navedeni, ispitivanje

### 3.3 Lime

Lime (Figure 3) is more widely used as a cement additive than a concrete additive. European norm EN197 - 1 provides two classes of Portland cement with lime whose labels are CEM II/L (or L-L instead of A-L) and CEM II/BL (or L-L instead of B-L). The former contains between 6 and 20% of lime and the latter 21- 35%.

Requirements that lime for cement should meet are the following:  $\text{CaCO}_3$  content should be greater than 75%, clay content, determined by methylene blue test, must not exceed 1.20g/100g, the total content of organic carbon must not exceed 0.20% for LL lime and 0.50% for L lime.

The presence of lime causes the acceleration of the hydration process and hydration shrinkage of concrete in the first few hours, because the particles of lime are used as additional cores for hydration.

### 4 RECYCLED AGGREGATE

As a sustainable solution to the problems of construction waste and the depletion of natural aggregates sites, the recycling process of deposited building materials, primarily concrete, has been imposed. Recycling and preservation of natural resources are unreservedly accepted by the construction industry but positive effects of this approach are somewhat limited, since the conditions for their application are still concealed. This is primarily related to the lack of space equipment for sorting construction rubble, lack of experience in the procedures of recycling waste materials, shortage of skilled workers and supervisors, lack of knowledge of the secondary materials market, of legislation in the field of environmental protection, etc [7].

The use of recycled aggregates in structures is still relatively new. Buck (1977) defines its beginning in the period immediately after the Second World War, when there was a tremendous need for building new facilities and infrastructure and at the same time, clearing the existing ruins. After that, the use of recycled aggregates stopped but during 70s the US started to re-use recycled aggregates in non-construction purposes, mainly as fill material and different fillings in road engineering [8]. Due to the above mentioned reasons, testing of recycled

recikliranog agregata (ne samo betonskog) i njegova primena danas su aktuelniji no ikad, jer je potreba za agregatom na svetskom nivou dostigla 26.8 milijardi tona godišnje [15]. Primera radi, Sjedinjene Države godišnje recikliraju oko 140 miliona tona betonskog otpada. Prema podacima iz godišnjeg izveštaja Evropske asocijacije za agregat (2010), reciklirani agregat čini 5% ukupne proizvodnje agregata u Evropskoj uniji, gde je Nemačka najveći proizvođač (60 miliona tona), a slede Velika Britanija (49 miliona tona), Holandija (20 miliona tona) i Francuska (17 miliona tona). U Australiji se oko 50% betonskog otpada reciklira, dok se u Japanu imponantnih 98% betonskog otpada pretvara u reciklirani agregat [5].

Procenjuje se da u Republici Srbiji godišnje nastaje oko milion tona građevinskog otpada i otpada od rušenja. Ovaj otpad završava na deponijama komunalnog otpada, a koristi se i kao inerten materijal za prekrivanje otpada na deponiji. Reciklaža građevinskog otpada praktično ne postoji [12].

Tehnološki postupak proizvodnje recikliranog agregata podrazumeva drobljenje komada starog betona na zrna određene veličine i njihovo prosejavanje, čemu prethodi odvajanje metalnih delova magnetnim separatorom i ručno ili mašinsko uklanjanje stranih materija. Zrno recikliranog agregata dobijeno ovakvim postupkom recikliranja sastoji se od zrna (ili dela zrna) prirodnog agregata i cementnog maltera originalnog betona, koji ga delimično ili potpuno obavija. Prisustvo starog cementnog maltera, koji je manje zapreminske mase i veće poroznosti od zrna prirodnog agregata, značajno utiče na niz fizičko-mehaničkih svojstava, kako recikliranog agregata, tako i betona na bazi recikliranog agregata, odnosno uslovljava „lošija” svojstva recikliranog u odnosu na prirodni agregat. Zbog toga su se u svetu u poslednjih nekoliko godina razvila istraživanja u smislu unapređivanja tehnologije recikliranja i dobijanja recikliranog agregata koji bi po svojstvima, odnosno kvalitetu, bio praktično identičan prirodnom agregatu. Radi uklanjanja cementnog kamena sa zrna agregata razvijeno je nekoliko naprednih tehnologija recikliranja, pre svega u Japanu. Jedna od tih tehnologija jeste takozvana „metoda zagrevanja i struganja”. Na ovaj način, dobija se 35% do 45% čistog krupnog agregata, 30% do 35% čistog sitnog i 18% do 35% finog praha od cementnog maltera u zavisnosti od temperature zagrevanja (300-700°C).

Druga tehnologija je hemijski tretman klasično proizvedenog recikliranog agregata. Prethodnim potapanjem recikliranog agregata u blage rastvore hlorovodonične, sumporne ili fosforne kiseline moguće je odstraniti deo cementnog maltera i poboljšati svojstva agregata, bez značajnijeg povećanja sadržaja hlorida i sulfata u njemu. Pomenuta procedura sastoji se iz potapanja recikliranog agregata u kiselu sredinu u trajanju od 24h, pri temperaturi od oko 20°C, a zatim se vrši ispiranje destilovanom vodom kako bi se u najvećoj mogućoj meri uklonile primenjene kiseline. Pre samog spravljanja betona, agregat stoji u vodi 24 časa. Da se ne bi smanjio kvalitet agregata (pH vrednost), koncentracija kiseline u rastvoru treba da bude oko 0.1 mol. Ovim postupkom moguće je smanjiti upijanje vode kod recikliranog agregata za 7–12% [9,6]. Sve navedene napredne tehnologije recikliranja, odnosno poboljšanja kvaliteta, iako omogućavaju proizvodnju kvalitetnog

aggregates (not just concrete) and their application are more relevant today than ever, because the need for aggregates globally reached 26.8 billion tons per year [15]. For example, the US annually recycles about 149 million tons of concrete waste. According to the data from the annual report of the European Association for aggregates (2010), recycled aggregates make 5% of the total production of aggregates in the European Union, where Germany is the largest producer, followed by Great Britain (49 million tons), the Netherlands (20 million tons) and France (17 million tons). In Australia, around 50% of the concrete waste is recycled, while in Japan, the impressive 98% of concrete waste is turned into recycled aggregate [5].

It is estimated that in the Republic of Serbia, about 1 million tons of construction waste and demolition waste is annually produced. This waste ends up in landfills of municipal waste, and is also used as inert material for coverage of waste at landfills. Recycling construction waste actually does not exist [12].

Technological process for the production of recycled aggregates involves crushing pieces of old concrete to a certain grain size and their sieving, which is preceded by the separation of metal parts, using magnetic separator, and manual or mechanical removal of foreign substances. Grains of recycled aggregate, obtained by this recycling process, consist of grains (or grain parts) of natural aggregates and cement mortar of original concrete which partially or completely wraps them. The presence of old cement mortar, which is of less density and higher porosity than grains of natural aggregates, significantly affects a number of physical and mechanical properties, of both recycled aggregate and concrete with recycled aggregate, i.e. causes “worse” properties of recycled aggregate compared to natural aggregate. Therefore, numerous researches have been carried out worldwide with the aim of improving recycling technologies and obtaining recycled aggregates that would be practically identical to natural aggregate in their properties or quality. In order to remove cement stone from an aggregate grain, a number of advanced recycling technologies have been developed, primarily in Japan. One of these technologies is called “the method of heating and abrasion”. Thus, they obtain 35% to 45% of pure coarse aggregate, 30% to 35% of pure small aggregate, and 18 % to 35% of fine powder of cement mortar, depending on the heating temperature (300 – 700°C).

Other technology is chemical treatment of classically produced recycled aggregate. By previous submerging of recycled aggregate in a mild solution of hydrochloric, phosphoric and sulphuric acid, it is possible to remove a part of cement mortar and improve aggregate properties without a significant increase of the content of chloride and sulphate in it. The mentioned procedure consists of immersing recycled aggregate in an acidic environment for 24 hours at a temperature of about 20°C, and then the applied acids are removed to the maximum extent possible, by washing with distilled water. Before making concrete, aggregate is left in water for 24 hours. In order to sustain the quality of the aggregate (ph value), concentration of acid in solution should be about 0.1mol. This method can reduce the absorption of water in recycled aggregate for 7-12% [9,6]. All of these advanced recycling technologies, although enable the

recikliranog agregata potpuno ekvivalentnog prirodnom, nemaju za sada širu primenu, jer su znatno skuplje od tradicionalnih tehnologija. Metode s termičkim tretmanom agregata su i energetski zahtevnije, što dovodi u pitanje korist od recikliranja i povoljan uticaj na zaštitu životne sredine [11].

## 5 SOPSTVENO EKSPERIMENTALNO ISPITIVANJE

### 5.1 Sastav betonskih mešavina

Za potrebe eksperimentalnog dela rada napravljeno je devet različitih trofrakcijskih betonskih mešavina. Korišćeni su cement PC 42.5R (Holcim Popovac); mineralni dodaci: mleveni krečnjak (proizvođač „Jelen Do“), elektrofilterski pepeo (iz Termoelektrane „Nikola Tesla“ B u Obrenovcu), i silikatna prašina (proizvod Sikafume, proizvođača građevinske hemije SIKA); prirodni agregat (Luka „Leget“ – Sremska Mitrovica), reciklirani agregat dobijen drobljenjem srušenog potpornog zida u kamenolomu Ostrovica kod Niša. Etaloni su spravljani sa svakim od dodataka i prirodnim agregatom; kod mešavina K50, P50 i S50, frakcija 8/16 mm zamenjena je recikliranim agregatom, a kod mešavina K100, P100 i S100, obe krupne frakcije (4/8 i 8/16 mm) zamenjene su recikliranim. U svim mešavinama korišćen je superplastifikator ViscoCrete 5380 (proizvođač SIKA), čije je doziranje izvršeno prema preporuci proizvođača. Kriterijum pri projektovanju mešavina bio je postizanje iste konzistencije betona, tj. slump - flow klase SF2, koja obuhvata uobičajenu primenu betona i podrazumeva rasprostiranje od 66 do 75 cm. Prilikom spravljanja betonskih mešavina, najpre je agregat mešan s polovinom potrebne vode u trajanju od oko 30 sekundi, a zatim su dodavane ostale komponente. Kada je korišćen reciklirani agregat, dodata je količina vode koju agregat upije za 30 minuta (II frakcija 2.22%, III frakcija 1.5%), mada ovaj princip nije mogao dosledno da se primeni.

Na svežem betonu urađena su ispitivanja: zapreminske mase, fluidnosti - slump flow test prema EN 12350-8, viskoznosti -  $T_{500}$  test prema EN 12350-8, sposobnosti prolaza između armature - L box test prema EN 12350-10, otpornosti na segregaciju - sieve segregation test prema EN 12350-11.

Na očvrslom betonu urađena su ispitivanja: zapreminske mase, čvrstoće pri pritisku, čvrstoće pri zatezanju savijanjem, skupljanja, vodonepropustljivosti, upijanja vode i SEM analize (skenirajuća elektronska mikroskopija).

Sastav betonskih mešavina prikazan je u tabeli 1.

production of high-quality recycled aggregates, fully equivalent to natural aggregates, have no wider application because they are significantly more expensive than traditional technologies. Methods of thermal treatment of aggregates are also more energy-demanding, which brings into question the benefits of recycling and its favourable impact on environmental protection.

## 5 MY OWN EXPERIMENTAL RESEARCH

### 5.1 Composition of Concrete Mixes

For the purposes of the experimental work, nine three-fraction concrete mixes have been made. Cement PC 42.5R (Holcim Popovac) has been used as well as mineral additives: lime (manufacturer „Jelen Do“), fly ash (from the power plant „Nikola Tesla B“ in Obrenovac), and silica fume (product of Sikafume, a manufacturer of building chemicals SIKA); natural aggregate (Luka „Leget“, Sremska Mitrovica), recycled aggregate obtained by crushing demolished retaining wall in the quarry Ostrovica, near Nis. Control concrete was made with each of the additives and a natural aggregate; in mixes K50, P50 and S50, fraction 8/16mm was replaced by the recycled aggregate, and in mixes K100, P100 and S100, both coarse fractions (4/8 and 8/16) were replaced by recycled fractions. In all the mixes, superplasticizer ViscoCrete 5380 (manufacturer SIKA) has been used, which was dosed according to the manufacturer. The criterion in the designing mixes was to achieve the same consistency of concrete, i.e. slump-flow class SF2, which includes the usual uses of concrete and involves spreading from 66 to 75cm. While making concrete mixes, the aggregate was first mixed with half of the required water for a period of about 30 seconds, and then other components were added. When used recycled aggregate, the amount of water which was absorbed by the aggregate in 30 minutes (II fraction 2.22%, III fraction 1.5%) was added, although this principle could not be consistently applied.

The fresh concrete tests were done for density, fluidity - slump flow test according to EN 12350-8, viscosity -  $T_{500}$  test according to EN 12350-8, the ability of the passage between the reinforcement - L box test according to EN 12350-10, segregation resistance - Sieve segregation test according to EN 12350-11.

The hardened concrete tests were done for density, compressive strength, tensile strength by bending, shrinkage, water impermeability, water absorption, and SEM analysis (Scanning Electron Microscopy).

Composition of concrete mixes is shown in Table 1.

Tabela 1. Sastav betonskih mešavina  
Table 1. Concrete mixes

	cement (cement) (kg/m <sup>3</sup> )	ml.krečnjak (lime) (kg/m <sup>3</sup> )	el.pepeo (fly ash) (kg/m <sup>3</sup> )	sil.prašina (silica fume) (kg/m <sup>3</sup> )	0/4mm (kg/m <sup>3</sup> )	4/8mm (kg/m <sup>3</sup> )	8/16mm (kg/m <sup>3</sup> )	voda (water) (kg/m <sup>3</sup> )	VSC5380 (kg/m <sup>3</sup> )
EK	400	120	0	0	770.86	306.28	532	170.8	4.94
EP	400	0	120	0	770.86	306.28	532	192.66	4.94
ES	400	0	0	52	770.86	306.28	532	185.71	4.94
K50	400	120	0	0	809.14	306.28	505.43	182.86	5.08
P50	400	0	120	0	809.14	306.28	505.43	214.28	5.08
S50	400	0	0	52	809.14	306.28	505.43	197.14	5.08
K100	400	120	0	0	809.14	306.28	505.43	189.5	5.08
P100	400	0	120	0	809.14	306.28	505.43	221	5.08
S100	400	0	0	52	809.14	306.28	505.43	208.6	5.08

## 5.2 Rezultati ispitivanja

Rezultati ispitivanja svežeg betona prikazani su u tabeli 2.

## 5.2 Test Results

The test results for concrete in the fresh state are shown in Table 2.

Tabela 2. Rezultati ispitivanja svežeg betona  
Table 2. Test results for concrete in the fresh state

bet. mešavina (concrete mix)	zaprem. masa (density) kg/m <sup>3</sup>	rasprostiranje (Slump-flow) cm	T500 s	L – kutija (L-box) H1/H2	test na situ, % (sieve segregation)
EK	2418	73	4	1	12.4
EP	2288	70	4	0.94	11
ES	2416	66	6	0.91	6.8
K50	2362	70	5	0.96	12
P50	2279	70	5	0.95	7.8
S50	2324	67	5	0.94	5.2
K100	2347	69	5	1	10
P100	2298	66	6	0.91	5.5
S100	2359	66	6	0.92	7.5

Rezultati ispitivanja zapreminske mase betona u očvrslom stanju, prema SRPS EN 12390 – 7 : 2010, nakon dva, sedam i 28 dana, prikazani su u tabeli 3.

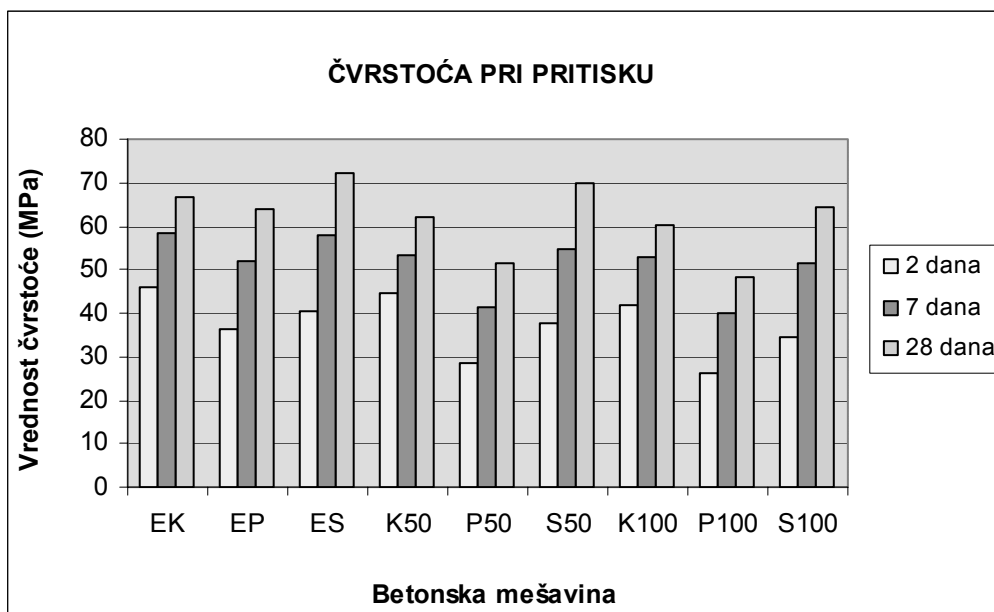
The test results for density of concrete in the hardened state, according to SPRS EN 12390 – 7:2010, after 2, 7 and 28 days are shown in Table 3.

Tabela 3. Rezultati ispitivanja zapreminske mase betona (kg/m<sup>3</sup>)  
Table 3. Test results for density (kg/m<sup>3</sup>)

	EK	EP	ES	K50	P50	S50	K100	P100	S100
2 dana	2396	2262.4	2366.4	2356.5	2313.5	2313	2363.5	2284.2	2312
7 dana	2469.2	2289.7	2361.8	2370	2315.5	2315.8	2352.9	2292.5	2338.6
28 dana	2426.7	2306.2	2376.3	2401.7	2314	2325	2357	2303.3	2333

Ispitivanje čvrstoće pri pritisku obavljeno je na kockama ivice 15 cm. Rezultati ispitivanja čvrstoće pri pritisku nakon dva, sedam i 28 dana, prikazani su na grafiku 1.

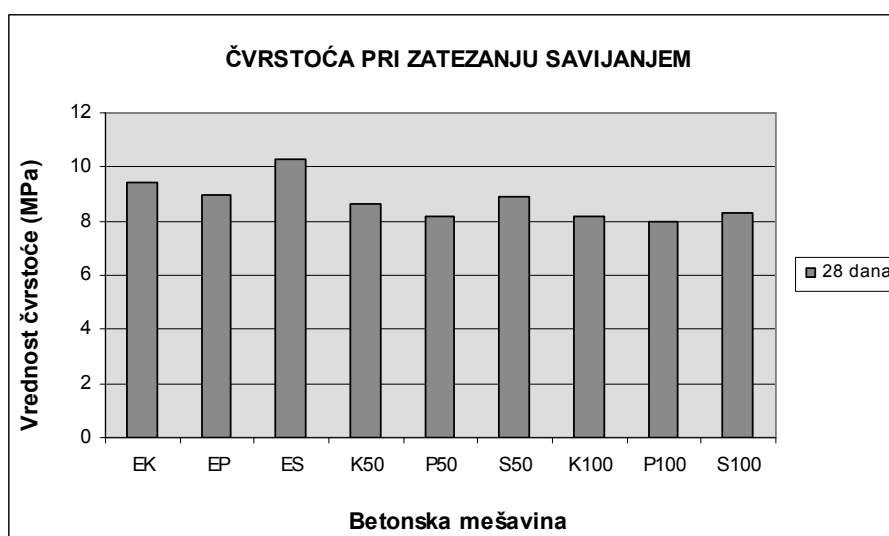
Testing compressive strength was carried out on the cubes with edges of 15cm. The test results for compressive strength after 2, 7 and 28 days are shown in Chart 1.



*Grafik 1. Čvrstoća pri pritisku*  
*Chart 1. Compressive strength*

Ispitivanje čvrstoće na zatezanje savijanjem obavljeno je nakon 28 dana na uzorcima dimenzija 12x12x36 cm. Rezultati su prikazani na grafiku 2.

Testing tensile strength by bending was done after 28 days on the samples of dimensions 12x12x36cm. The results are shown on Chart 2.



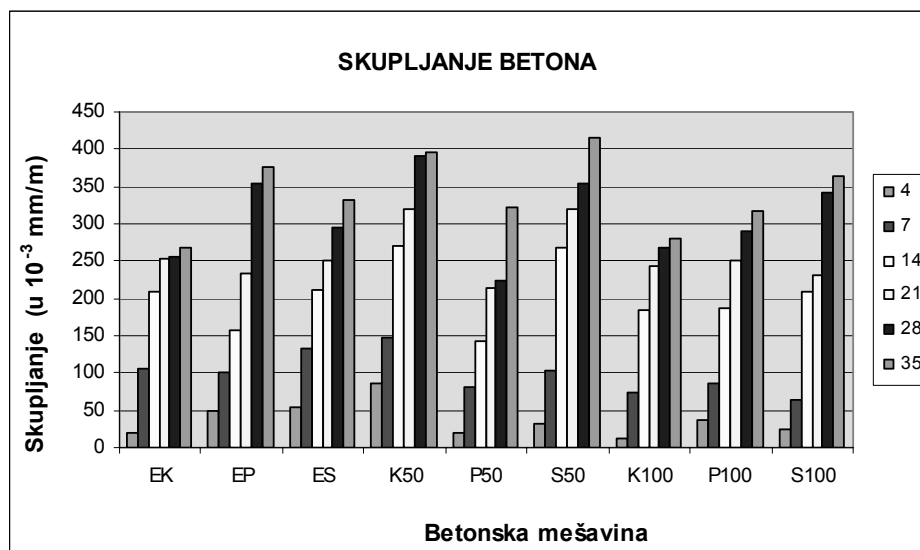
*Grafik 2. Čvrstoća pri zatezanju savijanjem*  
*Chart 2. Tensile strength by bending*

Ispitivanje skupljanja izvršeno je na uzorcima dimenzija 12x12x36 cm, u svemu prema SRPS U.M1.029. Nakon 72 h od završetka izrade, uzorci se vade iz vode i izlažu kondicioniranim termohigrometrijskim uslovima. Izabrano je da to budu  $70 \pm 5\%$  vlažnost vazduha i konstantna temperatura od  $20 \pm 4\text{ }^\circ\text{C}$ , što je standardom propisano za konstrukcije i elemente koji će biti u slobodnom prostoru. Prvo merenje se vrši nakon  $72 \pm 0.5$  h nakon završetka izrade uzoraka, a zatim posle četiri i sedam dana. Nakon ovoga, dalja

Shrinkage test was done on the samples of dimensions 12x12x36cm, all in accordance with SRPS UM1.029. 72 hours after the samples are made they are taken out from the water and exposed to thermo hygrometric conditions. We chose it to be  $70 \pm 5\%$  air humidity and a constant temperature of  $20 \pm 4\text{ }^\circ\text{C}$ , which is the standard prescribed for structures and elements located in free space. First measurement was done  $72 \pm 0.5$  h hours after the samples were made, and then after 4 and 7 days. After this, further measurements were

merjenja rade se nakon svakih narednih sedam dana, dok se proces ne stabilizuje. Rezultati ispitivanja skupljanja betona nakon četiri, sedam, 14, 21, 28 i 35 dana prikazani su na grafiku 3.

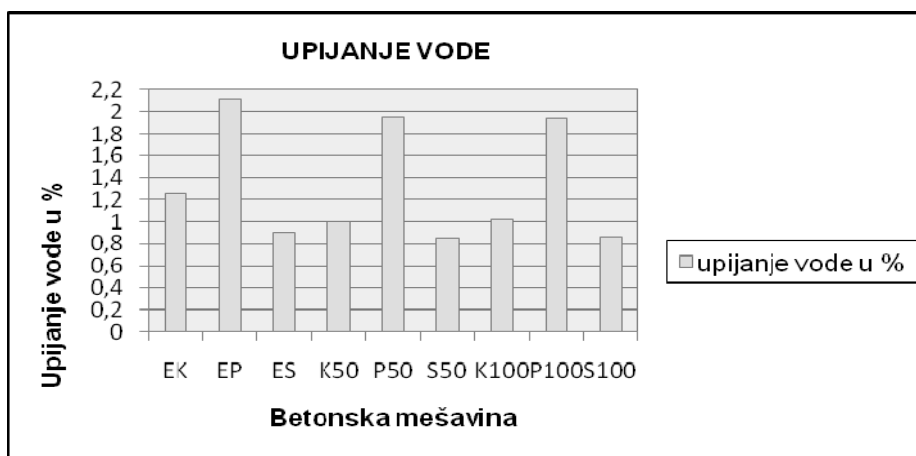
done after every seven days, until the process stabilized. The results of shrinkage tests after 4, 7, 14, 21, 28, and 35 days, are shown in Chart 3.



Grafik 3. Skupljanje betona  
Chart 3. Shrinkage

Ispitivanje upijanja vode urađeno je na uzorcima dimenzija 12x12x36 cm, metodom postupnog potapanja. Rezultati ispitivanja upijanja vode nakon 28 dana prikazani su na grafiku 4.

Water absorption test was done on the samples of dimensions 12x12x36cm, by the method of gradual immersion. The test results for water absorption after 28 days are shown in Chart 4.



Grafik 4. Upijanje vode  
Chart 4. Water absorption

Ispitivanje vodonepropustljivosti rađeno je na uzorcima dimenzija 200x200x150 mm, pri starosti betona od 28 dana, u svemu prema SRPS U.M1.015:1998. Uzorci su 24 časa izloženi dejstvu vode pod pritiskom od 1 bara, sledećih 48 časova pritisku od 3 bara, i na kraju poslednja 24 časa ispitivanja, pritisku od 7 bara. Nakon ovoga se polome i meri se dubina prodora vode. Kod uzoraka s krečnjakom i silikatnom prašinom, zabeležen je prodor vode od oko 2 cm, dok je kod uzoraka s pepelom prodor vode iznosio 8-10 cm.

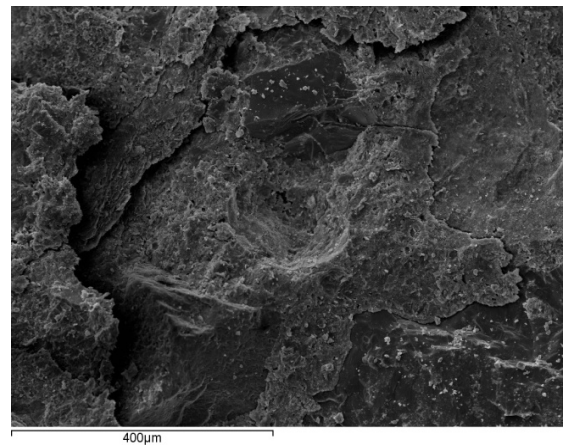
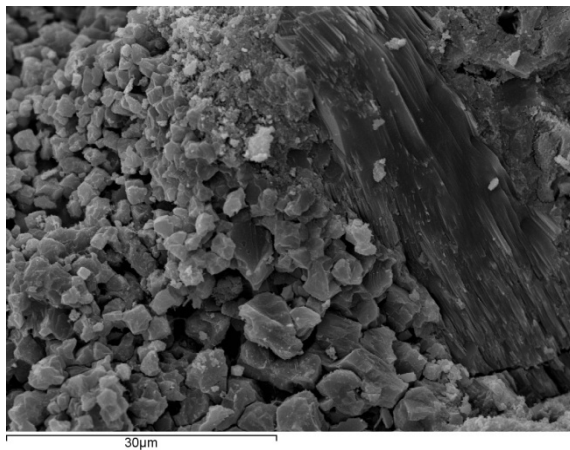
Water permeability testing was done on the samples of dimensions 200x200x150mm, in concrete at an age of 28 days, all in accordance with SRPS U.M1.015:1998. The samples were exposed to water under pressure of 1 bar for 24 hours; then the following 48 hours of 3 bars and finally, the last 24 hours of testing, under pressure of 7 bars. After this, they were broken and the depth of water ingress is measured. With the samples with lime and silica fume, ingress of water of about 2cm was recorded, while with the samples with fly ash, ingress of water was 8-10 cm.



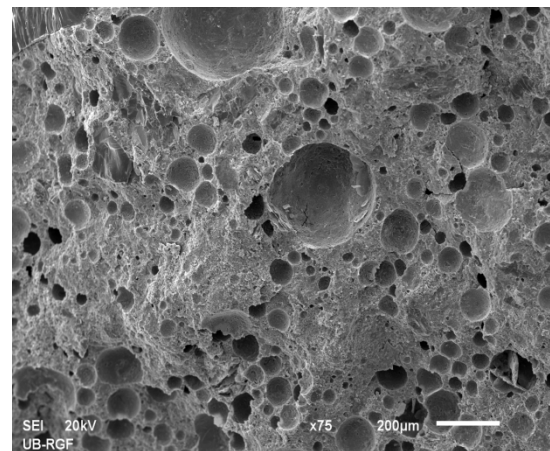
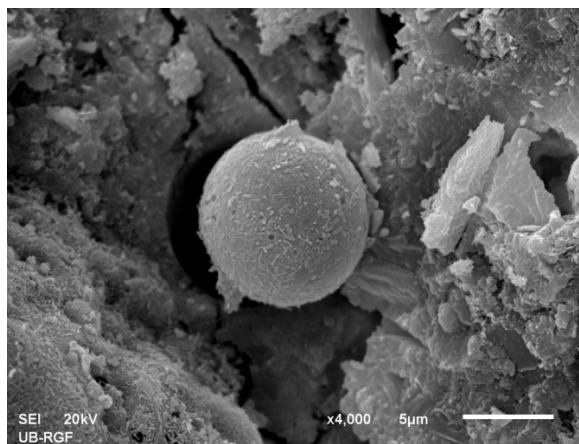
*Slika 4. Ispitivanje vodonepropustljivosti*  
*Figure 4. Waterpermeability testing*

Skenirajuća elektronska mikroskopija (SEM analiza) omogućava da se „zaviri“ u strukturu spravljenih betona i bolje objasne rezultati koji su dobijeni ispitivanjima (slike 5-7).

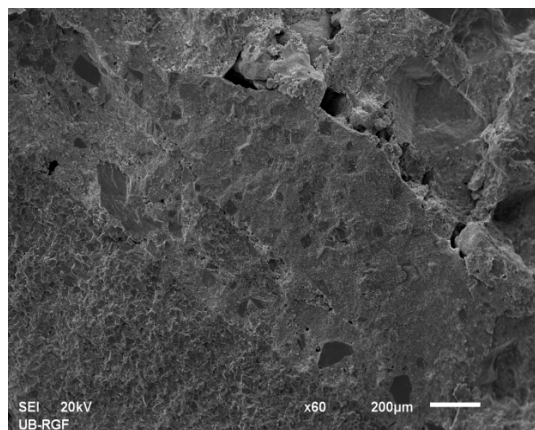
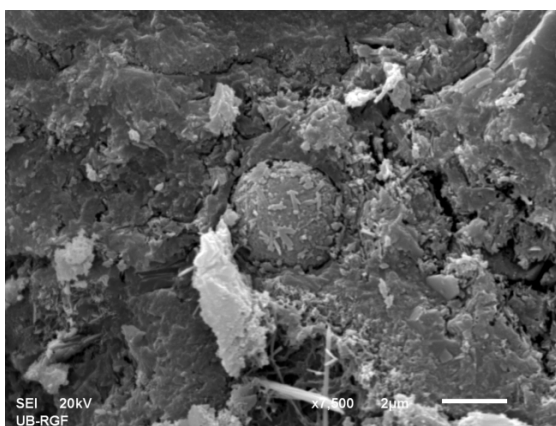
Scanning electron microscopy (SEM analysis) enables to “look into” the structure of concrete made and to better explain the results obtained by testing (Figures 5-7).



*Slika 5. Mikrostruktura betona s mlevenim krečnjakom*  
*Figure 5. Microstructure of the concrete with lime*



*Slika 6. Mikrostruktura betona sa elektrofilterskim pepelom*  
*Figure 6. Microstructure of the concrete with fly ash*



Slika 7. Mikrostruktura betona sa silikatnom prašinom  
Figure 7. Microstructure of the concrete with silica fume

## 6 ANALIZA REZULTATA

Rasprostiranje svežeg betona iznosilo je od 66 do 73 cm, što sve projektovane mešavine svrstava u klasu SF2, koja odgovara najčešćoj primeni betona u građevinarstvu. Najmanju pokretljivost imale su betonske mešavine sa silikatnom prašinom, kao i mešavine s recikliranim agregatom, jer je oštrovično zrno ovog agregata teže „pomeriti” prilikom razlivanja betona. Najveće rasprostiranje izmereno je kod etalona s krečnjakom - 73 cm, a najmanje kod etalona sa silikatnom prašinom, mešavine sa silikatnom prašinom i krupnim recikliranim agregatom i mešavine s pepelom i krupnim recikliranim agregatom - 66 cm.

$T_{500}$  je vreme za koje beton dostigne 500 mm, a meri se prilikom izvođenja slump-flow testa. Predstavlja proveru viskoznosti mešavine; za klasu SF2 preporučuje se interval od 3.5 do 6.0 s, u koji se sve mešavine „uklapaju”. Rezultati su u opsegu od 4 do 6 s, pri čemu su najsporije bile betonske mešavine sa silikatnom prašinom. Vreme duže od 2 s svrstava ih u klasu viskoznosti VS2.

Sve mešavine zadovoljavaju kriterijum da odnos visina betona na krajevima L-boxa bude najmanje 0.8, a kako je ispitivanje rađeno s tri armaturne šipke (što je i zahtev za gušće armirane konstrukcije), njihova klasa je PA2 (engl. passing ability = sposobnost prolaza). Rezultati testa kreću se u opsegu 0.91 – 1.0, pri čemu su najbolje rezultate (najbliže 1.0) postigle mešavine s krečnjakom. Najveća razlika na krajevima L box-a izmerena je kod mešavina sa silikatnom prašinom, što je i logična posledica njihovog najmanjeg rasprostiranja. Ni u jednom slučaju nije zabeleženo zaglavljivanje zrna agregata između šipki armature.

Test na situ pokazao je da su sve mešavine otporne na segregaciju i pripadaju klasi SR2 (<15%), pri čemu veće rasprostiranje znači manju otpornost na segregaciju.

Najveću zapreminsku masu u svežem stanju imao je etalon s krečnjakom  $2418 \text{ kg/m}^3$ , gotovo istu kao i etalon sa silikatnom prašinom ( $2416 \text{ kg/m}^3$ , tj. za 0.08% manju), dok je najmanja zapreminska masa određena kod mešavine P50 (pepeo i reciklirana III frakcija)  $2279 \text{ kg/m}^3$  za 5.7% manja. Uopšte, mešavine s pepelom imale su najmanje zapreminske mase, oko  $70 \text{ kg/m}^3$

## 6 THE RESULTS ANALYSIS

Fresh concrete was spread from 66 to 73cm which designed mixes of class SF2 which fits in most common use of concrete in construction. Mixes with silica fume had the slightest mobility, as well as mixes with recycled aggregate, because grains with sharp edges were more difficult to "move" while levelling concrete. The largest spreading was recorded in control concrete with lime - 73cm, and the smallest in control concrete with silica fume, in mixes with silica fume and coarse recycled aggregate, and in mixes with fly ash and coarse recycled aggregate - 66.

$T_{500}$  is the time that concrete reaches 500mm, and it is measured when doing slump-flow test. It represents a check of viscosity of the mix; the recommended interval for class SF2 is from 3.5 to 6.0s, and all mixes "fit" into it. The results are in the range of 4 – 6s, wherein concrete mixes with silica fume were the slowest. Time longer than 2s puts them in viscosity class VS2.

All mixes meet the criterion that height ratio of concrete at the ends of L-box is at least 0.8 and their class is PA2 as the testing was done with three reinforcement rods which is a requirement for thicker reinforced construction. The test scores are in the range of 0.91 – 1.0, wherein mixes with lime achieved the best results (nearest to 1.0). The biggest difference at the ends of L box was measured in mixes with silica fume, which is a logical consequence of its minimum spreading. Blocking of aggregate grains between reinforcement rods was not recorded in any case.

Sieve test shows that all mixes are resistant to segregation and they belong to class SR2 (<15%), while larger spreading means lower resistance to segregation.

Control concrete with lime had the highest density in the fresh state,  $2418 \text{ kg/m}^3$ , nearly the same as the control concrete with silica fume ( $2416 \text{ kg/m}^3$ , i.e. 0.08 lower), while minimum density was found in the mix P50 (fly ash and recycled III fraction)  $2279 \text{ kg/m}^3$ , 5.7% lower. Generally speaking, mixes with fly ash had the lowest density, about  $70 \text{ kg/m}^3$  lower, compared to the corresponding mixes with lime and silica fume.

While designing concrete mixes, in order to obtain the same consistency because of the use of recycled



manje u odnosu na odgovarajuće mešavine s krečnjakom i silikatnom prašinom.

Prilikom projektovanja sastava betonskih mešavina, a da bi se postigla ista konzistencija, zbog primene recikliranog agregata bilo je neophodno intervenisati u dva pravca: povećati količinu vode i smanjiti količinu III frakcije za 5%, istovremeno povećavajući količinu peska za 5%. Bez ovih intervencija u sastavu, nije bilo moguće postići samougradljivost mešavine, zbog oštrovičnog oblika zrna recikliranog agregata i samog granulometrijskog sastava (reciklirani agregat je imao 7% nadmerenih zrna). Najveća promena vodocementnog faktora bila je kod betonskih mešavina sa elektrofilterskim pepelom, pri istoj količini mineralnog dodatka (i svim ostalim komponentama), u etalon s pepelom je dodato 21.86 kg (12.8%) vode u odnosu na etalon s krečnjakom; u mešavinu sa III recikliranom frakcijom 31.42 kg (17.2%) u odnosu na odgovarajuću mešavinu s krečnjakom, a u mešavinu s recikliranom II i III frakcijom 31.5 kg (16.6%). Silikatna prašina ima mnogo sitnije čestice od krečnjaka i pepela, tako da je njeno doziranje bilo 52 kg/m<sup>3</sup> betona, tj. 13% mase cementa (uobičajena dozaža je 10–15%). U etalon sa silikatnom prašinom dodato je 14.91 kg (8.7%) vode u odnosu na etalon s krečnjakom, i po 14.28 kg (7.8%) i 19.1 kg (10.1%) u odnosu na mešavine s krečnjakom i recikliranim agregatom. Zahtevana klasa konzistencije postignuta je pri najmanjem vodocementnom faktoru kod mešavina s krečnjakom, dok je najviše vode bilo potrebno kod mešavina s pepelom. Najmanji vodocementni faktor zabeležen je kod etalona s krečnjakom – 0.43 (ujedno i najmanji vodopraškasti faktor – 0.33), a najveći kod mešavine s pepelom i obe krupne reciklirane frakcije – 0.55. Najveći vodopraškasti faktor imala je mešavina sa silikatnom prašinom i obe krupne reciklirane frakcije – 0.46. Treba napomenuti da su betonske mešavine s krečnjakom pri najmanjem sadržaju vode u odnosu na ostale mešavine imale najveće prečnike rasprostiranja i najbolja svojstva samougradljivosti.

Najveću zapreminsku masu u očvrslom stanju nakon dva dana imala je betonska mešavina etalon s krečnjakom, a najmanju etalon s pepelom (razlika 133.6 kg/m<sup>3</sup> tj. 5.6%). Ovaj trend se održao i nakon sedam dana s tim što je razlika iznosila 179.5 kg/m<sup>3</sup> (7.3%). Nakon 28 dana, etalon s krečnjakom imao je najveću zapreminsku masu, 2426.7 kg/m<sup>3</sup>, za 123.4 kg/m<sup>3</sup> (5.1%) veću od mešavine s pepelom i obe krupne reciklirane frakcije, i za 120.5 kg/m<sup>3</sup> (5%) veću od etalona s pepelom. Zapreminska masa u očvrslom stanju kod mešavina sa silikatnom prašinom kretala se od 2312 kg/m<sup>3</sup> (S100, dva dana) do 2366.4 kg/m<sup>3</sup> (ES, 28 dana); to su vrednosti „između” odgovarajućih kod krečnjaka i pepela. Treba imati u vidu da je za spravljanje betonskih mešavina korišćeno 52 kg silikatne prašine i po 120 kg mlevenog krečnjaka i pepela.

Najveću vrednost čvrstoće pri pritisku, nakon dva dana imao je etalon s krečnjakom, a najmanju mešavina s pepelom i obe krupne reciklirane frakcije – P100. Razlika je iznosila 19.8 MPa (43%). Nakon sedam dana, etalon s krečnjakom i silikatnom prašinom imali su gotovo iste čvrstoće (58 MPa), dok je mešavina P100 dostigla 40.18 MPa (razlika 17.82 MPa, tj. 30.7%). Nakon 28 dana, najveću vrednost čvrstoće dostigao je etalon sa silikatnom prašinom, 72.31 MPa, a najmanju mešavina P100, 47.2 MPa (razlika 25.11 MPa, tj.

aggregate, it was necessary to intervene in two directions: to increase the amount of water and to reduce the amount of III fraction by 5%, simultaneously increasing the amount of sand by 5%. Without these interventions in the composition, it was impossible to achieve self-compacting of mixes because of the sharp-edged grain shape of recycled aggregates and granulometric composition itself (recycled aggregate had 7% of oversized grains). The greatest change of the water-cement ratio was found in concrete mixes with fly ash; at the same amount of mineral additive (and all other components), 21.86 kg (12.8%) of water was added into the control concrete with fly ash compared to the control concrete with lime; in the mix with III recycled fraction 31.42 kg (17.2%) compared to the appropriate mix with lime and in the mix with I and III fraction 31.5 kg (16.6%). Silica fume has much smaller particles than lime and fly ash, so that its dosage was 52 kg/m<sup>3</sup> of concrete, i.e. 13% by the mass of cement (the usual dosage is 10 – 15%). We added 14.91 kg (8.7%) of water into the control concrete with silica fume compared to the control concrete with lime and 14.28 kg (7.8%) and 19.1 kg (10.11%) compared to mixes with lime and recycled aggregate. The required class of consistency was obtained at the lowest water-cement ratio in mixes with lime, while the highest amount of water was needed in mixes with fly ash. The lowest water-cement ratio was recorded in the control concrete with lime – 0.43 (at the same time the lowest water-cement ratio - 0.33), and the highest in mixes with fly ash and both two coarse recycled fractions – 0.46. It is necessary to point out that concrete mixes with lime, at the lowest content of water compared to other mixes, had the largest diameters of spreading and the best properties of self-compacting.

The highest density in the hardened state after two days was recorded in the control concrete with lime, and the lowest in the control concrete with fly ash (the difference 133.6 kg/m<sup>3</sup> i.e.5.6%). This trend was held even after 7 days excepting that the difference amounted 179.5 kg/m<sup>3</sup> (7.3%). After 28 days, control concrete with lime had the highest density, 2426.7 kg/m<sup>3</sup>, 123.4 kg/m<sup>3</sup> (5.1%) higher than the mix with fly ash and both two coarse recycled fractions, and 120.5 kg/m<sup>3</sup> (5%) higher than control concrete with fly ash. Density in the hardened state in mixes with silica fume ranged from 2312 kg/m<sup>3</sup> (S100, 2days) to 2366.4 kg/m<sup>3</sup> (ES, 28days); those are the values “between” the corresponding values in lime and fly ash. It should be borne in mind that, for making concrete mixes, we used 52 kg of silica fume and 120 kg of lime and 120 kg of fly ash.

The highest value of the compressive strength after 2 days was recorded in the control concrete with lime, and the lowest in the mix with fly ash and both two coarse recycled fractions – P100. The difference was 19.8 MPa (43%). After 7 days, control concrete with lime and control concrete with silica fume had nearly the same compressive strength (58MPa), while the mix P100 reached 40.18 MPa (the difference 17.82 MPa, i.e.30.7%). After 28 days, the highest value of strength was found in the control concrete with silica fume, 72.31 MP, and the lowest in the mix P100, 47.2 MPa (the difference 25.11 MPa, i.e. 34.7%). Considering mixes with lime, it can be concluded that the differences in the obtained strength, when using natural and recycled

34.7%). Posmatrajući mešavine s krečnjakom, može se zaključiti da su razlike u dostignutoj čvrstoći pri upotrebi prirodnog i recikliranog agregata relativno male, iznose 4.51 MPa (6.8%) i 6.38 MPa (9.6%) – poređenje etalona s mešavinama kod kojih je zamenjena jedna, odnosno obe krupne frakcije. Kod mešavina s pepelom razlika je 12.3 MPa (19.2%) i 16.8 MPa (26.2%). Veća razlika u čvrstoćama u okviru mešavina s pepelom može da se objasni neujednačenim kvalitetom recikliranog agregata, koji predstavlja glavni problem njegove primene. U grupi mešavina sa silikatnom prašinom, razlika između etalona i druge dve mešavine iznosila je 2.61 MPa (3.6%) i 7.81 MPa (10.8%). Najbrži priraštaj čvrstoće imale su mešavine sa silikatnom prašinom. Kod svih betonskih mešavina s rečnim agregatom zabeležen je lom po cementnoj pasti, dok je kod mešavina s recikliranim agregatom zabeležen lom po agregatu, bez obzira na vrstu mineralnog dodatka.

Razlike u rezultatima čvrstoće pri zatezanju savijanjem nisu velike. Vrednosti čvrstoće pri zatezanju u opsegu su od 7.97 MPa (P100) do 10.31 MPa (ES). Razlika između ovih vrednosti je 2.34 MPa (22.7%).

Dostupni podaci iz literature kao i lična prethodna istraživanja [2] pokazuju da je nezahvalno predviđati ili nalaziti neku zakonitost kada je skupljanje betona u pitanju. Obavljena merenja pokazuju da je najveće skupljanje imala betonska mešavina sa silikatnom prašinom i III recikliranom frakcijom, S50, a najmanje etalon s krečnjakom EK, pri čemu je razlika 56%. Ne može se izvući nikakva pravilnost u ovim rezultatima: mešavine sa III recikliranom frakcijom imale su veće skupljanje od mešavina sa II i III recikliranom frakcijom, pri čemu su razlike kod krečnjaka i silikatne prašine bile izraženije nego kod betona s pepelom. Ako se klasifikacija betona vrši prema mineralnom dodatku, najveće skupljanje imale su mešavine sa silikatnom prašinom; ukoliko je kriterijum agregat, među etalonima najveće skupljanje imao je etalon s pepelom (29% više od etalona s krečnjakom i 11.7% više od etalona sa silikatnom prašinom), među mešavinama sa III recikliranom frakcijom S50 (4.8% više od mešavina s krečnjakom i 22.8 % više od mešavina s pepelom), a među mešavinama sa II i III recikliranom frakcijom S100 (22.8% više od mešavina s krečnjakom i 13.2% više od mešavina s pepelom).

Upijanje vode kreće se u opsegu 0.85% (mešavina S50) do 2.12% (mešavina EP). Najveće upijanje vode imale su mešavine s pepelom, a najmanje mešavine sa silikatnom prašinom, što je potpuno u skladu sa ostvarenom strukturom betona, koja je, kako su SEM analize pokazale, bila najporoznija kod betonskih mešavina s pepelom. Prosečno upijanje vode kod mešavina sa silikatnom prašinom iznosilo je 0.9%, kod mešavina s mlevenim krečnjakom 1% , a kod mešavina s pepelom 2%.

Kod ispitivanja vodonepropustljivosti, prodor vode u beton s krečnjakom i silikatnom prašinom bio je veoma mali, oko 2 cm, tako da su ove mešavine praktično bile nepropustljive, dok je kod mešavina s pepelom zabeležen veći prodor vode, oko 10 cm, što je posledica povećane poroznosti ovih betona. Prema kriterijumu da prodor vode ne sme biti veći od 4 cm [4] betoni s letećim pepelom smatrali bi se propustljivim.

aggregate, are relatively small, 4.51 MPa (6.8%) and 6.38 MPa (9.6) – comparison of control concrete with mixes in which one or both coarse fractions are replaced. In mixes with fly ash, the difference is 12.3 MPa (19.2%) and 16.8 MPa (26.2%). Greater difference in strength among mixes with fly ash can be explained by the uneven quality of recycled aggregate, which represents a major problem of their application. In the group of mixes with silica fume, the difference between the control concrete mix and other two mixes was 2.61 MPa (3.6%) and 7.81 MPa (10.8%). The fastest increment of strength was found in mixes with silica fume. In all concrete mixes with natural aggregate, a failure was recorded through cement paste, while in mixes with recycled aggregate, the failure was found through aggregate, no matter which mineral additive was used.

Differences in the results of tensile strength by bending are not great. The values of strength by bending are in the range of 7.97 MPa (P100) to 10.31 MPa (ES). The difference between these values is 2.34 MPa (22.7%).

Available data from the literature, like my own previous researches [2] show that it is difficult to predict or find regularities when shrinkage of concrete is in question. The measurements done show that the largest shrinkage was found in the concrete mix with silica fume and III recycled fraction, S50, and the smallest in the control concrete with lime EK, wherein the difference is 56%. No regularities can be drawn from these results: mixes with III recycled fraction had greater shrinkage than mixes with II and III recycled fraction, wherein differences in lime and silica fume were more pronounced than in concrete with fly ash. If classification of concrete is done according to the mineral additive, the largest shrinkage was found in mixes with silica fume; if the criterion is aggregate, the largest shrinkage among control concrete mixes, was found in the control concrete with fly ash (29% more than in the control concrete with lime and 11.7% more than in the control concrete with silica fume); among mixes with III recycled fraction S50 (4.8% more than in mixes with lime and 22.8% more than in mixes with fly ash), and among mixes with II and III recycled fraction S100 (22.8% more than in mixes with lime and 13.2% more than in mixes with fly ash).

Water absorption is in the range of 0.85% (mix S50) to 2.12% (mix EP). The highest water absorption was recorded in the mixes with fly ash, and the lowest in the mixes with silica fume, which is absolutely in accordance with the achieved concrete structure, which was, according to SEM analyses, the most porous in concrete mixes with fly ash. Average water absorption in mixes with silica fume was 0.9%, in mixes with lime 1%, and in mixes with fly ash 2%.

When testing water impermeability, the ingress of water into the concrete with lime and silica fume, was very small, about 2cm, so as these mixes were practically impermeable, while in the mixes with fly ash, larger ingress of water was noted, about 10cm, which is the consequence of the increasing porosity of these concretes and, according to the criterion, that penetration of water must not be larger than 4cm [4], concretes with fly ash can be considered permeable.

## 7 ZAKLJUČCI

Na osobine svežeg samougrađujućeg betona utiču i vrsta mineralnog dodatka i vrsta primenjenog agregata. Najbolja svojstva samougradljivosti postižu se upotrebom mlevenog krečnjaka. Ovi betoni su imali najbolju fluidnost, viskoznost, nakon prolaska kroz armaturu bili su potpuno horizontalni, ali se zbog najvećeg rasprostiranja kod njih javila najmanja otpornost na segregaciju. Mešavine s pepelom imale su najbolji odnos prečnika rasprostiranja (fluidnosti) i otpornosti na segregaciju. Zbog toga što su veoma sitne (oko 100 puta sitnije od zrna cementa ili pepela) s jako velikom površinom zrna ( $15000\text{--}20000\text{ m}^2/\text{kg}$ ), čestice silikatne prašine značajno povećavaju koheziju betona i nepovoljno utiču na samougradljivost svežeg betona. Mešavine sa silikatnom prašinom bile su teško pokretne, imale najmanje prečnike rasprostiranja, ali i najveću otpornost na segregaciju. Primena recikliranog agregata, zbog oštroičnog oblika zrna koji povećava trenje, takođe nepovoljno utiče na svojstva samougradljivosti betona, te je bilo neophodno intervenisati u smislu smanjenja III odnosno povećanja I frakcije za 5%, kako bi se postigla željena konzistencija.

Uticao silikatne prašine na čvrstoću betona pri pritisku: silikatna prašina je pucolan i za njeno aktiviranje neophodno je prisustvo kalcijum-hidroksida. On nastaje u procesu hidratacije cementa tako da silikatna prašina može da se aktivira tek kada cement počne da reaguje. Kako beton počinje da vezuje i očvršćava, pucolanska aktivnost silikatne prašine postaje dominantna reakcija. Zbog veće specifične površine i višeg sadržaja silicijum-dioksida, silikatna prašina je mnogo reaktivnija od letećeg pepela. Ova pojačana reaktivnost prvobitno će znatno pojačati brzinu hidratacije  $\text{C}_3\text{S}$  frakcije cementa, ali se nakon dva dana proces normalizuje. Kako silikatna prašina reaguje i stvara hidrate kalcijum-silikata, šupljine i pore u betonu se popunjavaju, pri čemu nastali kristali povezuju prostor između čestica cementa i zrna agregata. Ako se ovom efektu doda i samo fizičko prisustvo silikatne prašine u mešavini, jasno je da će betonska matrica biti veoma homogena i gusta, a rezultat će biti poboljšana čvrstoća i nepropusnost, što se i jasno vidi na SEM slikama. Pored ovoga, zbog svoje veličine, čestice silikatne površine mogu da izazovu i „mikrofiler“ efekat, dodatno popunjavajuću tranzitnu zonu u betonu.

Uticao letećeg pepela na čvrstoću betona pri pritisku: kada se leteći pepeo doda betonu, počinje pucolanska reakcija između silicijum-dioksida ( $\text{SiO}_2$ ) i kalcijum-hidroksida ( $\text{Ca}(\text{OH})_2$ ) ili kreča, koji je nusprodukt hidratacije Portland cementa. Slaba pucolanska reakcija odvija se tokom prvih 24 sata na  $20^\circ\text{C}$ . Zbog toga se za datu količinu cementa, s povećanjem sadržaja letećeg pepela postižu niže rane čvrstoće. Prisustvo letećeg pepela usporava reakciju alita u okviru Portland cementa u ranom stadijumu. Međutim, produkcija alita kasnije se ubrzava zahvaljujući stvaranju jezgara hidratacije na površini čestica letećeg pepela. Kalcijum- hidroksid utiskuje se na površinu staklastih čestica, reagujući sa  $\text{SiO}_2$  ili  $\text{Al}_2\text{O}_3\text{-SiO}_2$  rešetkom. Sporiji priraštaj čvrstoće betona s letećim pepelom onemogućava njegovu primenu tamo gde se očekuju velike rane čvrstoće, što se može rešiti primenom akceleratora. Dostupna literatura zbog ovog razloga upućuje na projektovanje i

## 7 CONCLUSIONS

Properties of self-compacting concrete are affected both by a kind of mineral additive and a kind of the applied aggregate. Best properties of self-compacting are achieved by using lime. These concrete mixes had the best fluidity and viscosity, after passing through reinforcement they were absolutely horizontal, but because of the largest spreading, they had minimum segregation resistance. Mixes with fly ash had the best ratio of diameter of spreading (fluidity) and segregation resistance. Since they are very small (about 100 times smaller than cement or ash grains), and have very large area of grain ( $15\ 000\text{ to }20\ 000\text{ m}^2/\text{kg}$ ), particles of silica fume significantly increase concrete cohesion and adversely affect the fresh concrete self-compacting. Use of recycled aggregates, due to a sharp-edged shape of grains which increases adhesion, also adversely affects the properties of self-compacting concrete, so it was necessary to intervene in the sense of reducing III or increasing I fraction by 5%, in order to achieve the desired consistency.

Effect of silica fume on the compressive strength of concrete: silica fume is pozzolan which is activated by calcium hydroxide. Calcium hydroxide is formed in the process of cement hydration so that silica fume can be activated only when cement begins to react. As concrete starts to bind and harden, pozzolanic activity of silica fume becomes the dominant reaction. Due to the high specific area and higher content of silicon dioxide, silica fume is much more reactive than fly ash. This increased reactivity will initially significantly intensify hydration rate of  $\text{C}_3\text{S}$  cement fraction, but after two days the process becomes normal. As silica fume reacts and forms calcium silicate hydrates, voids and pores in the concrete are filled, wherein crystals formed connect the space between cement particles and aggregate grains. If this effect is added by the physical presence of silica fume in the mix, it is clear that the concrete matrix will be very homogenous and dense, resulting in improved strength and impermeability, which is clearly seen in SEM pictures. Besides, owing to their size, silica fume particles can cause “micro filler” effect, additionally filling transit zone of concrete.

Effect of fly ash on the compressive strength of concrete: when fly ash is added to concrete, there is pozzolanic reaction between the silicon dioxide ( $\text{SiO}_2$ ) and calcium hydroxide ( $\text{Ca}(\text{OH})_2$ ) or lime, which is a by-product of hydration of Portland cement. Weak pozzolanic reaction occurs during the first 24 hours at a temperature of  $20^\circ\text{C}$ . That is why, for a given amount of cement, with increasing fly ash content, lower early compressive strength is achieved. The presence of fly ash slows the reaction of alite in Portland cement at an early stage. Meanwhile, production of alite later accelerates thanks to the creation of cores of hydration on the surface of fly ash particles. Calcium hydroxide is pressed in the surface of the glassy particles, reacting with  $\text{SiO}_2$  or  $\text{Al}_2\text{O}_3\text{-SiO}_2$  grid. Slower early strengths of concrete with fly ash prevent its application where high early strength is expected, which can be solved by using accelerator. Therefore, the available literature refers to the design and monitoring of the 90 day compressive strength of concrete. SEM analyses evidently show extremely spongy, i.e. porous structure of the concrete

praćenje 90-dnevne čvrstoće betona. SEM analize jasno pokazuju izuzetno sunderastu, tj. poroznu strukturu betona s letećim pepelom bez obzira na vrstu primenjenog agregata.

Utjecaj mlevenog krečnjaka na čvrstoću betona pri pritisku: SEM analize ukazuju na postojanje čestica krečnjaka u betonu i nakon 28 dana, a s druge strane, priraštaj dvodnevne čvrstoće potvrđuje da ove čestice predstavljaju jezgro za hidrataciju  $C_3S$  i  $C_2S$ , te tako ubrzavaju reakcije hidratacije, što ide u prilog tezi da je mleveni krečnjak hemijski inertan.

Razlike u čvrstoći pri pritisku između betona sa silikatnom prašinom i krečnjakom ne prelaze 10% pri istoj količini cementa, pri čemu je beton s krečnjakom imao bolje performanse u svežem stanju, što treba imati u vidu, posebno ako se uključi i ekonomski faktor.

Razlike u čvrstoći pri pritisku između betona s pepelom i betona sa silikatnom prašinom kreću se od 13% (kod etalona) do 37% kod betona s krupnim recikliranim agregatom, pri čemu betoni s pepelom imaju veću ekološku vrednost, jer rešavaju problem deponovanja ogromnih količina letećeg pepela.

Rezultati ispitivanja čvrstoće pri zatezanju savijanjem ujednačeni su i pokazuju da vrsta mineralnog dodatka i agregata ne utiče na vrednost ove čvrstoće.

Skupljanje u cementnoj pasti povećano je kada se koristi silikatna prašina, o čemu treba posebno voditi računa, što je u skladu s dostupnim literaturnim podacima. Ne može se utvrditi zakonitost skupljanja, niti izvesti neki uopšten zaključak, već se skupljanje kod svakog od ovih betona mora posebno i pažljivo pratiti.

Najmanje upijanje vode zabeleženo je kod betonskih mešavina sa silikatnom prašinom, a najveće kod betona s pepelom. Ipak, ova razlika nije previše velika (oko 1%) s obzirom na sunderastu građu betona s pepelom, što se može objasniti manjim sadržajem otvorenih pora veličine 1–10  $\mu m$ , kroz koje je najbrži transport vode, a što je opet u vezi s pucolanskom aktivnošću letećeg pepela da učestvuje u C-S-H formacijama i popunjava pore.

Svi betoni su imali dobru vodonepropustljivost osim mešavina s letećim pepelom, što je u skladu sa ostvarenom mikrostrukturom.

Velika eksploatacija prirodnog agregata ozbiljno je ugrozila rečne ekosisteme, tako da je na nekim mestima i zabranjena. Pored ovoga, sve veća udaljenost prirodnih nalazišta od mesta gradnje svakako utiče na cenu materijala. S druge strane, u urbanim sredinama postoje znatne količine betonskog otpada koji nastaje prilikom izgradnje ili rušenja starih objekata, te je izražen problem deponovanja ovakvog materijala. Razvijene, ekološki svesne zemlje, mnogo polažu na recikliranje sirovina i za odlaganje na deponije (koje oduzimaju korisno zemljište) naplaćuju novčane kazne. Drobljenjem betonskog otpada dobija se reciklirani agregat koji se može „vratiti” u proizvodnju.

Glavni problem primene recikliranog agregata jeste povećana poroznost koja je posledica postojanja zaostale stare cementne paste na zrnima agregata. Postojanje stare cementne paste osnovni je uzročnik neujednačenosti kvaliteta agregata i dovodi do smanjenja čvrstoće pri pritisku betona. Postoje postupci „čišćenja” agregata koji poskupljuju beton, ali treba imati u vidu ekološku korist njegove upotrebe.

with fly ash, no matter which aggregate is used.

The effect of lime on the compressive strength of concrete: SEM analyses show the presence of lime particles in concrete even after 28 days, and on the other hand, two day increment of strength confirms that these particles constitute the core for hydration  $C_3S$  and  $C_2S$ , so that they accelerate the reactions of hydration, which supports the thesis that lime is chemically inert.

Differences in compressive strength between concrete with silica fume and concrete with lime do not exceed 10% at the same quantities of cement, wherein concrete with lime had better performances in the fresh state, what should be borne in mind, particularly if the economic factor is included.

Differences in compressive strength between concrete with fly ash and concrete with silica fume are from 13% (in control concrete) to 37% in concrete with coarse recycled aggregate, wherein concrete mixes with fly ash have greater ecological value, because they solve the problem of depositing huge quantities of fly ash.

The test results of tensile strength by bending are uniform and show that type of mineral additive and aggregate fails to affect the value of this strength.

Shrinkage in the cement paste is increased when silica fume is used, which has to be taken into account, and it is in accordance with the data available from the literature. It is impossible to determine the legality of shrinkage or draw a general conclusion about it, but shrinkage of each of the concrete must be specifically and carefully monitored.

The lowest water absorption was recorded in concrete mixes with silica fume and the highest in mixes with fly ash. However, this difference is not too great (about 1%), due to the sponge-like composition of concrete with ash, which can be explained by the lower content of open pores of size 1 – 10  $\mu m$  through which water transport is the fastest, and which is again related to the pozzolanic activity of fly ash to participate in C-S-H formations and to fill pores.

All concrete mixes had good water impermeability except mixes with fly ash, which is in accordance with the achieved microstructure.

Great exploitation of natural aggregates has seriously endangered river ecosystems, so that it is in some places forbidden. Besides, long distances of natural deposits from building sites surely affect the price of materials. On the other hand, in urban areas, there are significant amounts of concrete waste generated during construction or demolition of old buildings, so there is a problem of depositing such material. Developed, ecologically conscious countries, invest a lot in the recycling of raw materials and they charge penalties for the waste disposal at landfills (that take away useful land). When crushing concrete waste, recycled aggregate is obtained and it can be “returned” to production.

The main problem of using recycled aggregate is its increased porosity, caused by the remained old cement paste on aggregate grains. This is the main reason for uneven quality of aggregates and it causes a decrease in the compressive strength of concrete. There are “cleaning” procedures that raise the price of concrete, but the environmental benefits should be borne in mind.

While designing concrete mixes, it is of great use to

Prilikom projektovanja betonskih mešavina, veoma je korisno poznavati poreklo recikliranog agregata - što je prvobitni beton bio kvalitetniji, to će i novospravljeni imati bolje karakteristike. Poželjno je i da agregat bude spravljen od betona iste marke, kako bi mu kvalitet bio što je moguće ujednačeniji.

Količina upotrebljenog recikliranog agregata ne utiče značajnije na vrednosti čvrstoće pri zatezanju savijanjem.

Količina recikliranog agregata utiče na upijanje vode tako što s povećanjem količine recikliranog agregata raste i procenat upijanja vode kao posledica veće poroznosti.

Samougrađujući betoni s recikliranim agregatom mogu biti vodonepropustljivi. Na ovu osobinu utiču kapilarna poroznost starog cementnog kamena zaostalog na agregatu, kao i kapilarna poroznost cementnog kamena novog betona. Ukoliko je agregat dobijen drobljenjem betona male poroznosti, vodonepropustljivost novog betona zavisiće od ostvarene strukture novog cementnog kamena.

Primenom sva tri ispitivana mineralna dodatka mogu se dobiti samougrađujući betoni visokih performansi. U tome prednjači silikatna prašina, ali ako se ima u vidu ekonomska i ekološka komponenta elektrofilterskog pepela, kao i relativno mala razlika u dobijenim rezultatima, pepeo neizostavno treba uzeti u obzir. Uz to, upotreba recikliranog agregata (uz pojačana ispitivanja) čini da ovakvi betoni s pravom ponesu naziv ekološki. Nedovoljna istraženost ovog područja otvara širok spektar mogućnosti za dalja ispitivanja u smislu varijacije količine cementa, kombinovanja različitih podataka i sličnog.

## ZAHVALNOST

U radu je prikazan deo istraživanja koje je pomoglo Ministarstvo za nauku i tehnološki razvoj Republike Srbije, u okviru tehnološkog projekta TR 36017 pod nazivom: Istraživanje mogućnosti primene otpadnih i recikliranih materijala u betonskim kompozitima, sa ocenom uticaja na životnu sredinu, u cilju promocije održivog građevinarstva u Srbiji.

## 8 LITERATURA REFERENCES

- [1] Bjegović D., Serdar M., Jelčić Rukavina M., Baričević A., Pezer M.: Mogućnost približavanja betonske industrije cirkularnom modelu kroz industrijsku simbiozu, Građevinski materijali i konstrukcije 57 (2014) 4, str. 31–42.
- [2] Despotović I.: Svojstva i tehnologija samougrađujućeg betona sa posebnim osvrtom na mogućnost upotrebe recikliranog agregata za njegovo spravljanje, magistarski rad, Građevinsko arhitektonski fakultet, Niš 2009.
- [3] Despotović I.: Uticaj različitih mineralnih podataka na osobine samougrađujućeg betona, doktorska disertacija, Građevinsko-arhitektonski fakultet, Niš 2015.
- [4] Gomez-Soberon J.: Porosity of recycled concrete with substitution of recycled concrete aggregate :An experimental study, Cement and Concrete Research 32 (2002), pp.1301– 1311.
- [5] Janssen G., Hendriks C.F.: Sustainable use of recycled materials in building construction, Advances in Building Technology, Volume 2 (2002), pp.1399–1407.
- [6] Jevtić D., Zakić D., Savić A.: Specifičnosti tehnologije spravljanja betona na bazi recikliranog agregata, Materijali i konstrukcije 52 (2009)1, str. 52–62.
- [7] Malešev M., Radonjanin V., Marinković S.: Recycled Concrete as Aggregate for Structural Concrete Production, Sustainability 2010, 2, str. 1204-1225, doi:10.3390/su2051204.

know the origin of a recycled aggregate – the more qualitative the original concrete was, the better characteristics the newly made concrete have. It is preferable that the aggregate is made of concrete of the same brand so that its quality will be as uniform as possible.

The values of tensile strength by bending are insignificantly affected by the amount of the recycled aggregate used.

The amount of recycled aggregate affects the absorption of water in the sense that with increasing the amounts of recycled aggregates, the percentage of water absorption is also increased, as a consequence of greater porosity.

Self-compacting concretes with recycled aggregates can be water impermeable. This property can be affected both by capillary porosity of the old cement stone remained on the aggregate, and capillary porosity of the cement stone of the new concrete. If the aggregate is obtained by crushing concrete of low porosity, water impermeability of the new concrete will depend on the achieved structure of the new cement stone.

Using all three tested mineral additives, high performance self-compacting concretes can be obtained. Silica fume is ahead, but having in mind economic and ecological component of fly ash, as well as relatively small difference in the obtained results, fly ash should necessarily be taken into account. Besides, the use of recycled aggregates (with increased testing) makes these concretes ecological rightly considered. Insufficient research in this area opens up a wide range of options for further testing, in terms of variations in the amount of cement, combining different additives, etc.

## ACKNOWLEDGEMENTS

The work reported in this paper is a part of the investigation within the research project TR 36017 "Utilization of by-products and recycled waste materials in concrete composites in the scope of sustainable construction development in Serbia: investigation and environmental assessment of possible applications", supported by the Ministry for Science and Technology, Republic of Serbia. This support is gratefully acknowledged.

- [8] Meyer C.: The greening of the concrete industry, *Cement & Concrete Composites* 31 (2009), pp. 601-605.
- [9] Murali G., Vivek Vardhan C.M., Rajan G., Janani G.J., Shifu Jajan N., Ramya sri R.: Experimental study on recycled aggregate concrete, *International Journal of Engineering Research and Applications (IJERA)*, ISSN: 2248-9622, Vol. 2, Issue 2, Mar-Apr 2012, pp.407-410.
- [10] Newman J., Chao B.S.: *Advanced concrete Technology*, Elsevier, 2003, p.280.
- [11] Radonjanin V., Malešev M., Marinković S.: Mogućnosti primene starog betona kao nove vrste agregata u savremenom građevinarstvu, *ZAŠTITA MATERIJALA* 51 (2010) broj 3, str. 178 – 188
- [12] Trumić M., Trumić M.: Uloga pripreme u reciklaži otpada i održivom razvoju Srbije, naziv monografije: Stanje i perspektive pripreme mineralnih sirovina u Srbiji, Izdavač: Inženjerska akademija Srbije, Beograd, (2011), str. 73-93.
- [13] Corinaldesi V., Moriconi G.: Influence of mineral additions on the performance of 100% recycled aggregate concrete, *Construction and Building Materials* 23 (2009), pp. 2869–2876.
- [14] [www.siliconsources.com](http://www.siliconsources.com)
- [15] [www.waste-environment.vin.bg.ac.rs](http://www.waste-environment.vin.bg.ac.rs)

## REZIME

### SVOJSTVA SAMOUGRAĐUJUĆEG BETONA SPRAVLJENOG S RECIKLIRANIM AGREGATOM I RAZLIČITIM MINERALNIM DODACIMA

Iva DESPOTOVIĆ

Po svojoj tehnologiji, samougrađujući beton nakon unošenja u oplatu ne zahteva vibriranje. Ugrađivanje ovog betona u svakom delu, ili u svakom uglu oplata, uključujući i njene teško pristupne delove, ostvaruje se bez ikakvih spoljnih sila, osim sile gravitacije, tj. njegove sopstvene težine. Ovakva svojstva postižu se dodavanjem betonu hemijskih dodataka superplastifikatora, najčešće u kombinaciji s novom vrstom aditiva za modifikaciju viskoziteta i/ili primenom određene količine finog mineralnog dodatka - praha. Moguće je koristiti različite mineralne dodatke, pri čemu upotreba onih koji predstavljaju industrijski nusprodukt (poput letećeg pepela) ima višestruke ekološke koristi.

Nedostatak prirodnog agregata u urbanim sredinama i sve veće rastojanje između nalazišta kvalitetnog prirodnog agregata i gradilišta, prisilili su graditelje da razmotre mogućnosti zamene prirodnog agregata recikliranim materijalima (građevinska keramika, zgura, beton i tako dalje). S druge strane, u urbanim sredinama često se javlja velika količina betonskog otpada čije uklanjanje i deponovanje predstavlja ekološki problem.

Predmet ovog rada je analiza svojstava i tehnologije samougrađujućeg betona s različitim mineralnim dodacima (mlevenim krečnjakom, letećim pepelom i silikatnom prašinom), prirodnim i recikliranim agregatom, pri čemu su pravljeni mešavine bez recikliranog agregata, s trećom recikliranom frakcijom i s drugom i trećom recikliranom frakcijom.

**Ključne reči:** samougrađujući beton, mleveni krečnjak, leteći pepeo, silikatna prašina, reciklirani agregat, ekološki aspekt

## SUMMARY

### PROPERTIES OF SELF-COMPACTING CONCRETE MADE OF RECYCLED AGGREGATES AND VARIOUS MINERAL ADDITIVES

Iva DESPOTOVIC

By its technology, Self-Compacting Concrete does not need compaction by vibration. Compaction of this concrete, in every part, or in every corner of the formwork, including its hardly available parts, is done without any external forces except its own weight. These properties are achieved by adding superplasticizers, commonly with new Viscosity Modification Admixtures, or/and determined amount of powders. It is possible to use different mineral additions, where the use of those which are industrial by-products (like fly ash) has multiple environmental benefits.

Lack of natural aggregate in urban areas and increasing distance between deposits of high-quality natural aggregate and building sites, forced building contractors to analyze possibility of replacing of natural aggregate with recycled materials (masonry, slag, concrete, etc.). On the other hand, huge amount of old concrete exists in urban areas and its removal and deposition is a big ecological problem.

Aim of this paper is analysis of properties and technology of Self-Compacting Concrete with different mineral additions (lime, fly ash and silica fume), natural and recycled aggregate, considering mixes without recycled aggregate, with third recycled fraction, and with second and third recycled fractions.

**Key words:** Self - Compacting Concrete, lime, fly ash, silica fume, recycled aggregate, ecological aspect

# KORISNI KONCEPTI U PRIMENI NOVE AUSTRIJSKE METODE ZA GRADNJU TUNELA (NATM)

## USEFUL CONCEPTS FOR APPLICATION OF NEW AUSTRIAN TUNNELLING METHOD IN TUNNEL CONSTRUCTION (NATM)

Vojkan JOVIČIĆ  
Jasmin BUČO  
Nermin ŠEHAGIĆ  
Alaga HUSIĆ

PREGLEDNI RAD  
REVIEW PAPER  
UDK: 624.191.1(436)  
doi: 10.5937/grmk1504021J

### UVOD

Tunele poznajemo kao podzemne prostore koji služe za transport ljudi i/ili materijala. Tunelske konstrukcije su rezultat specifične podzemne građevinske aktivnosti; izvode se iskopom stenske mase ili tla, pri čemu se statička ravnoteža obezbeđuje pomoću interakcije tunelske obloge i stenske mase odnosno tla oko tunela. Potporne mere za postizanje ravnoteže pri iskopu (primarna podgrada) obuhvataju tunelsku oblogu i različite oblike ojačanja stenske mase ili tla. Tuneli po pravilu imaju male dimenzije poprečnog preseka u odnosu na svoju dužinu, pri čemu niveleta tunela, osim u primeru hidrotehničkih tunela, ne odstupa bitnije od horizontale.

Upotreba NATM metode predstavljena je za tunele na autoputevima, koji imaju specifične dimenzije i zahteve u pogledu oblika. Na slici 1 prikazan je tipičan karakteristični poprečni presek autoputnog tunela bez podnožnog svoda. Dimenzije autoputnog tunela prilagođene su svetlom profilu približnih dimenzija 9,0 m x 5,5 m, pri čemu je visina tunela nad kotom nivelete približno 7 m. Ukupna površina iskopa ovakvog tunela kreće se od 85 m<sup>2</sup> za tunel bez podnožnog svoda do 100 m<sup>2</sup> za tunel s podnožnim svodom. Zaključci o primeni NATM metode u ovom članku primenjivi su na sve tunele pribli-

### INTRODUCTION

Tunnels are universally known as underground structures used for the transport of people and/or materials. Tunnel structures are the result of the specific underground engineering activity; they are excavated in the rock or soil mass and equilibrium is achieved within the interaction of tunnel lining and the rock mass or soil around the tunnel cavity. The support measures needed to reach the equilibrium during the excavation (primary support) encompass tunnel lining and the different support elements of rock mass or soil reinforcement. Tunnels are by rule elongated structures in which the vertical alignment, except in the case of hydro-technical tunnels, does not significantly deviate from horizontality.

The use of NATM is presented in the paper for the motorway tunnels, which have specific dimensions and the conditions with regard to their shape. The typical characteristic cross section of a two-lane motorway tunnel without invert is shown in Figure 1. The dimensions for the motorway tunnel are adapted to the required "profile of light" of approximate dimensions of 9,0m x 5,5m, wherein the free height of the tunnel is some 7m above the roadway. The total excavation surface of this tunnel is some 85m<sup>2</sup> if without the invert and some 100 m<sup>2</sup> for a tunnel with the invert. The con-

---

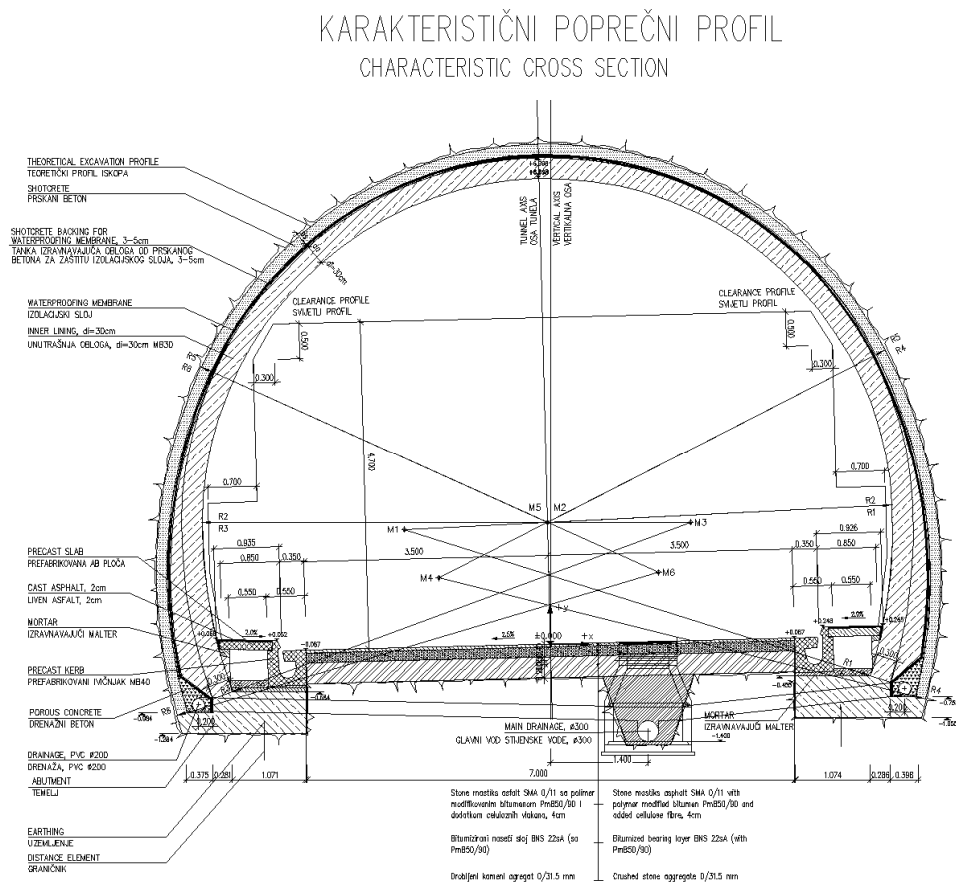
Vojkan Jovičić, IRGO – Institut za rudarstvo, geotehnologiju in okolje, Slovenčeva 93, 1000 Ljubljana, Slovenija  
Jasmin Bučo, JP Autoceste FBiH, Braće Fejića bb, 88000 Mostar, Bosna in Hercegovina  
Nermin Šehagić, PPG d.o.o, Hamdije Čemerlića 2/9, 71000 Sarajevo, Bosna in Hercegovina  
Alaga Husić, SAC T&C Paromlinska 53H, 71000 Sarajevo, Bosna in Hercegovina

---

Vojkan Jovicic, IRGO – Institut for Mining, Geotechnology and Environment, Slovenčeva 93, 1000 Ljubljana, Slovenia  
Jasmin Buco, JP Autoceste FBiH, Braće Fejića bb, 88000 Mostar, Bosna and Hercegovina  
Nermin Šehagic, PPG d.o.o, Hamdije Čemerlića 2/9, 71000 Sarajevo, Bosna and Hercegovina  
Alaga Husic, SAC T&C d.o.o Paromlinska 53H, 71000 Sarajevo, Bosna and Hercegovina

žnih dimenzija kao što su dimenzije tunela prikazanog na slici 1.

clusions about the application of the NATM method given in this paper are applicable to all tunnels of the approximate dimensions as given in Figure 1.



Slika 1. Karakteristični poprečni presjek autoputnog tunela  
Figure 1. Characteristic cross section of a highway tunnel

Tuneli na auto-putevima obično su kraći od dužine koja je rentabilna za gradnju s TBM strojem. Stoga, skoro u svim slučajevima gradnje tunela u regionu u posljednje dve decenije bila je izabrana NATM metoda odnosno SCL metoda (Sprayed Concrete Lining). Metoda SCL, to jest metoda upotrebe mlaznog betona za primarnu oblogu tunela, svakako je tehničko primerenije ime nego NATM. U literaturi se često nailazi na kritični odnos do uopštene upotrebe imena NATM, jer je mlazni beton najverovatnije bio prvi put primenjen za oblogu tunela u Australiji u tridesetim godinama prošlog veka. U našem regionu je izraz NATM odomaćen jer je shvaćen u širem smislu i zbog toga će biti korišćen u nastavku.

Osnovne koncepte NATM metode posle Drugog svetskog rata postavili su austrijski inženjeri Rabcewicz, Müller i Pacher (Golser, 1976), pri čemu je zanimljivo to što je metoda dobila svoje prve aplikacije tek u šezdesetim godinama prošlog veka u Venecueli. Metoda se pokazala kao ekonomski veoma efikasna, jer je osnovna ideja iskorišćavanje samonosivosti stenske mase. To uzrokuje manju potrebu za ugrađivanjem elemenata primarne podgrade i samim tim - ekonomičniju gradnju.

Very often, the motorway tunnels are shorter than what would be the economical tunnel length for the use of Tunnel Boring Machine (TBM). This was the reason that all the tunnels that were built in the region in the last two decades were constructed using the NATM method. This method is also known as the SCL (Sprayed Concrete Lining) method, which is technically more accurate use of terminology implying the utilisation of the shotcrete as the material for the tunnel primary lining. There is a lot of criticism for the overall use of the term NATM found in the literature as the first use of the shotcrete for the tunnel lining probably happened in the nineteen thirties in Australia. However, the term NATM is commonly used in our region in a wider sense and so it is preferred term used also in the continuation of this paper.

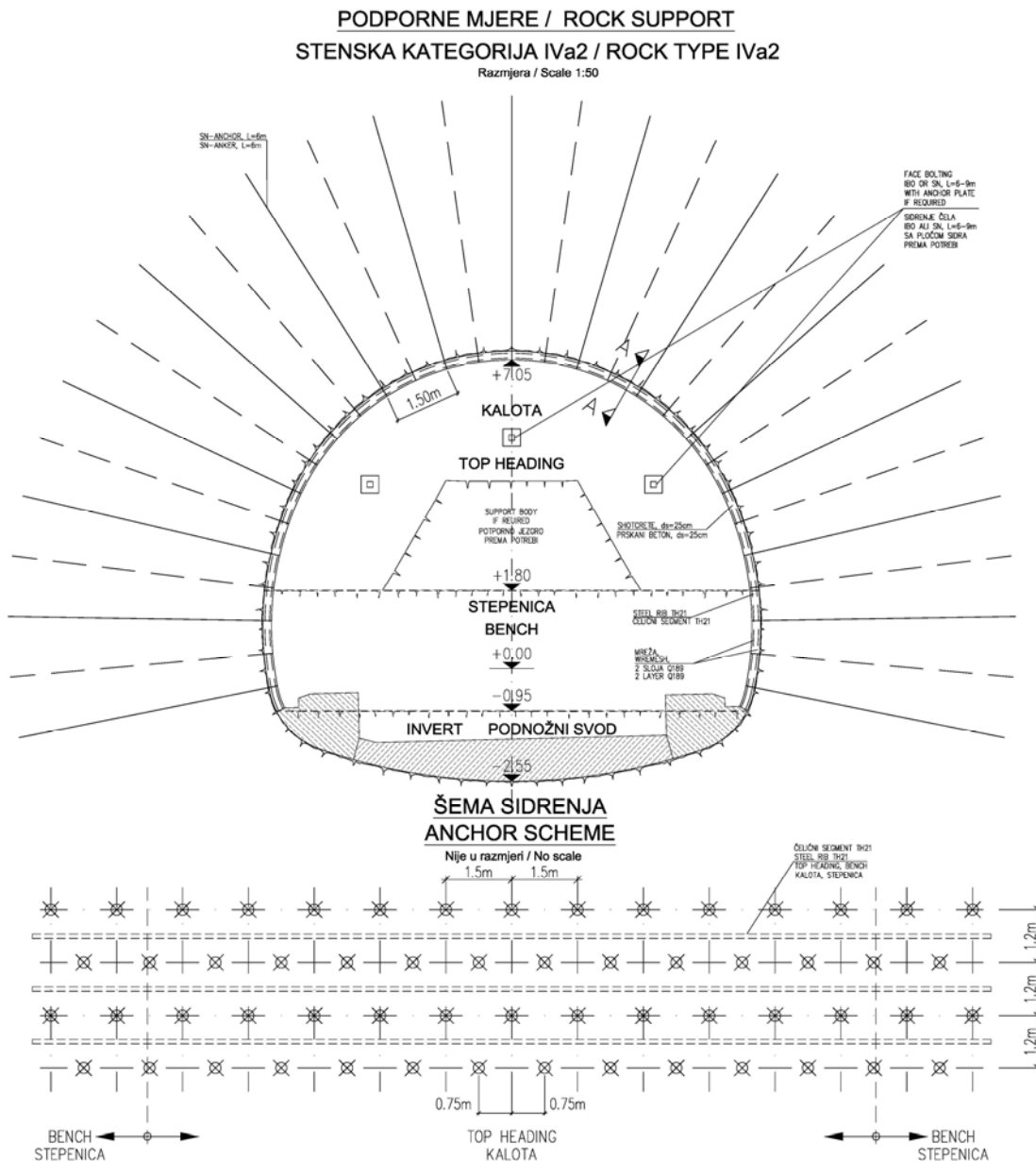
The basic concepts of the NATM method were laid out by Austrian engineers Rabcewicz, Müller and Pacher (Golser, 1976). It is interesting to note that the first application of this method was carried out in Venezuela in the nineteen sixties. The method was proven to be economically very efficient as the basic philosophy is based on the use the self-capacity of the rock mass, which reduces the need for the embedment of the man-



Elementi primarne podgrade, tipične za NATM, jesu: obloga od prskanog (mlaznog) betona i stenska sidra koja se ugrađuju radialno. U slabijim geološkim uslovima, obloga od mlaznog betona armirana je s čeličnim armaturnim mrežama i koriste se čelični lukovi za privremenu stabilizaciju iskopa. Alternativno, za određene geološke uslove može se uspješno koristiti primarna obloga od mikroarmiranog betona (Jovičić i dr., 2009). Za stabilizaciju čela iskopa koriste se i podgradni elementi u uzdužnom smeru, kao što su: koplja, sidra za stabilizaciju ugrađena u čelo iskopa (fiber-glass) i/ili cevni kišobran (pipe-roof). Na slici 2 prikazani su tipični elementi podgrade za NATM i njihov raspored u ravni tunela.

made elements of the primary support.

The typical elements of the primary lining in NATM are: a) the shotcrete lining and b) the rock bolts, which are installed radially. In the poorer geological conditions the shotcrete lining is reinforced with steel meshes and steel sets are used for the temporary support. Alternatively, in certain geological conditions a microfiber shotcrete can be used for the primary lining (Jovičić et al., 2009). The supporting elements in longitudinal direction typically used for stabilisation of the head of excavation comprise fibre-glass anchors and/or pipe roof, as appropriate. The typical elements of primary support in NATM are shown in Figure 2 including their layout in the plane of the tunnel.



Slika 2. Tipični elementi primarne podgrade za NATM  
Figure 2. Typical supporting elements for NATM

NATM možemo posmatrati kao filozofiju projektovanja tunela, zasnovanu na sledećim konceptima: a) nosivost stenske mase oko otvora tunela mobilise se do maksimalno mogućeg stepena; b) to se postiže kontrolisanim praćenjem radijalnih deformacija u tunelu i drugih pokazatelja stabilnosti iskopa; c) elementi primarne podgrade ugrađuju se u skladu s geološkim uslovima gradnje; d) napredovanje iskopa tunela sinhronizira se s vremenskom komponentom razvoja radijalnih deformacija.

U smislu metode izgradnje, za NATM je karakteristično sledeće: a) otvor tunela kopa se u sekvencama i obično je u poprečnom smeru podeljen na kalotu, stepenicu i podnožni svod (vidi sliku 2); b) sekvenca iskopa u uzdužnom smeru prilagođena je geološkim uslovima gradnje, pri čemu je ključni faktor prelaz iz trodimenzionalnih graničnih uslova - 3D (blizina čela iskopa) na dvodimenzionalne - 2D (udaljeno čelo iskopa); c) izbor i frekvencija ugradnje potpornih elemenata prilagođeni su geološkim uslovima gradnje. U nastavku su prikazane teorijske osnove metode NATM, koje čine osnovu za njenu adekvatnu primenu u praksi.

## TEORIJSKE OSNOVE ZA NATM

### Metoda Konvergencije-Relaksacije

Ciljevi rešavanja naponsko-deformacijskog problema tunelske konstrukcije jesu dokaz njegove stabilnosti i određivanje naponsko-deformacijskog odziva stenske mase. To se dobija na osnovu izračunavanja stanja napona, deformacija i pomeranja u stenskoj masi i primarnoj podgradi tunela koji odgovara konačnom ravnotežnom stanju koje zadovoljava uslove trajnosti.

Načelno, iskop tunela prolazi različite uslove gradnje, tako da sistem primarne podgrade mora tome biti prilagođen. Svrha statičkih proračuna jeste da dokažu stabilnost iskopa tunela u različitim geološkim uslovima i s različitim visinama nadsloja. Pri proračunu, treba imati u vidu to da iskop tunela izaziva relaksaciju početnih napona u stenskoj masi koja se zatim preraspodeli u interakciji između same stenske mase i podgrade. Ključni elementi podgrade tunela jesu pasivna stenska sidra (rock-bolts), koja se ugrađuju radijalno i koja obavljaju funkciju prenosa uticaja rasterećenja i omogućavaju mobilizaciju stenske mase u blizini otvora i po dubini.

U periodu građenja, naponsko-deformacijska analiza iskopa tunela trodimenzionalni (3D) je granični problem. Tada se javlja uticaj čela iskopa, na osnovu koga stenska masa u uzdužnom smeru ispred tunela preuzima i deo radijalnih opterećenja. Kada se čelo iskopa udalji dovoljno daleko od posmatranog poprečnog preseka, granični problem prelazi iz trodimenzionalnih (3D) uslova u dvodimenzionalne (2D) uslove ravnog stanja deformacije. Zbog toga se proračuni stabilnosti tunela u rutinskom projektovanju načelno rade primenom 2D modela za konačno stanje, pri čemu se posredno uvode 3D efekti - kao simulacija

The NATM can be understood as a design philosophy, which is based on the following concepts: a) the capacity of the rock-mass is mobilised to the highest degree, b) this is achieved by controlled monitoring of the convergence (radial) deformations and the other indicators during the excavation of the tunnel, c) the elements of primary support are installed with respect to the current geological conditions, d) the progress of the excavation and the primary support of the tunnel is synchronised with the time component of the development of the radial deformations.

From the point of view of the construction method, the NATM concepts are as follows: a) the tunnel cavity is excavated in sentences so that the cross section is usually divided into the top, the bench and the invert (see Figure 2), b) the sequence of excavation in longitudinal section is adapted to the geological conditions, wherein the key factor becomes the transition from 3D boundary conditions (near to the head of excavation) to the 2D boundary conditions (far from the head of excavation) and c) the selection and the frequency of the installation of the elements of the primary support are chosen according to the current geological conditions. The theoretical background of the NATM, which is the basis for its utilisation in practise, is shown in continuation.

## THEORETICAL BACKGROUND OF NATM

### Convergence – Confinement method

The aim of solving the stress-deformation problem of tunnel structure is the proof of stability and control of deformations. This is done by resolving the state of stresses, deformations and movements in the rock mass and the primary support of the tunnel for a particular cross section. The numerical analysis is carried out for the final equilibrium stage of the construction considering the long term performance and sustainability of tunnel structure.

In general, the excavation of the tunnel is traversing through different building conditions so that the primary support system must be fully adapted, as appropriate. The purpose of the static calculations is to prove the stability of tunnel excavation for different geological conditions and for different amounts of overburden. The excavation of the tunnel is causing the relaxation of the initial ground stresses, which is in turn redistributed within the interaction between the rock mass and the tunnel primary support. The key elements of the primary support are the rock bolts, which are installed radially, perpendicular to the direction of the excavation. The rock bolts are enabling the mobilisation of the rock mass in the vicinity of the cavity and enable the transfer of the relaxation load deeper into the rock mass of better capacity.

The stress-strain deformation analyses is a 3D (three dimensional) boundary value problem only in the time of tunnel excavation. During that time there is the presence of the head of excavation so that the load is taken by rock mass also in longitudinal direction ahead of the tunnel. When the head of excavation is moved further from the observed cross section, the boundary value

procesa gradnje.

Načelno, u okolini tunela razlikujemo tri naponska stanja odnosno tri zone (slika br. 3):

- Stanje pre iskopa

Zona 1 - Netaknuta stenska masa. Uticaj prirodno napregnute stenske mase u unutrašnjosti budućeg tunela statički je ekvivalentan srednjem početnom naponu ( $p = p_0$ )

• 3D stanje u kome se oseća uticaj blizine čela iskopa

Zona 2 - Čelo iskopa. Stanje posle iskopa i pre ugradnje podgrade, kontaktni napon na konturi jednak je nuli ( $p = 0$ ), deo opterećenja preuzima stenska masa ispred čela iskopa, granični problem je trodimenzionalan.

• 2D stanje u kome se ne oseća uticaj blizine čela iskopa

Zona 3 - Stabilizovan iskop. Stanje posle ugradnje podgrade je takvo da je uticaj podgrade statički ekvivalentan kontaktnom naponu na konturi -  $p$ ; granični problem je dvodimenzionalan.

problem is transferred from 3D conditions to 2D (two-dimensional) conditions of plane strain. This is the reason that the static calculations of tunnel stability are routinely carried out in 2D conditions, and the 3D effects and boundary conditions are taken indirectly into the account.

In this context, we differentiate three different stress conditions around the tunnel, that is three different zones shown in Figure 3:

- State before the excavation

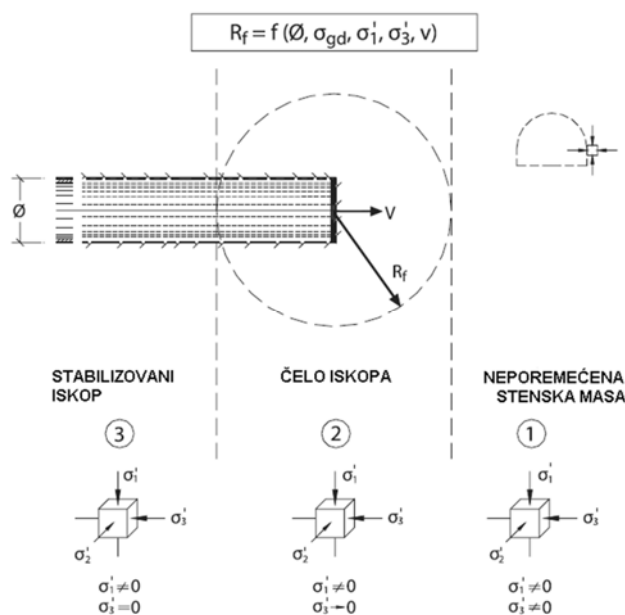
Zone 1 - Undisturbed Rock Mass. The influence of naturally stressed rock mass in the interior of future tunnel, which is equal to the in-situ mean effective stress, ( $p = p_0$ ).

• 3D state in which the proximity of the head of the excavation is felt

Zone 2 - Head of excavation. For the stress state after the excavation and before the installation of primary support the contact stress on the contour is equal zero ( $p = 0$ ), part of the loading is taken by the rock mass in front of the head of excavation, the boundary value problem is three-dimensional.

• 2D state in which the proximity of the head of excavation is not felt

Zone 3 - Stable excavation. State of excavation after installation of primary support is established so that influence of the support is statically equivalent to the contact stress on the contour, the boundary value problem is 2D.



Slika 3. Karakteristične zone stanja napona u toku etapnog iskopa tunela  
Figure 3. Characteristic stress state zones during the tunnel excavation

U savremenoj inženjerskoj praksi, granični problem interakcije stenske mase i podgrade tunela rešava se numeričkim putem i to najčešće primenom metode konačnih elemenata. Za dobijanje opšte slike o stabilnosti tunela i određivanja primerenih ulaznih podataka za numeričke analize potrebno je prethodno proveriti jednostavnije analitičke postupke koji imaju potvrđene teorijske osnove. Jedna od najkorisnijih metoda za tu svrhu jeste takozvana metoda Konvergen-

In contemporary engineering practice, solving boundary value problem of interaction of the rock mass and the tunnel support is usually performed by numerical methods; in particular the Finite Element Method is used most frequently. For the general picture on tunnel stability and for selection of appropriate input parameters it is necessary to check more simple analytical procedures, which have confirmed theoretical background. One of the most useful methods for this purpose is the

cije-Relaksacije (Convergence-Confinement Method), koja će ovde biti objašnjena u kratkim crtama.

Metoda Konvergencija-Relaksacije ima dvojni svrhu kada se koristi u sprezi s numeričkim analizama i to: a) za ocenu globalne stabilnosti tunela na pojedinačnim odsecima i b) za određivanje ulaznih parametara za numeričke analize, odnosno za posredno uvođenje 3D uticaja u 2D analizu.

Za rešavanje problema stabilnosti po metodi Konvergencija-Relaksacija potrebno je istovremeno analizirati: a) naprezanje na konturi tunela koje je rezultat relaksacije napona izazvanog iskopom tunela (Relaksacija) i b) radijalne deformacije i pomeranja konture tunelskog iskopa (Konvergencija). Osnovne proračunske pretpostavke metode Konvergencija-Relaksacija jesu sledeće: a) stenska masa se tretira kao izotropni kontinuum; b) granični problem je 2D; c) nadslonj je visok, odnosno tunel je dubok ( $H/D > 4$ ), gde je  $H$  visina nadslonja, a  $D$  je prečnik tunela; d) tunel je kružnog oblika ( $R$  je radijus tunela); e) važi ravno stanje deformacija nakon uspostavljanja 2D graničnih uslova; f) početno naponsko stanje je za  $k_0 = \sigma_h / \sigma_v = 1$ ; ( $\sigma_h$  – horizontalni napon je jednak  $\sigma_v$  – vertikalnom naponu). Iako prikazane pretpostavke predstavljaju umnogome idealizovane uslove koji se ne mogu naći u realnim tunelima, smatra se da su za potrebe određivanja globalne stabilnosti pri projektovanju autoputnih tunela načelno prihvatljive (autoputni tuneli s podnožnim svodom su jajasto-kružnog oblika s približnim poluprečnikom  $R=5,5m$ ; naponsko stanje u stenskoj masi, usled delovanja tektonskih sila, verovatno je blizu  $k_0=1$ ; stenska masa se može posmatrati kao kontinuum ukoliko uticaj diskontinuiteta nije dominantan, i dr.).

U smislu razvoja deformacija, ponašanje stenske mase u blizini iskopa tunela, opisano karakterističnom krivom relaksacije, prikazano je na slici 4.a. Usled relaksacije, naponi u stenskoj masi opadaju i javljaju se pomeranja na konturi. Naponi opadaju od vrednosti početnih napona  $\sigma_0$  do vrednosti 0, pri čemu se stenska masa odziva elastično do vrednosti  $p_i \geq p_{cr}$  odnosno plastično u slučaju da je relaksacija veća i da je  $p_i < p_{cr}$ , pri čemu je  $p$  srednja vrednost glavnih napona u stenskoj masi,  $p_i$  – stepen relaksacije napona i  $p_{cr}$  – granična vrednost.

Ponašanje podgrade definisano je karakterističnom krivom otpora podgrade (slika 4.b), pri čemu je uvedena pretpostavka njenog elastično-idealno plastičnog ponašanja. To znači da je u interakciji sa stenskom masom odziv podgrade, koja je instalirana pri pomeranju  $u_{in}$ , na početku linearno elastičan (koeficijent podgrade  $k_s$ ), a zatim pri dostizanju nosivosti odnosno maksimalne vrednosti  $p_{max}$  idealno plastičan.

Ravnoteža interakcije između primarne podgrade i stenske mase uspostavlja se kada karakteristična kriva podgrade preseče karakterističnu krivu stenske mase (slika 5) u tački s koordinatama  $p_{eq}$ ,  $u_{eq}$ , pri čemu je  $p_{eq}$  ekvivalentni napon i  $u_{eq}$  – odgovarajuće ekvivalentno pomeranje pri kome je uspostavljena ravnoteža.

Convergence-Confinement Method, which will be explained here in short form.

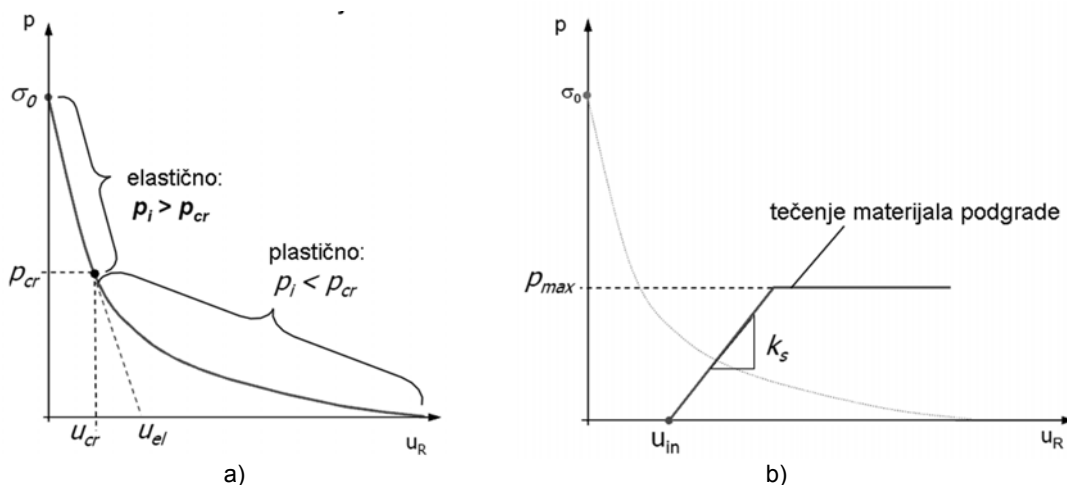
Convergence-Confinement Method has a double purpose in connection with the more advanced numerical analyses. It is used for: a) evaluation of global stability of the tunnels at particular sections and b) determination of input parameters for numerical analyses, in particular for the gradual integration of 3D effects into 2D analyses.

To provide with the solution using the Convergence-Confinement Method it is necessary to analyse in parallel: a) stresses on the contour of the tunnel, which are the result of the stress relaxation caused by excavation of the tunnel (Relaxation) and b) movements of the contour of the tunnel excavation caused by relaxation (Convergence). The main calculation assumptions of the Convergence-Confinement Method are: a) the rock mass is an isotropic continuum, b) the boundary value problem is 2D, c) the tunnel is deep ( $H/D > 4$ ),  $H$  is the height of overburden,  $D$  is the diameter of the tunnel d) the tunnel contour is of circular shape,  $R$  is tunnel radius, e) the plane strain deformation state is established for 2D boundary conditions and f) the in situ stress state is hydrostatic, that is  $k_0 = \sigma_h / \sigma_v = 1$ , where  $\sigma_h$  and  $\sigma_v$  are in situ horizontal and vertical stress, respectively. The given assumptions are idealisation of real circumstances. However, they are considered accurate enough for evaluation of global stability of a motorway tunnel (motorway tunnels with the invert are egg shaped but close to approximate circle with the radius of  $R=5,5m$ : the stress state in the rock mass is affected by the tectonic forces and is likely to be close to hydrostatic state with  $k_0=1$ , the rock mass can be regarded as continuum, if the discontinuities are relatively small to the dimensions of the tunnel, which is very often, etc)

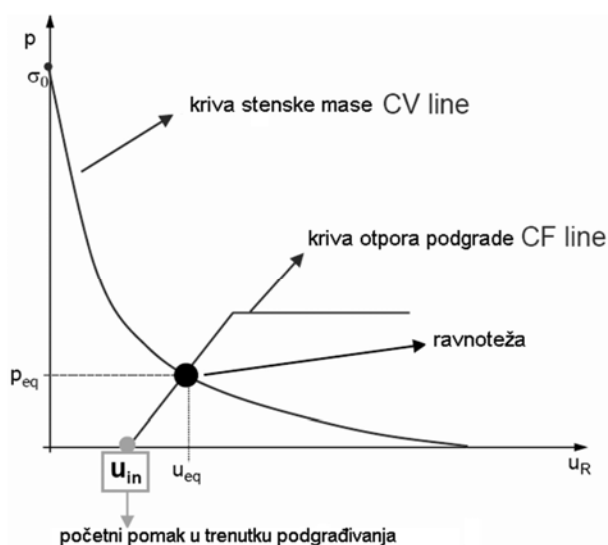
In terms of the deformation pattern the behaviour of the rock mass in the vicinity of the tunnel is described by the characteristic relaxation curve of the rock mass, which is shown in Figure 4a. The movements on the tunnel contour  $u$  are caused by relaxation of the stresses due to the excavation of the tunnel cavity. The stresses in the rock mass are decreasing from the in-situ values  $\sigma_0$  up to zero and the response of the rock mass is elastic within the region  $p_i > p_{cr}$  and plastic if the relaxation becomes larger than  $p_i \leq p_{cr}$ , where  $p_i$  is the amount of relaxed stress and  $p_{cr}$  is the boundary value.

The behaviour of the lining is defined with the characteristic curve of the lining resistance (Figure 4b), considering the assumptions that the behaviour is elastic-plastic. This means that the interaction between the rock mass and the lining (which is installed at the convergence movement  $u_{in}$ ) results in the firstly elastic response (the coefficient of lining stiffness response  $k_s$ ) and secondly, after the capacity of the lining is reached at  $p_{max}$ , in the ideally plastic response.

The equilibrium of interaction between the primary lining and the rock mass is established when the characteristic curve of the lining intersects relaxation curve of the rock mass (Figure 5) in the point with the coordinates  $p_{eq}$ ,  $u_{eq}$ , where  $p_{eq}$  is the equilibrium stress and the  $u_{eq}$  the equilibrium movement. The aim of the NATM method is to use most of the capacity of the rock mass and in the same time that there is enough reserve in the capacity of lining, as schematically presented in Figure 5.



Slika 4. Karakteristične krive odziva: a) stenske mase i b) podgrade na iskop tunela  
 Figure 4. Characteristic curves of: a) rock mass and b) tunnel support response to tunnel excavation



Slika 5. Tačka preseka krive stenske mase i krive otpora podgrade  
 Figure 5. Point of intersection for curves of rock mass and tunnel support

U smislu iskorišćenja nosivosti stenske mase, od ključnog značaja je dostizanje tačke ravnotežnog stanja, što je posledica interakcije stenske mase i primarne podgrade. U slučaju da se podgrada ugradi prekasno, može doći do tako velikih deformacija da se progresivni lom stenske mase ne može više sprečiti. Takođe, ako nosivost podgrade nije zadovoljavajuća, podgrada može dostići granicu izdržljivosti pre dostizanja ravnoteže. U oba slučaja, podgradna konstrukcija neće imati efekta, jer nije uspostavljeno ravnotežno stanje, te dolazi do rušenja u tunelu.

Trenutak postavljanja podgrade određuje se na osnovu uslova stabilnosti nepodgrađene stenske mase i tehnološkog ograničenja deformacije konture, s ciljem da ne dođe do nastanka potprofila. Inženjerski gledano, stanje konačne ravnoteže mora imati određeni faktor sigurnosti - kako u odnosu na nosivost podgrade, tako i u odnosu na nosivost stenske mase.

In terms of utilisation of the capacity of rock mass it is of key importance to achieve equilibrium on the optimal place, as a result of preferred interaction of the rock mass and the lining. If the lining is installed too late for a given schedule of excavation (i.e. too far from the head of excavation), there would be too much deformation of the rock mass and the progressive failure might occur. Also, if the lining is of insufficient capacity, it can collapse before the equilibrium point is ever reached. In both cases the supporting structure is without effect, as equilibrium will not be reached and the failure of the rock mass can occur.

The moment of the installation of the tunnel lining and the supporting elements is defined on the conditions of the stability of the unsupported tunnel and the technological limit of the amount of deformation for the tunnel contours so that the under-profile does not occur. From the engineering point of view, the state of the final equilibrium should have a certain factor of safety in terms of both the lining and the rock mass capacity.

## Dinamika gradnje: prelazak iz 3D graničnih uslova na 2D granične uslove

Cilj postupka metode Konvergencija-Relaksacija jeste određivanje uslova za pravovremenu ugradnju primarne podgrade koja ima zahtevanu nosivost, tako da se dostigne ravnoteža i s time zahtevana stabilnost tunela. Pritom, treba uzeti u obzir da inicijalni pomak stenske mase ( $u_{in}$ ), u trenutku postavljanja podgrade, zavisi od stepena relaksacije stene ( $\lambda$ ), koji je u funkciji transfera s 3D graničnih uslova na 2D granične uslove ravne deformacije. To je direktno povezano sa udaljenošću nepodgrađenog dela tunela od čela iskopa tunela. Pri gradnji tunela taj razmak manifestuje se kao korak u tehnološkoj sekvenci iskopa i primarnog podupiranja tunela.

Panet i Guénot (1982) modelirali su transfer s 3D graničnih uslova na 2D granične uslove ravne deformacije uvodeći fiktivni pritisak  $\sigma_r^f$  koji deluje unutar tunela. Vrednost fiktivnog pritiska određena je iz inicijalnog napona  $\sigma_r^o$  koristeći izraz:

$$\sigma_r^f = (1 - \lambda) \cdot \sigma_r^o \quad (1)$$

$$\lambda = 1 - \frac{p}{p_o} \Rightarrow p = p_o (1 - \lambda) \quad (2)$$

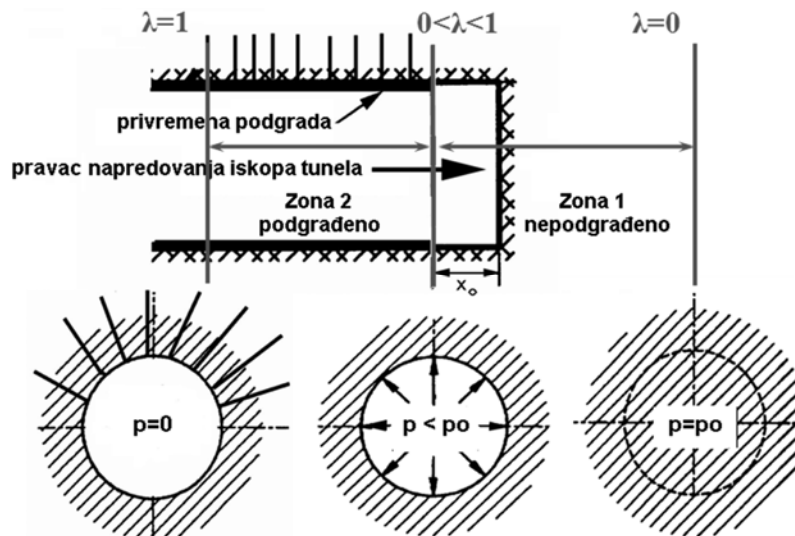
U gornjem izrazu,  $\lambda$  predstavlja koeficijent redukcije napona kojim uvodimo 3D efekte čela iskopa u 2D model proračuna tunela. Na određenoj udaljenosti ispred čela iskopa je  $\lambda=0$  (uslovi su potpuno 3D,  $\sigma_r^f = \sigma_r^o$ , odnosno  $p=p_o$ ), dok se ta vrednost povećava sve do  $\lambda=1$  (uslovi su potpuno 2D,  $\sigma_r^f = 0$  odnosno  $p=0$ ) na rastojanju od približno dva do tri prečnika tunela iza čela iskopa (slika 6).

## Schedule of construction: the transition from 3D to 2D boundary conditions

The aim of the application of Convergence-Confinement Method is the determination of the conditions for timely installation of the primary lining of required capacity, so that the equilibrium can be achieved and with this the required stability of tunnel excavation. In this sense it should be taken into account that the initial movement ( $u_{in}$ ) depends on the degree of the relaxation of the rock mass ( $\lambda$ ). The degree of the relaxation of the rock mass ( $\lambda$ ) is the function of transfer from the 3D boundary conditions to the 2D boundary conditions of plane strain, that is, the function of distance from supported part of the tunnel to the advancing head of excavation. This is seen in the technological sequence of tunnel construction as the one step of excavation and the primary support of the tunnel.

Panet and Guénot (1982) modelled the transfer from 3D to 2D boundary conditions by introducing the fictive supporting stress  $\sigma_r^f$  (Figure 6) acting within the tunnel cavity. The value of the fictive supporting stress is derived from the initial stress  $\sigma_r^o$  using the relationships:

in which  $\lambda$  is the coefficient of stress reduction. At a certain distance in front of the head of excavation  $\lambda=0$  (the conditions are fully 3D,  $\sigma_r^f = \sigma_r^o$ , that is  $p=p_o$ ), and this value increases up to  $\lambda=1$  (the conditions are fully 2D,  $\sigma_r^f = 0$ , that is  $p=0$ ). The 2D conditions are realised at the distance that is approximately 2 to 3 times the diameter  $D$  of the tunnel.



Slika 6. Model prelaza sa 3D graničnih uslova na 2D granične uslove ravne deformacije (Kavvadas 2004)  
Figure 6. Model of transition from 3D boundary conditions to 2D plain strain boundary conditions (Kavvadas, 2004)

Uvođenje prelaza s 3D graničnih uslova na 2D granične uslove stanja ravne deformacije u samom

The introduction of the transfer from 3D to 2D boundary conditions is done in three steps: (1)

postupku numeričke analize sprovodi se u tri faze, tako da se vrši: (1) evaluacija početnog stanja napona; (2) delimično uvođenje opterećenja izazvanog iskopom proporcionalno koeficijentu  $\lambda$ , da bi simulirali deformacije nastale pre podgrađivanja - (modeliranje 3D uslova); (3) aktivacija podgrade i uvođenje preostalog opterećenja proporcionalno vrednosti  $(1-\lambda)$  - (prelazak na 2D uslove). Ključnu ulogu pri modeliranju 3D efekta ima koeficijent  $\lambda$ . U nastavku će biti prikazane promjenljive od kojih koeficijent  $\lambda$  zavisi, kao načini i postupci za ocenu njegove vrednosti.

Panet je uzdužni raspored deformacija nepodgrađenog tunela opisao empirijskom kvadratnom funkcijom, koristeći se rezultatima analitičkog rešenja za problem osno-simetričnog modela tunela u elastičnoj steni (slika 7), što je analitički prikazano jednačinom:

$$\frac{u_r}{u_r^{\max}} = 0,25 + 0,75 \cdot \left[ 1 - \left( \frac{0,75}{0,75 + x/R} \right)^2 \right] \quad (3)$$

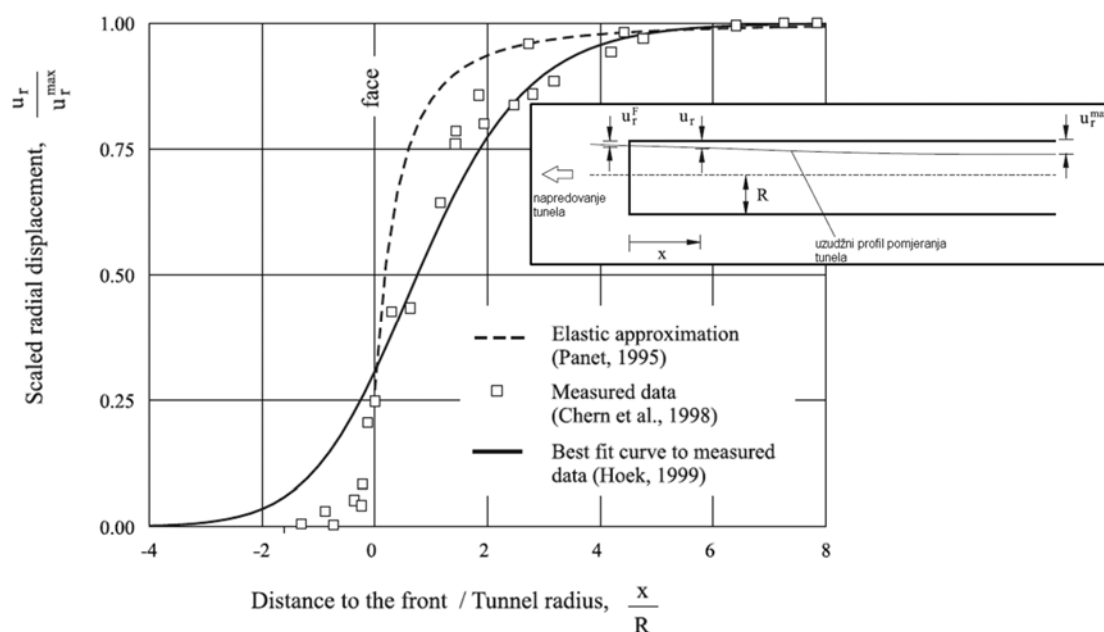
pri čemu je  $u_r$  konvergentno pomeranje na rastojanju  $x$  od čela iskopa,  $u_r^{\max}$  maksimalno konvergentno pomeranje za 2D granične uslove ravne deformacije;  $R$  je radijus tunela.

evaluation of the in-situ stresses, (2) partial introduction of the load caused by the relaxation of the in-situ stresses in proportion to coefficient  $\lambda$ , so that we simulate deformation occurred before the installation of the support system - (modelling of 3D conditions) and (3) activation of support and introduction of the rest of the relaxation load up to the full relaxation proportional to  $(1-\lambda)$  - (transfer to 2D conditions). The key role in modelling 3D effect is proper choice of the coefficient  $\lambda$ . The main variables that influence the value of  $\lambda$  and procedures for their determination will be shown in continuation.

Panet has described longitudinal distribution of the unsupported tunnel with an empirical quadratic function, using the closed form analytical solution for the problem of axi-symmetrical tunnel in elastic continuum (Figure 7) given in the following equation:

In which  $u_r$  is the convergence movement at distance  $x$  from the head of excavation,  $u_{r\max}$  is the maximum convergence movement for 2D boundary value conditions of plane strain;  $R$  is the radius of the tunnel.

$$\frac{u_r}{u_r^{\max}} = \left[ 1 + \exp\left(\frac{-x/R}{1,10}\right) \right]^{-1,7} \quad (4)$$



Slika 7. Uzdužni raspored radijalnog pomeranja nepodgrađenog tunela (prilagođeno za Hoek-om, 1999)  
Figure 7. Longitudinal distribution of radial displacements in unsupported tunnel (adapted after Hoek, 1999)

Na slici 7 takođe je prikazana empirijska kriva kojom je Hoek (1999) opisao uzdužni raspored deformacija nepodgrađenog tunela, koristeći terenske podatke i rezultate svojih numeričkih analiza. Hoek-ova empirijska kriva prikazana u jednačini 4 razlikuje se od Panet-ove, jer je predviđena za upotrebu pri manjoj nosivosti

The empirical curve derived by Hoek (1999), also presented in Figure 7, is given in equation 4. Hoek derived the curve using the in-situ measured data and the results of the back analyses. Hoek empirical curve is different from Panet's curve, and is more appropriate for the use for rock mass of low capacity, that is, in the case

stenske mase, odnosno u slučajevima kada je odziv stenske mase elasto-plastičan.

Iz gornje slike jasno je uočljivo da je odnos između  $u_r$  i  $u_{r,max}$ , odnosno dužina zone uticaja 3D efekta i brzina njegovog opadanja sa udaljavanjem od čela, zavisna od nosivosti stenske mase i nivoa opterećenja koje ona trpi zbog relaksacije napona izazvanog iskopom tunela. Nivo relaksacije napona direktno je proporcionalan visini nadsloja nad tunelom (relaksacija napona je veća za dublje i manja za pliće tunele).

## PRORAČUN KOEFICIJENTA STABILNOSTI $N_s$

Pri oceni uslova stabilnosti u tunelu, treba uzeti u obzir da su mogući različiti tipovi rušenja, u zavisnosti od dva vodeća kriterijuma: a) relativne veličine tunela u odnosu na veličinu blokova koji grade stensku masu; b) nosivosti stenske mase u odnosu na stepen rasterećenja, koji je izazvan iskopom tunela. Pri tome su moguća dva karakteristična mehanizma: a) diskretni mehanizam nestabilnosti (nestabilnost blokova); b) mehanizam nestabilnosti praćen razvojem deformacija koje su prethodno prikazane pomoću koncepta Konvergencije-Relaksacije.

Odnos između nosivosti stenske mase i stepena relaksacije jeste ključni faktor stabilnosti iskopa tunela za stenske mase umerene do male nosivosti. Taj odnos opisuje se pomoću parametra koji se imenuje kao faktor stabilnosti tunela  $N_s$ .

Faktor stabilnosti tunela  $N_s$  povezan je s dubinom na kojoj je pozicioniran tunel i na kvalitet odnosno nosivost stenske mase koja je obično prikazana pomoću njene jednoosne čvrstoće na pritisak. Odnos ove dve veličine - definisan vrednošću  $N_s$  - jeste pokazatelj stabilnosti naponsko-deformacijskog stanja u stenskoj masi u toku iskopa tunela. Faktor stabilnosti nepodgrađenog tunela definiše se relacijom:

$$N_s = \frac{2p_o}{\sigma_{cm}} \quad (5)$$

gde je,

$p_o = 1/3(\sigma_v + 2k_0\sigma_h)$  – srednja vrednost napona na dubini tunela;

$\sigma_{cm}$  - jednoosna čvrstoća stenske mase na pritisak.

Za određivanje vrednosti jednoosne čvrstoće stenske mase na pritisak  $\sigma_{cm}$  koristi se više različitih metoda. Na slici 8 prikazan je postupak (Hoek I dr., 2002) određivanja  $\sigma_{cm}$  pomoću takozvane GSI klasifikacije (Marinos in Hoek, 2001; Marinos in dr, 2011), pri čemu je  $\sigma_{ci}$  jednoosna čvrstoća na pritisak intaktnog uzorka stenske mase, koji se obično dobija iz laboratorijskih rezultata. GSI klasifikacija ima u vidu sve bitne elemente stanja diskontinuiteta u stenskoj masi (npr. veličinu, raspored, uslojenost, frekvencu, orijentaciju, zapunu).

when interaction of the rock mass and the lining lead to the response that is elastic-plastic.

It can be seen in Figure 7 that the relationship between  $u_r$  and  $u_{r,max}$  indirectly describes the length of the zone of influence of the 3D effect and also the gradient of its decrease with the advance of the head of excavation. This decrease is related to the capacity of the rock mass and the level of loading that is transferred to it due to the stress relaxation caused by the excavation of the tunnel. The amount of stress relaxation is directly proportional to the depth of the tunnel (i.e. the relaxation is smaller for a shallow tunnel).

## CALCULATION OF THE STABILITY COEFFICIENT $N_s$

The conditions of tunnel stability involve possibilities for different types of failure considering two criteria: a) size of the tunnel relative to the size of the blocks that form the rock mass and b) capacity of rock mass relative to the degree of stress relaxation caused by the tunnel excavation. In this sense the two governing mechanisms are possible: a) discrete type of failure mechanism (wedge instability) and b) mechanism of stability that is followed by development of deformation as previously described using the Convergence-Confinement Method.

The relationship between capacity of the rock mass and the degree of stress relaxation is key factor of stability of tunnel excavation. This relationship is described by using the parameter Factor of Tunnel Stability annotated  $N_s$ .

$N_s$  is directly related to the height of overburden ( $H$ ) and the bearing capacity of the rock mass. The ratio between those two values, defined as  $N_s$ , is the index indicator of stress-strain state, which can be expected in the rock mass after the excavation of the un-supported tunnel. Factor of Tunnel Stability  $N_s$  is defined as:

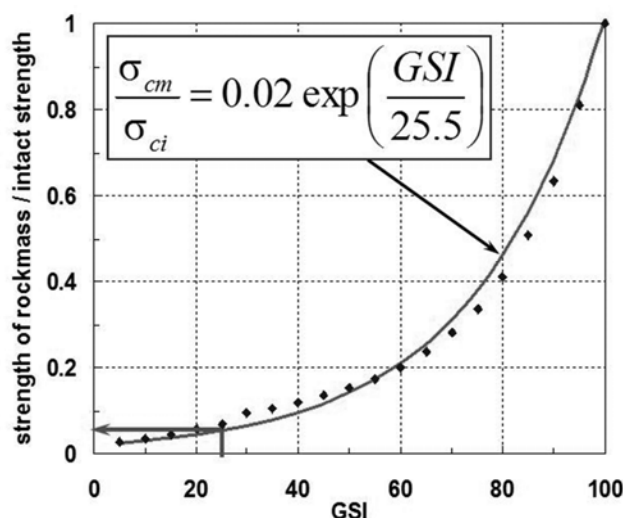
where,

$p_o = 1/3(\sigma_v + 2k_0\sigma_h)$  - mean effective stress at tunnel depth

$\sigma_{cm}$  - uniaxial strength of the rock mass domain.

Uniaxial strength of the rock mass domain  $\sigma_{cm}$  can be determined using several different methods. The procedure (Hoek et al., 2002), that is based on the GSI classification (Marinos and Hoek, 2001; Marinos et al., 2011) is shown in Figure 8, in which  $\sigma_{ci}$  is the uniaxial strength of the intact rock mass usually obtained from the laboratory tests. The GSI classification takes into account all the important aspects of the rock mass discontinuities in the observed rock mass domain (size, distribution, layering, frequency, orientation, filling and etc.)





Slika 8. Postupak određivanja vrednosti jednoosne čvrstoće stenske mase na pritisak  $\sigma_{cm}$  na osnovu klasifikacijskog indeksa stenske mase GSI i vrednosti za jednoosnu čvrstoću intaktno stene  $\sigma_{ci}$  (po Hoek i dr., 2002).  
 Figure 8. The method of determination of uniaxial strength of rock mass  $\sigma_{cm}$  based on the classification index of rock mass GSI and the value of uniaxial strength of intact rock mass  $\sigma_{ci}$  (after Hoek et.al, 2002)

Ukoliko je odziv stenske mase elastičan, vrednost faktora stabilnosti jeste  $N_s \leq 1$ . Za vrednosti faktora  $N_s > 1,0$  odziv stenske mase je elastoplastičan, odnosno deo stenske mase u najbližoj okolini nepodgrađenog tunela jeste plastificiran. Na slici 9 šematski je prikazana promena veličine i oblika plastificirane zone stene oko tunela (Kavvadas, 2004), zavisno od veličine  $N_s$ .

U primeru podgrađenog tunela, jedan deo opterećenja preuzima podgrada tunela, tako da dubina plastifikacije stenske mase zavisi i od nosivosti podgrade. U određenom smislu, 3D efekat stabilnosti čela u funkciji je smanjivanja dubine plastifikacije, odnosno ona se ne može u potpunosti realizovati dok se iskop čela ne udalji dovoljno od posmatranog poprečnog preseka. Na taj način, stepen relaksacije, brzina napredovanja i deo opterećenja koji preuzima podgrada tunela direktno su povezani.

Uticao podgrada tunela možemo prikazati kao interni pritisak  $p$  koji deluje u otvoru tunela, pri čemu je  $p_0$  početni pritisak. Za  $k_0 = \sigma_h / \sigma_v = 1$  stanje je stepen relaksacije:

$$p = (1 - \lambda) p_0 \quad (6)$$

Može se pokazati da za linearno-elastične uslove iskopa kružnog tunela u homogenoj i izotropnoj stenskoj masi važi:

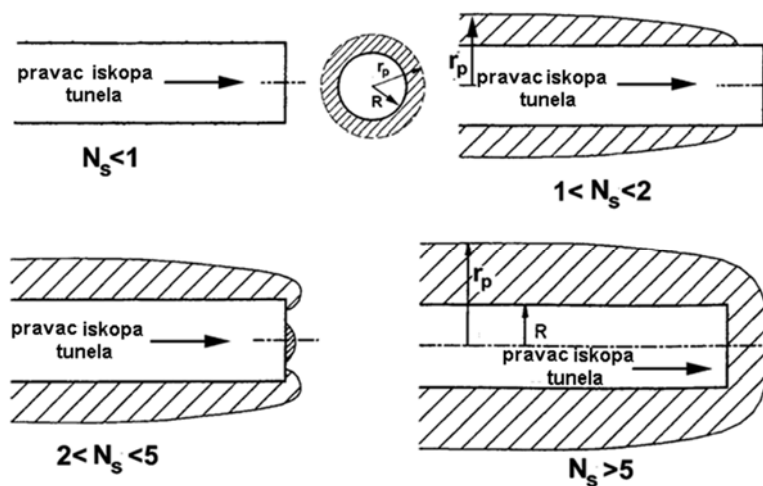
$$\sigma_\theta - \sigma_r = 2p_0 \lambda \quad (7)$$

In the case that the rock mass response is elastic, the value of  $N_s$  is less or equal one,  $N_s \leq 1$ . For the values of  $N_s > 1,0$  the rock mass responses is elastic-plastic, which means that certain amount of rock mass around the unsupported tunnel remains in plastic state. The change of the shape and the size of the plastic region around the tunnel with the change of  $N_s$  (Kavvadas, 2004) are schematically shown in Figure 9.

In the case of supported tunnel, one part of the relaxation load is taken by the supporting elements, so that the depth of the plastic zone around the tunnel is related to the capacity of the lining and the installed rock bolts. In a certain sense, the 3D effect of the stable head of excavation is in the function of the decrease of the depth of plasticization, which means that it cannot be fully materialised until head of excavation is not advanced enough from the observed cross section. By these means, the development of relaxation, the timing of the advancement and the part of the loading taken by the tunnel supporting system are directly correlated.

The influence of the tunnel lining can be presented as internal pressure  $p$ , which acts within the interior of the tunnel, where  $p_0$  represents the initial hydrostatic pressure. For the hydrostatic state  $k_0 = \sigma_h / \sigma_v = 1$ , the degree of relaxation is expressed as:

It can be shown that for linearly-elastic conditions the conditions of the tunnel excavation of the circular tunnel in homogeneous and isotropic rock mass is:



$$\frac{r_p}{R} = \left[ \left( \frac{2}{k+1} \right) \frac{N_s + \frac{2}{k-1}}{(1-\lambda)N_s + \frac{2}{k-1}} \right]^{\frac{1}{k-1}}$$

Slika 9. Veličina i oblik plastificirane zone oko nepodgrađenog tunela u zavisnosti od vrednosti  $N_s$  (Kavvadas, 2004),  $R$  - radijus tunela,  $r_p$  - radijus plastične zone oko tunela,  $k$  - koeficijent  $k = \text{tg}^2(45 + \varphi/2)$ ,  $\varphi$  - ugao smičuće otpornosti stenske mase.

Figure 9. The size and shape of plasticised zone around unsupported tunnel depending on value  $N_s$  (Kavvadas, 2004),  $R$  - tunnel radius,  $r_p$  - radius of plasticised zone around the tunnel,  $k$  - coefficient  $k = \text{tg}^2(45 + \varphi/2)$ ,  $\varphi$  - angle of shear resistance of the rock mass.

Pri čemu je  $\sigma_r$  radijalni i  $\sigma_\theta$  tangencijalni napon. Ukoliko je njihova razlika (devijator napona) veća od jednoaksijalne čvrstoće  $\sigma_{cm}$  dolazi do plastifikacije stenske mase. Iz prethodne jednačine vidi se da je to direktno zavisno od faktora relaksacije  $\lambda$ . To znači, postoji granična vrednost koeficijenta relaksacije  $\lambda = \lambda_{cr}$ , (Kavvadas, 2004), pri kojoj se stenska masa plastificira:

where is  $\sigma_r$  radial and  $\sigma_\theta$  tangential stress that acts in the rock mass around the cavity. The difference between  $\sigma_r$  radial and  $\sigma_\theta$  tangential stress is the deviator stress. If deviator stress is greater than uniaxial rock mass strength  $\sigma_{cm}$  plasticization around the tunnel cavity occurs. It can be seen that this is directly related to the degree of relaxation  $\lambda$ . This means that there is a certain value of the degree of relaxation  $\lambda = \lambda_{cr}$ , (Kavvadas, 2004) which will lead to the plasticization of the rock mass. This  $\lambda_{cr}$  can be calculated as:

$$\lambda_{cr} = 1 - \left( \frac{2}{1+k} \right) \left( \frac{N_s - 1}{N_s} \right) \quad (8)$$

gde je  $k = \text{tg}^2(45 + \varphi/2)$ ,  $\varphi$  je ugao smičuće otpornosti stenske mase.

where  $k = \text{tg}^2(45 + \varphi/2)$  and  $\varphi$  is the angle of shear resistance of the rock mass.

Iz toga sledi da je stenska masa oko tunela u elastičnom stanju ako je:

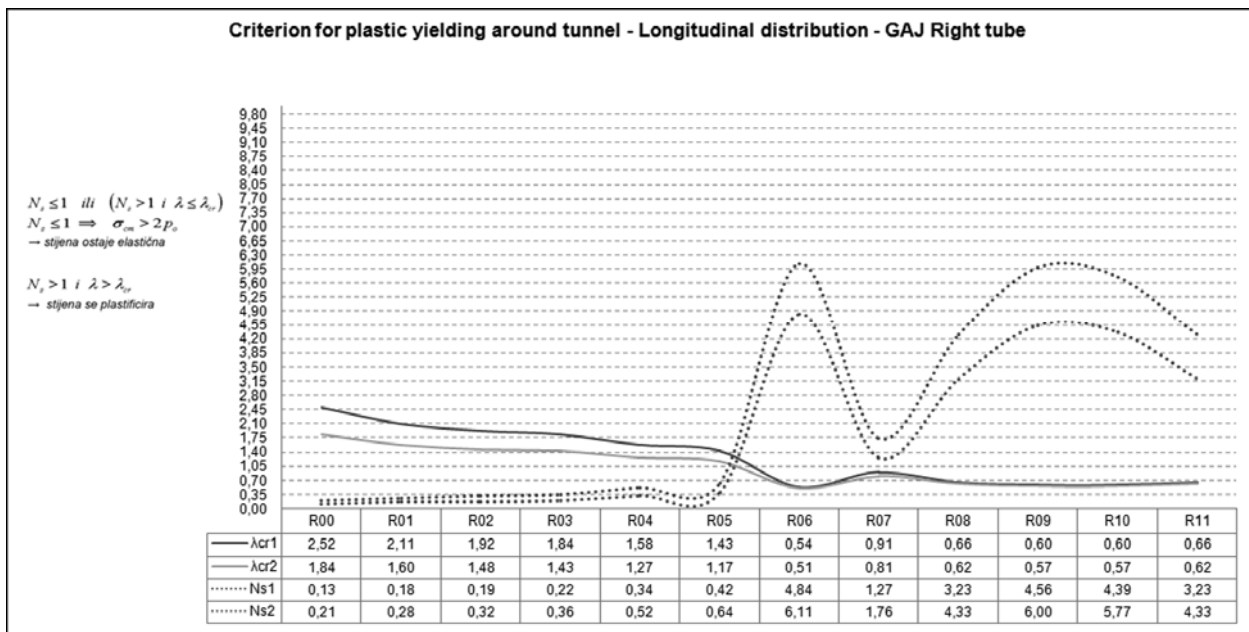
This means that the rock mass around the tunnel cavity is inelastic state:

$$N_s \leq 1 \quad \text{or} \quad (N_s > 1 \quad \text{i} \quad \lambda \leq \lambda_{cr}) \quad (9)$$

ili u plastičnom stanju ako je

or in the plastic state if:

$$N_s > 1 \quad \text{and} \quad \lambda > \lambda_{cr} \quad (10)$$



Slika 10 Raspodela faktora  $N_s$  i  $\lambda_{cr}$  po sektorima duž ose tunela GAJ  
Figure 10 The distributon of factors  $N_s$  and  $\lambda_{cr}$  along the sections of tunnel Gaj

Ukoliko želimo da pri  $N_s > 1$  stanje u okolini tunela ostane elastično, moramo postići to da relaksacija napona usled iskopa tunela ne prelazi vrijednost  $\lambda_{cr}$ . To znači da moramo ugraditi oblogu dovoljne nosivosti na određenoj distanci od čela iskopa, koja obezbeđuje da 3D efekat još uvek zadržava potrebni nivo relaksacije napona.

Prilikom tumačenja vrednosti koeficijenta  $N_s$ , potrebno je imati u vidu to da je on izveden na osnovu teorije kontinuuma i da njegova vrednost od  $N_s \leq 1$  ne garantuje stabilnost tunela u slučaju nepovoljno orijentisanih pukotina u stenskoj masi. U tom slučaju, potrebno je izvesti proračune stabilnosti protiv ispadanja blokova, koji mogu da prouzrokuju rušenja u tunelu.

Za vrednosti  $N_s \geq 1,0$  glavni mehanizam odziva stenske mase zasnovan je na njenoj smičućoj otpornosti i elastoplastičnom ponašanju. U tim slučajevima, redovno se proverava stabilnost upotrebom numeričkih analiza i to najčešće metodom konačnih elementa. Za te analize potrebno je korektno proceniti raspodelu koeficijenta relaksacije  $\lambda_{cr}$  uzduž tunela. To se potom koristi da se opredeli skup numeričkih analiza sa upotrebom metode konačnih elemenata, da bi se izvršilo dimenzionisanje potpornih mera na različitim odsecima u tunelu.

Na slici 10 prikazana je raspodela faktora  $N_s$  i  $\lambda_{cr}$  po sektorima različitih kombinacija nadsloja i geoloških uslova duž ose tunela Gaj, koji je izveden na AC Sarajevo – Tarčin u BiH. Na osnovu slike možemo uočiti da su na određenim deonicama vrednosti  $N_s$  manje od 1 (to je bio deo tunela s niskim nadslojem u krečnjacima), dok na određenim deonicama prelaze vrednosti i od 6,0 (to je bio deo tunela u slaboj stenskoj masi s višim nadslojem). U praktičnom smislu, to je značilo da su za vrednosti od  $N_s \geq 6,0$  numeričke analize ukazale na potrebu opsežnijih potpornih mera tj. jače primarne obloge i dužih stenskih sidara, kao i na manje predviđeno rastojanje od čela iskopa do zatvaranja

In the other words, if we want to achieve that for  $N_s > 1$  state remains elastic around the tunnel, we must achieve that relaxation of stresses caused by excavation of the tunnel does not exceed values that correspond to  $\lambda_{cr}$ . This means that we have to install the supporting system (lining and the rock bolts) of given capacity at a certain distance from the head of excavation enabling conditions in which the 3D effect actually contains the amount of relaxation at the required level.

In the interpretation of the Factor of Tunnel Stability  $N_s$  it should be considered that this concept was derived on the theory of continuum mechanics and that the value  $N_s \leq 1$  does not necessarily guaranty stable conditions for unfavourable layering of discontinuities in the rock mass. In this case a wedge analyses should be carried out to prove or mitigate possible instabilities in the tunnel.

For the values of  $N_s \geq 1,0$  the main mechanism of the rock mass response is based on its shearing resistance and elastic plastic behaviour. In these cases the numerical analyses for the proof of tunnel stability are routinely carried out using Finite Element Method. The appropriate approach for these analyses is to first determine the distribution of the coefficient of relaxation  $\lambda_{cr}$  along the tunnel. This was then used to devise the set of Finite Element analyses, which will cover all significant variations in the  $N_s$  values and define the appropriate primary support systems for different tunnel sections.

The distribution of  $N_s$  and  $\lambda_{cr}$  along the tunnel Gaj, which was constructed on Motorway Sarajevo-Tarčin in Bosnia and Herzegovina, is shown in Figure 10. The distribution is shown for different combinations of the amount of overburden and appropriate geological conditions that varied along the tunnel. It can be seen in the figure that at the certain tunnel sections the values of  $N_s$  are less than 1 (e.g. shallow part of the tunnel in hard limestone), wherein in some sections the values of  $N_s$  are exceeding 6,0 (e.g. deeper part of the tunnel in poor

podnožnog svoda. Na slici su prikazani proračuni  $N_s$  i  $\lambda_{cr}$  za različite vrednosti koeficijenta  $K_0$  i to za  $K_0=1-\sin\varphi$  i  $K_0=1,0$ , što se smatralo logičnim graničnim vrednostima za koeficijent pritiska tla u stanju mirovanja.

## ZAVRŠNE NAPOMENE I ZAKLJUČAK

U skladu s principima NATM, dozvoljen je - čak i poželjan - određeni nivo plastifikacije oko otvora tunela, ali on ne sme prekoračiti dužinu sidara. U idealnim okolnostima, plastifikacija ne prelazi dubinu od 3 m do maksimalno 6 m, što odgovara približnoj vrednosti  $N_s=5-6$ . U slučajevima kada  $N_s$  prekorači vrednost 7, možemo očekivati teškoće pri gradnji tunela, jer je to približno i granica upotrebljivosti koncepta NATM.

Ako to dozvoljava nosivost stenske mase, pravilo je da treba težiti da njen odziv ostane pretežno elastičan. To garantuje dugoročnu trajnost tunela, odnosno manju zavisnost njegove stabilnosti od materijala ugrađenih u njegovu podgradu. Ključno pitanje na koje projektant mora odgovoriti jeste na kojem rastojanju od čela iskopa se javlja vrednost  $\lambda_{cr}$  i kakvu oblogu treba ugraditi na tom mestu da bi odziv stenske mase bio pretežno elastičan odnosno plastičan do željenog nivoa.

U numeričkim analizama potrebno je težiti tome da se usvoji vrijednost  $\lambda$  koja je bliska vrednosti za  $\lambda_{cr}$ , jer to omogućava dimenzionisanje podgrade koja će zadovoljiti potrebu dominantnog elastičnog odziva stenske mase. Ukoliko je vrednost faktora stabilnosti tunela  $N_s < 1,0$ , to implicira višu vrednost za  $\lambda$  jer stenska masa ima zahtevanu nosivost, tako da samo mali deo opterećenja preuzima primarna podgrada. U skladu s tim, unutrašnje sile u oblozi biće relativno male i obratno, manji  $\lambda$ -faktor znači veće unutrašnje sile i manje deformacije stenske mase.

Vrednost  $\lambda$ -faktora - koja se koristi kao ulazni podatak za numeričke analize - utvrđuje se na bazi teorijskih pretpostavki i ocene nosivosti odnosno kvaliteta stenske mase. Svakako, najrealnija ocena vrednosti  $\lambda$ -faktora i interakcije potpornog sistema i stenske mase postiže se povratnim statičkim analizama. Za efikasnu primenu povratnih analiza potrebno je obezbediti podatke na osnovu tekućeg praćenja svih važnih pokazatelja interakcije stenske mase i potpornih elementa. U tu svrhu, u toku građenja tunela, potrebno je kontinuirano: a) vršiti geološko kartiranje čela iskopa i valorizaciju parametra čvrstoće stenske mase; b) dnevno meriti radialne deformacije u tunelu; c) po potrebi, ugrađivati i interpretirati merne profile za određivanje pomeranja po dubini stenske mase i stepena mobilizacije stenskih sidara. Merni profili (tj. ekstenzometri i merna sidra) po pravilu se koriste u slučaju pojave slabijih geoloških uslova. Na osnovu dobijenih informacija pokazatelja stanja u tunelu i rezultata povratnih analiza, projektant dobija mogućnost da pravilno odluči o eventualnoj promeni podgradnog sklopa radi optimizacije gradnje tunela.

Prethodna objašnjenja osnovnih pojmova principa NATM jesu osnova za uspešno, sigurno i ekonomski opravdano građenje tunela. U praksi je to, nažalost,

rock). In the sections with the values of  $N_s \geq 6,0$  the numerical analyses were used to dimension the elaborate primary support including stronger primary lining, longer rock bolts and the requirement for the short distance from the head of excavation to the closing of the tunnel invert. The calculations of  $N_s$  and  $\lambda_{cr}$  in the figure are given for the different values of the coefficient of earth pressure at rest  $K_0$  for  $K_0=1-\sin\varphi$  and  $K_0=1,0$ , which are considered to be appropriate boundary values.

## THE FINAL REMARKS AND CONCLUSIONS

In accordance to the principles of NATM, certain level of plasticization around the cavity of the tunnel is desirable, but its size must not exceed the length of the rock bolts. In the ideal circumstances the depth of plasticization around the tunnel should be kept around 3m and should not exceed 6m, which corresponds to the approximate value of  $N_s=5-6$ . In cases when  $N_s$  exceeds the value of 7,0 one can expect difficulties during the tunnel construction, as this indicates practical limit for successful use of NATM.

As a rule (if the self-capacity of the rock mass allows for it) one should strive to keep the rock mass in predominantly elastic state as this complements to the durability of tunnel construction, that is, ensures less dependence on the materials installed in the tunnel (e.g. tunnel lining and rock bolts). The key question that designer should answer is at what distance from the head of excavation is the value of  $\lambda_{cr}$  and what type of primary support at that position should be installed so that the response of the rock mass remains elastic or becomes plastic up to the desired level.

If possible, during the execution of the finite element analyses, the value of  $\lambda$  should be chosen to be close to  $\lambda_{cr}$ , as this will result into the dimension of the primary lining within the required elastic response of the rock mass. If the value of Factor of Tunnel Stability is  $N_s < 1,0$  this implies higher value for  $\lambda$  as the rock mass have the required capacity and only a small fraction of the relaxation is taken by the supporting system. The opposite is also true; the lower value of  $\lambda$  implies higher internal forces in the lining and less deformation of the rock mass.

The value of the coefficient  $\lambda$ , which is used as the input parameter for the numerical analyses, is determined from the described theoretical concepts and the prediction of the rock mass quality. However, the most realistic determination of the factor  $\lambda$  and interaction between the supporting system and the rock mass is evaluated using the back analyses. For the efficient use of back analyses it is necessary to obtain all the relevant information with regard to the interaction of the rock mass and the tunnel lining. For this purpose a permanent monitoring of the key indicators is carried out during the tunnel construction: a) geological mapping of the head of excavation and evaluation of the quality of the rock mass, b) daily assessment of the convergence movement in the tunnel, and c) if necessary the installation and interpretation of measuring profiles for determination of the movements of the rock mass and the degree of mobilisation of rock bolts. The measuring profiles (e.g. extensometers and measuring anchors) are typically installed within the poor geological conditions. On the basis of the interpretation of the indicators of the

veoma teško dostići, jer se kontinuirano praćenje gradnje tunela ne izvodi pravovremeno i kvalitetno. To posleđično onemogućava pravovremeno donošenje pravilnih odluka u smislu prilagođavanja primarne podgrade u skladu s promenom uslova gradnje.

Sve pokazatelje uspešnosti gradnje u praksi kontinuirano prati projektant u okviru projektantskog nadzora. Projektantski nadzor obuhvata prikupljanje informacija o geološkim i hidrogeološkim uslovima gradnje, praćenje merenja radijalnih pomeranja na konturi iskopa, praćenje rezultata drugih mernih profila, izvršenje povratnih analiza stabilnosti iskopa tunela i pravovremeno predlaganje promene podgradnog sistema ako je to potrebno.

Za uspešno delovanje projektantskog nadzora moraju biti jasno određene obaveze i dužnosti svih aktera gradnje: izvođača, inženjera, investitora i projektanta. Osnovni odnosi moraju biti definisani fleksibilnim tipom ugovora koji omogućava optimizaciju gradnje i sprečava nepotrebno trošenje finansijskih sredstava, kao i materijalnih i ljudskih resursa. Iskustvo autora govori u prilog tome da se samo u tom slučaju dobijaju zadovoljavajući rezultati i iskorišćavaju potencijali koje u sebi nosi pravilna upotreba metode NATM. U suprotnom, gradnja tunela može biti nepotrebno skupa i neefikasna, s pogubnim finansijskim posledicama za investitora i izvođača. Postizanje fleksibilne ugovorne strukture koja je bazirana na crvenoj knjizi FIDIC-a (naplaćivanje prema izvedenim količinama) po iskustvu projektanta jeste najprimerenije rešenje za aplikaciju principa NATM u tunelogradnji.

state in the tunnel and the results of the back analyses, the designer becomes able to achieve the correct decisions with regard to eventual change of the supporting system and thus optimisation of tunnel construction.

Understanding of the basic NATM principles presented in the paper is the basis for successful, safe and economically viable tunnel construction. Unfortunately, in practise, this is usually difficult to achieve as the permanent monitoring is not carried out on time and with required quality. In consequence, the well-timed and correct decisions are not taken and there is no appropriate change of primary support to conform the change in boundary conditions.

The permanent evaluation of indicators of tunnel construction should be carried out by the designer within the process of designer supervision. The designer supervision comprises the acquisition of geological and hydrogeological data, monitoring of the convergence movements on the excavation contour, monitoring and interpretation of the results of the measuring profiles, execution of the back analyses for the evaluation of tunnel stability and propositions for the change of supporting system when appropriate.

For a successful execution of the designer supervision it is necessary that all the actors in construction: designer, contractor, engineer, and client have clearly defined roles. The relationships should be defined within the flexible contractual framework that enables the optimisation of construction and prevent unnecessary wasteful use of resources: human, material and financial. The experience of the authors is such that only under those circumstances there are satisfactory results and proper utilisation of the potential of NATM. Otherwise, the tunnel construction can be unnecessary expensive bringing up deadly financial consequences to the client and/or to the contractor. The establishment of flexible contractual framework within the red book of the FIDIC type of contract (admeasurement) is the most appropriate solution for application of NATM in practice by the experience of the authors.

## LITERATURA LITERATURE

- [1] Hoek, E. 1999. Support for very weak rock associated with faults and shear zones Distinguished lecture for the opening of the International Symposium on Rock Support and Reinforcement Practice in Mining, Kalgoorlie, Australia, 14-19 March, 1999.
- [2] Hoek E. Carranza Torres, C. & Corkum, B. 2002. Hoek-Brown failure criterion – 2002 edition. Proceedings of the Fifth North American Rock Mechanics Symposium (NARMS-TAC) (Eds: Hammah, R., Bawden, W., Curran, J. & Telesnicki, M.), 1, 267-273. University of Toronto Press, Toronto.
- [3] Golser J., 1976, The New Austrian Tunneling Method (NATM), Theoretical Background & Practical Experiences. 2nd Shotcrete conference, Easton, Pennsylvania (USA), 4-8 Oct 1976.
- [4] Jovičić, Vojkan, ŠUŠTERŠIĆ, Jakob, VUKELIĆ, Željko. The application of fibre reinforced shotcrete as primary support for a tunnel in flysch. Tunn. undergr. space technol.. [Print ed.], 2009, vol. 24, no. 6, str. 723-730. [COBISS.SI-ID 946015] FA - construction & building technology ; 19/49
- [5] Kavvadas, M. 2004. Design of Underground Structures. University Notes. Specialised Master Design and Construction of Underground Works. National Technical, University of Athens
- [6] Marinos, P., Hoek, E. 2001. Estimating the geotechnical properties of heterogeneous rock masses of Flysch. Bull. Eng. Geol. Env., 60: 85–92.
- [7] Marinos, V., Fortsakis, P., Proutzopoulos, G. 2011. Estimation of geotechnical properties and classification of geotechnical behaviour in tunnelling for flysch rock masses. V: Proceedings of the 15th European Conference on Soil Mechanics and Geotechnical Engineering. IOS Press. pp. 435-440.
- [8] Panet, M. and Guénot, A. 1982. Analysis of convergence behind face of a tunnel. In Proc. Tunnelling'82, pp. 197–203. IMM, London.

## REZIME

### KORISNI KONCEPTI U PRIMENI NOVE AUSTRIJSKE METODE ZA GRADNJU TUNELA

Vojkan JOVIČIĆ  
Jasmin BUČO  
Nermin ŠEHAGIĆ  
Alaga HUSIĆ

U članku su predstavljeni koncepti razvijeni u dugogodišnjoj praksi pri projektovanju i gradnji tunela primenom Nove austrijske metode (New Austrian Tunnelling Method - NATM). Cilj članka jeste da predoči osnovne teorijske koncepte ove metode i da iznese iskustva kako pri projektovanju tunela, tako i pri aplikaciji tih principa na konkretnim primerima. Prikazana su uputstva za primenu korisnih koncepta prilikom dimenzionisanja primarne podgrade, kao i metodologija ocene stepena upotrebljivosti NATM metode za date granične uslove. U članku su takođe obrađeni postupci primene NATM metode u uslovima izvođenja radova, pri čemu je kao osnova za uspešan rad ispostavljena aktivna uloga projektanta i fleksibilnost ugovornih odnosa između investitora i izvođača.

**Ključne reči:** projektovanje, tuneli, NATM, SCL, stenska masa, nosivost

## SUMMARY

### USEFUL CONCEPTS FOR APPLICATION OF NEW AUSTRIAN TUNNELLING METHOD IN TUNNEL CONSTRUCTION

Vojkan JOVICIC  
Jasmin BUCO  
Nermin SEHAGIC  
Alaga HUSIC

The concepts that were developed in the long-standing practice in designing and constructing tunnels using New Austrian Tunnelling Method (NATM) are presented in the paper. The aim of the paper is to highlight the basic theoretical concepts and to expose the experience in the design and the application of NATM principles following the concrete examples. The procedures used in the application of these principles are also addressed in the paper, in which the active role of the designer and the contractual flexibility between the contractor and the client are seen as the key conditions for a successful work.

**Key words:** design, tunnels, NATM, SCL, rock mass, capacity

# KRITERIJUM STABILNOSTI DEFORMACIJE ELASTOPLASTIČNIH MATERIJALA

## CONDITIONS FOR STABILITY OF DEFORMATION IN ELASTO-PLASTIC MATERIALS

Selimir V. LELOVIĆ

ORIGINALNI NAUČNI RAD  
ORIGINAL SCIENTIFIC PAPER  
UDK: 691.175  
doi: 10.5937/grmk1504037L

### UVOD

Problem stabilnosti geomehaničkih materijala za tačno utvrđenu geometriju, granične uslove i karakter opterećenja, zahteva određivanje intervala parametara opterećenja, pri kojem naponsko-deformacijske veličine imaju konačne vrednosti. Gubitak stabilnosti može se posmatrati i kao početak loma materijala.

Od velikog praktičnog značaja jeste to da se odredi da li će posmatrana plastična deformacija - u trenutku kada je dostignuto ravnotežno stanje - povećati svoju dužinu za konačan (mali) inkrement i prestati s rastom (stabilan režim deformisanja) ili će nastaviti s nekontrolisanim rastom dok ne dođe do velikih priraštaja posmatranih deformacija (nestabilan režim deformisanja). Prelaz fizičkog (mehaničkog) sistema iz stabilnog režima deformisanja u nestabilan režim deformisanja često se naziva gubitak stabilnosti.

Granica ovog prelaza poznata je kao kritično stanje materijala, a njemu odgovarajuće opterećenje jeste kritično opterećenje. Potreban uslov za gubitak stabilnosti ponašanja materijala, gubitak jedinstvenosti rešenja i pojavu bifurkacije jeste promena znaka drugog izvoda funkcije rada na plastičnom deformisanju materijala (Drucker, 1950). S jedne strane, Drucker-ov postulat predviđa dovoljan uslov za stabilno ponašanje materijala, određena teorijska razmatranja ukazuju na to da je ovo možda samo potreban, ali ne i dovoljan uslov (Mroz, 1964). Ponašanje materijala postaje nestabilno kada počinje da se gubi eliptičnost tangente matrice krutosti. Ovaj početak nestabilnog ponašanja materijala povezan je s tačkom bifurkacije ili odstupanja od jedinstvenog rešenja na ravnotežnoj putanji (Mandel, 1964). Pojava

### INTRODUCTION

Stability of deformation for a geomechanical material under applied load, for defined geometry and boundary conditions, requires determination of the load interval where stress-strain properties have definite values. Loss of material stability may be considered as initiation of material failure.

From the practical point of view it is important to determine for the small increment in stress, if the plastic deformation increment was small (stable deformation occurred) or large (unstable deformation occurred). Losing the stability of deformation occurred at the boundary between these two regimes. The loading condition at the boundary is called the critical loading while material is called to be in a critical state.

The term "stability" is used here as a quasi-static response of a material under small increments of displacements. Necessary condition for the stability loss, as well as loss in unique relationship and appearance of bifurcation is the sign change in the second derivative of the work function (Drucker, 1950). Although from one point of view, Drucker's postulate provides a sufficient condition for material stability, some theoretical considerations have suggested that this is only a necessary condition (Mroz, 1964). Material instability occurs when ellipticity of the tangent stiffness matrix is lost. The beginning of unstable material behavior is connected with bifurcation point or deviation from the unique solution on the equilibrium path (Mandel, 1964). The onset of localized deformation is often associated with the satisfaction of the classical discontinuous bifurcation criterion. The localized deformation phenomena in

---

Selimir V. Lelović, Univerzitet u Beogradu Građevinski fakultet, Bulevar kralja Aleksandra br. 73, Beograd  
lelovic@grf.bg.ac.rs

---

Selimir V. Lelovic, University of Belgrade, Faculty of Civil Engineering, King Alexander Blvd., # 73, Belgrade  
lelovic@grf.bg.ac.rs

lokalizovane deformacije, u klasičnom smislu diskontinuiteta, obično je povezana s pojavom tačke bifurkacije. Fenomen lokalizacije deformacije u granularnim materijalima veoma je interesantan kako sa eksperimentalne, tako i sa analitičke tačke gledišta. Klasični rezultati za elastoplastični kontinuum izraženi preko kritične vrednosti modula ojačanja i odgovarajuća orijentacija trake klizanja (*shear band*) prikazani su u radovima (Hill, 1950), (Rudnicki i sar., 1975) i (Rice, 1976). U ovim radovima definisani su statički i kinematički uslovi za početak klizanja u granularnom materijalu. Matematički precizan kriterijum za određivanje položaja kritične tačke izveden iz generalnog razmatranja svojstvenih vrednosti tangentne matrice krutosti (Borst, 1988). Ovako postavljen kriterijum za određivanje kritične tačke vrlo je pogodan sa stanovišta praktične primene. Više autora primenilo je ovu metodologiju na granularne materijale, s tim što su koristili Mohr-Coulomb-ov kriterijum kao funkciju tečenja.

U ovom radu prvo su prikazana generalna razmatranja odnosa napon-deformacija i kriterijum za određivanje kritične tačke deformacije, zatim tri ilustrativna primera, poređenje dobijenih rezultata sa eksperimentalnim vrednostima i naposljetku - zaključak.

## KONSTITUTIVNE JEDNAČINE

U teoriji plastičnosti obično se zanemaruju uticaji brzine deformacije i temperaturnog polja. Tako dobijena teorija zove se izotermička teorija plastičnosti. Ograničićemo naša razmatranja na izotermički proces ( $T = \text{cons.} > 0$ ). Pomeranje tačke tela označićemo sa  $u(x)$ , gde su sa  $x$  označene pravougle Dekartove koordinate posmatrane tačke. Usvajajući pretpostavku o malim pomeranjima, tenzor deformacije može se napisati u obliku:

$$2\varepsilon_{ij} = u_{i,j} + u_{j,i} \quad (1)$$

gde zarez označava parcijalni izvod po odgovarajućoj koordinati. Veza između napona i elastične deformacije određena je Hukovim zakonom. Funkcija plastičnog potencijala za izotropan materijal može se napisati u obliku:

$$f = f(\sigma, q) \quad (2)$$

gde  $q$  označava određenu unutrašnju promenljivu stanja materijala (tj. njen tenzor). Uslov tečenja  $f = f(\sigma, q) = 0$  definiše površ tečenja u  $(\sigma, q)$  prostoru. Neka veliko  $Q$  označava izvod površi tečenja u odnosu na napon, a veliko  $R$  označava izvod u odnosu na unutrašnju promenljivu  $q$ :

$$Q(\sigma, q) = \frac{\partial f}{\partial \sigma}, R(\sigma, q) = \frac{\partial f}{\partial q} \quad (3)$$

Neka je  $P$  normala na površ tečenja koja označava pravac tečenja u odnosu na  $\sigma$ , onda ako je  $P = Q$  plastično tečenje se naziva asocijativno, dok se za slučaj

granular material are very interesting not only from the experimental point of view but numerical as well. Now classical results for elasto-plastic continuum derived from the critical values for the hardening modulus and corresponding orientation of the so called shear band were published by (Hill, 1950), (Rudnicki and Rice., 1975) and (Rice, 1976).

Static and kinematic conditions for the onset of slip (shear band) in granular materials were presented in those papers. Mathematically precise criteria to determine the critical point position is derived from general considerations of the values for the tangent of the material stiffness constants (Borst, 1988). Criteria established in such a way showed to be very useful for practical applications. Presented methodology was used by many authors, mostly employing the classical Mohr-Coulomb's type yield function.

In this paper, general points about the stress-strain relationship and the critical point deformation are given first; second two illustrative examples are given along with published experimental results; third analysis of the compared differences in critical loads and at the end are given conclusions.

## CONSTITUTIVE EQUATIONS

In theory of plasticity, rate of deformation and temperature effects are usually neglected. Such considerations are called isothermal plasticity. In this work considerations are restricted to isothermal processes ( $T = \text{cons.} > 0$ ). The displacement of a point in the body is characterized by  $u(x)$ , where  $x$  are the rectangular Cartesian coordinates of the point. Following the assumption of small displacements, the strain-displacement relations are:

where comma followed by an index represents partial differentiation with respect to the corresponding coordinate. Hooks law is defining the relationship between the increments in stress and deformation. The yield potential for an isotropic material is given by the following function:

where  $q$  signifies suitable set of internal state variables for geomaterial (tensor). The yield condition  $f = f(\sigma, q) = 0$  defines the yield surface in the  $(\sigma, q)$  space. Let  $Q$  denote the derivative of the yield surface with respect to the stress and  $R$  the derivative with respect to the internal variable  $q$ :

If  $P$  is normal to the yield surface and describes the flow direction with respect to  $\sigma$ , then if  $P = Q$  the plastic flow rule is called associative, where as if  $P \neq Q$



gde  $P \neq Q$  plastično tečenje naziva ne-asocijativno. Plastični deo priraštaja deformacije označen je kao:

$$\dot{\varepsilon}^p = \lambda P(\sigma, q), \lambda > 0 \quad (4)$$

gde je  $\lambda$  arbitrarni faktor proporcionalnosti. Pozitivni znak za  $\lambda$  je usled činjenice da plastično tečenje uključuje gubitak energije. Tačka iznad promenljive označava puni izvod promenljive u odnosu na vreme, koji je usled pretpostavke malih brzina isti kao i parcijalni izvod u odnosu na vreme. Efekti disipacije u materijalu koji prate deformaciju mogu se uzeti u obzir preko unutrašnje promenljive stanja. Brzina promene unutrašnje promenljive  $q$  predstavljena je nelinearnom funkcijom  $h$  koja sadrži  $\sigma$  i  $q$ ,

$$\dot{q} = \lambda h(\sigma, q) \quad (5)$$

Za infinitezimalne deformacije možemo izraziti tenzor deformacije kao zbir tenzora elastičnih i plastičnih deformacija:

$$\varepsilon = \varepsilon^e + \varepsilon^p \quad (6)$$

gde indeks  $e$  označava elastičan deo, i indeks  $p$  označava plastičnu promenu u polju deformacija kada se unutrašnja koordinata  $q$  promeni u  $q + \dot{q}$ . Razmatrajući materijale kod kojih se konstitutivno ponašanje može idealizovati u segmentno-linearnoj formi:

$$\dot{\sigma} = L : \dot{\varepsilon} \quad (7)$$

gde je  $L$  konstitutivni tenzor materijala,  $(:)$  označava dijadu. Jedna forma konstitutivne jednačine (6) može se izraziti:

$$\dot{\sigma} = C : \left( \dot{\varepsilon} - \frac{1}{R \cdot h} P(Q : \dot{\sigma}) \right) \quad (8)$$

gde je  $C$  tenzor inkrementa modula elastičnosti,  $h$  - brzina promene ojačavanja ili omekšavanja. Desna strana jednačine (7) može se napisati u odnosu na  $\dot{\varepsilon}$ , i poređenjem s jednačinom (6) dobija se sledeći odnos:

$$L = C - \frac{(C : P)(Q : C)}{Q : C : P - R \cdot h} \quad (9)$$

Ako se funkcija  $f$  može razviti u Tejlorov red do drugog stepena oko trenutnih vrednosti za deformaciju i plastične promenljive, može se dobiti sledeći izraz:

$$f(\varepsilon + \dot{\varepsilon}^*, q + \dot{q}^*) = f(\varepsilon, q) + \frac{\partial f}{\partial \sigma} : (L : \dot{\varepsilon}^*) + \frac{\partial f}{\partial q} \cdot \dot{q}^* + \frac{1}{2} \cdot \frac{\partial^2 f}{\partial \sigma \partial \sigma} : (L : \dot{\varepsilon}^*) : (L : \dot{\varepsilon}^*) + \frac{\partial^2 f}{\partial \sigma \partial q} : (L : \dot{\varepsilon}^*) \cdot \dot{q}^* + \frac{1}{2} \cdot \frac{\partial^2 f}{\partial q \partial q} \cdot \dot{q}^* \cdot \dot{q}^* \quad (10)$$

the plastic flow is called non-associative. The plastic part of the strain rate is expressed as:

where  $\lambda$  is an arbitrary factor of proportionality. The positive sign of  $\lambda$  is due to the fact that plastic flow involves dissipation of energy. A dot above the variable denotes the total derivative of that variable with respect to time which, under the approximation of small velocities is the same as the partial derivative with respect to time. The dissipative effects which accompany deformation may be accounted for by the use of internal state variables. The rate of change of the  $q$  is represented with a non-linear function  $h$  which includes the state variable  $\sigma$  and the complete internal state  $q$ ,

The infinitesimal macro strain field may be divided in accordance with the following equation:

where superscript  $e$  stands for the elastic part, and superscript  $p$  denotes inelastic change in a strain field during which  $q$  changes into  $q + \dot{q}$ . Considering the class of materials whose constitutive behaviour may be idealised as a piecewise-linear relation of the form:

where  $L$  is the tangent-compliance tensor of the material,  $(:)$  signifies the dyadic product. One particular form of the constitutive rate relation (6) may be expressed as:

where  $C$  is the tensor of incremental elastic module,  $h$  is the rate of hardening or softening. The right-hand side of equation (7) may be written in terms of  $\dot{\varepsilon}$ , and compared with equation (6) to make the following evident:

If the function  $f$  can be expanded in Taylor series to second order around the current values of the strain and plastic variables, then it can be used to obtain the following:

gde su svi izvodi određeni na  $\varepsilon, q$ . Promene u  $\varepsilon + \dot{\varepsilon}^*$  mogu se posmatrati kao varijacije u  $\dot{\varepsilon}^*$ , gde je  $\dot{\varepsilon}^* = \varepsilon_{,u}(\delta u)$  prva promena u (nelinearnom) operatoru za deformaciju-pomeranje  $\varepsilon(u)$  u odnosu na  $u$ . Sledeće veličine uvedene su da bi se jednačina (10) pojednostavila:

$$T(\sigma, q) = \frac{\partial^2 f}{\partial \sigma \partial \sigma}, U(\sigma, q) = \frac{\partial^2 f}{\partial \sigma \partial q}, V(\sigma, q) = \frac{\partial^2 f}{\partial q \partial q} \quad (11)$$

gde je  $T$  simetrični tenzor četvrtog stepena,  $U$  je simetrični tenzor drugog stepena, a  $V$  – scalar. Sada, jednačina (10) ima sledeći oblik:

$$f = f + Q : (L : \dot{\varepsilon}^*) + R \cdot \dot{q}^* + 1/2 \cdot T : (L : \dot{\varepsilon}^*) : (L : \dot{\varepsilon}^*) + U : (L : \dot{\varepsilon}^*) \cdot \dot{q}^* + 1/2 \cdot V \cdot \dot{q}^* \cdot \dot{q}^* \quad (12)$$

Treći član u jednačini (12) zove se drugi osnovni kvadratni oblik površi tečenja.

### ODREĐIVANJE KRITIČNE TAČKE

U analizi stabilnosti deformacije, određivanje kritične tačke jeste centralni problem.  $T, U, V$ , izrazi određeni relacijama (11), koeficijenti su druge osnovne kvadratne forme površi tečenja  $f = f(\sigma, q)$ . Izraz za normalnu krivinu posmatrane površi, možemo napisati u sledećem obliku:

$$\frac{1}{\rho} = \frac{T : (L : \dot{\varepsilon}^*) : (L : \dot{\varepsilon}^*) + 2U : (L : \dot{\varepsilon}^*) \cdot \dot{q}^* + V \cdot \dot{q}^* \cdot \dot{q}^*}{\left[ Q : (L : \dot{\varepsilon}^*) + R \cdot \dot{q}^* \right]^2} \quad (13)$$

Znak normalne krivine zavisi samo od znaka brojioca izraza na desnoj strani gornje jednačine. U proučavanju znaka normalne krivine, prema tome, mogu nastupiti tri slučaja:

$$1. \quad \delta = U^2 - T \cdot V < 0. \quad (14)$$

Imenilac izraza na desnoj strani uvek je pozitivna veličina, jer predstavlja kvadrat. Tada je brojilac potpuni kvadrat i ne menja znak, tj. krivina opet ostaje stalnog znaka u svim pravcima, ali postoji jedan pravac u kome je krivina jednaka nuli. Ovakve tačke površine zovu se eliptične, a za površinu se kaže da u takvoj tački ima eliptičnu krivinu. Znak krive uvek je pozitivan i prema koeficijentu  $T$ .

$$2. \quad \delta = U^2 - T \cdot V = 0. \quad (15)$$

Brojilac ne menja znak i krivina normalnih preseka u svim pravcima ima isti znak, izuzev u tački gde je nula. Takve tačke površine zovu se paraboličke tačke.

$$3. \quad \delta = U^2 - T \cdot V > 0. \quad (16)$$

where all derivatives are evaluated at  $\varepsilon, q$ . The variations in  $\varepsilon + \dot{\varepsilon}^*$  may be treated as variations in  $\dot{\varepsilon}^*$ , where  $\dot{\varepsilon}^* = \varepsilon_{,u}(\delta u)$  is the first variation of the (non-linear) strain-displacement operator  $\varepsilon(u)$  with respect to  $u$ . The following quantities are defined in order to express equation (10) in a simplified manner:

where  $T$  is a symmetric fourth-order tensor,  $U$  is a symmetric second-order tensor and  $V$  is a scalar. Now, equation (10) may be written as:

The third member in the equation (12) is called the second basic quadratic form of yield surface.

### CRITICAL POINT DETERMINATION

In the analysis of stability of deformation, the critical point determination is the central problem.  $T, U, V$  are the coefficient of the yield surface  $f = f(\sigma, q)$  given by equations (11). The normal curvature of the considered surface could be written in accordance with (12) as:

Its sign depends only on the sign of the numerator because denominator is always positive. There are three possible cases:

In the first case, the numerator does not change sign and curve has the same sign in all possible directions from the given point. In other word, normal vector to the possible cross-sections at a given point have the same directions. These points are called elliptical. The sign of the curve is always positive and towards the coefficient  $T$ .

The numerator still does not change sign and the curve has the same sign in all directions, except the one where it is equal to zero. These points are called parabolic.

Brojilac menja znak, tj. u posmatranoj tački postoje glavne normale suprotnih smerova za normalne preseke raznih pravaca. Normalna krivina u istoj tački u tom slučaju za razne pravce može biti pozitivna i negativna, a postoje dva pravca u kojima je krivina nula. Takva tačka površi zove se hiperbolička, a površina u toj tački ima hiperboličku krivinu. Klasifikacija tačaka jedne površi, odnosno utvrđivanje oblika površi u okolini posmatrane tačke, jasno ističe značaj i druge osnovne kvadratne forme površi. Na ovaj način, posmatranjem ravnotežne putanje sistema, odnosno analizom njegovog ponašanja u okolini kritične tačke, direktno se formulišu uslovi za egzistenciju granične tačke. Kompletan nelinearan odgovor jednog elastoplastičnog sistema formuliše njegovu ravnotežnu putanju, određujući pri tome i odgovarajuće singularne vrednosti. Zadatak stabilnosti definisan je putem oblasti dopustivih deformacija posmatranog elastoplastičnog materijala. Sračunavanjem diskretnih tačaka ravnotežne krive, zajedno sa odgovarajućim vrednostima  $\delta$ , definisane gornjim izrazima, nailazimo i na tačku u kojoj se menja znak ove veličine. Pri vrednosti funkcije  $\delta > 0$ , relacija postaje i potreban i dovoljan uslov za stabilnost ravnotežnog položaja posmatranog sistema za vreme opterećenja.

## PRIMERI ZA ILUSTRACIJU

U radu (Lelović, 2012) razmatrane su različite naponske putanje u trijaksijalnom opitu, za slučaj primene konstitutivnih jednačina HISS modela (Desai i sar., 1987), za granularni materijal. Invarijante napona uvedene su prema sledećim izrazima (naponi i deformacije su pozitivni u kompresiji):

$$I_1 = \sigma_{kk}, I_{2d} = \frac{1}{2} S_{ij} S_{ij}, I_{3d} = \frac{1}{3} S_{ij} S_{jk} S_{ki} \quad (17)$$

gde je  $I_1$  prva invarijanta napona, a  $I_{2d}$  i  $I_{3d}$  – druga i treća invarijanta devijatora napona.

U praktičnim proračunima se druga invarijanta koristi za definisanje oktaedarskog smičućeg napona  $\tau_{oct}$ , kao što se može videti iz sledeće jednačine

$$\tau_{oct}^2 = 2/3 \cdot I_{2d} \quad (17a)$$

Funkcija tečenja opšteg tipa (Desai i sar., 1987),  $f$  za asocijativnu plastičnost sa izotropnim ojačanjem je oblika:

$$f = p_a^{-2} I_{2d} - F_b \cdot F_s = 0 \quad (18a)$$

gde je:

$$F_b = -\alpha \left( \frac{I_1}{p_a} \right)^n + \gamma \left( \frac{I_1}{p_a} \right)^2, F_s = (1 - \beta S_r)^m \quad (18b)$$

$S_r$  je odnos napona dat u obliku  $S_r = 3\sqrt{3}/2 I_{2d}^{-\frac{3}{2}} I_{3d}$ ,  $\alpha$  je funkcija ojačanja,  $\gamma$  i  $\beta$  su parametri materijala, a  $p_a$  je atmosferski pritisak.  $F_b$  je osnovna funkcija koja prikazuje oblik funkcije tečenja u

In this case, numerator changes sign at the given point for different normal vectors. The sign of the curve can be either positive or negative, with two directions where the sign is equal to zero. These points are called the hyperbolic points. This approach allows the determination of the value for the critical loading. The complete non-linear response of an elasto-plastic system defines its deformation path. Stability will define its allowed deformations. Calculation of discrete points along the stability path may lead to the change of the  $\delta$  values in the normal curvature sign. The condition  $\delta > 0$  becomes necessary and sufficient for the stability of deformation. With the analysis of the stability path around the critical points, the limiting conditions become directly formulated.

## ILLUSTRATIVE EXAMPLES

Different loading paths and constitutive relations from the hierarchical single surface (HISS) [14] model for granular materials are described in this section. In order to describe the yield surface, the stress invariants are

where  $I_1$  is the first invariant of the stress tensor and  $I_{2d}$  and  $I_{3d}$  are the second and third invariants of the deviatoric stress tensor. For most practical calculations second invariant is used to define octahedral shear stress  $\tau_{oct}$  as shown in the following relationship:

The model is based on general yield potential,  $f$ , for the associative, isotropic hardening plasticity is given by

where:

$S_r$  is the stress ratio such that  $S_r = \frac{3\sqrt{3}}{2} I_{2d}^{-\frac{3}{2}} I_{3d}$ ,  $\alpha$  is hardening function,  $\gamma$  and  $\beta$  are material parameters, and  $p_a$  is atmospheric pressure.  $F_b$  is the basic function representing the shape of the yield

prostoru  $I_1 - \sqrt{I_{2d}}$ , a  $F_s$  je funkcija oblika u oktaedarskoj ravni. Funkcija ojačanja je data izrazom:

$$\alpha = a_1 \xi^{-\eta} \quad (19)$$

gde su  $a_1$  i  $\eta$  materijalni parametri za model izotropnog ojačanja,  $\xi$  je putanja plastične deformacije. Ukupna efektivna plastična deformacija  $\xi$  definisana je kao preko promene

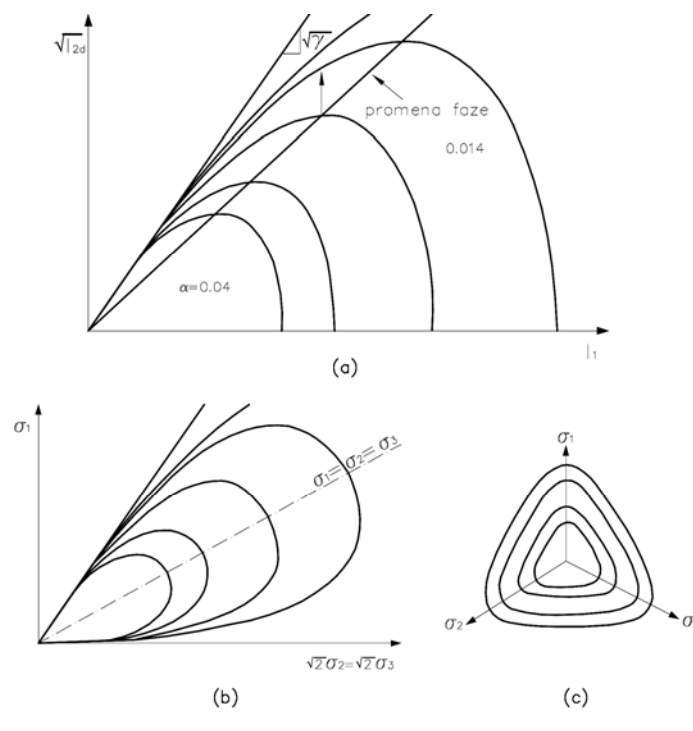
$$\dot{\xi} = \sqrt{p \dot{\epsilon}_{ij}^p p \dot{\epsilon}_{ij}^p} \quad (20)$$

gde se  $m = -0.5$  uzima za većinu (geotehničkih) materijala. Ovaj model uključuje osam materijalnih konstanti, od kojih su dve konstante elastične.

function in the  $I_1 - \sqrt{I_{2d}}$  space,  $F_s$  is the shape function which represents the shape in the octahedral plane. The hardening relation is given by

where  $a_1$  and  $\eta$  are material parameters for the hardening behaviour,  $\xi$  is the trajectory of the plastic strains. The accumulated effective plastic strain,  $\xi$ , is defined by the rate

With  $m = -0.5$  for most (geotechnical) materials. This model involves eight constants including two elastic. Factors such as non associative response, anisotropy, cycling loading, damage and softening are not considered.



Slika 1. Funkcija tečenja HISS (Desai, 1986): (a) u prostoru  $I_1 - \sqrt{I_{2d}}$ ; (b) u trijaksijalnoj ravni; (c) u devijatorskoj ravni  
 Figure 1. Yield function HISS (Desai, 1986): (a) in space  $I_1 - \sqrt{I_{2d}}$ ; (b) triaxial plane; (c) deviatoric plane

Iz relacije (18) eksplicitni izrazi za gradijente funkcije tečenja dobijaju se diferenciranjem

From relationship (18) the explicit expressions for the gradients of yield function are found by differentiation as follows

$$\frac{\partial f}{\partial \sigma_{ij}} = p_a^{-1} F_s \left[ n \alpha (I_1 / p_a)^{n-1} - 2 \gamma (I_1 / p_a) \right] \delta_{ij} + \left( p_a^{-1} - 1.5 m F_s^{\frac{m-1}{m}} F_b S_r I_{2d}^{-1} \right) S_{ij} + m F_s^{\frac{m-1}{m}} F_b A_{ij} \quad (21a)$$

$$\frac{\partial f}{\partial \xi} = -a_1 \eta \xi^{-(\eta+1)} (I_1/p_a)^n F_s \quad (21b)$$

$$\begin{aligned} \frac{\partial f}{\partial \sigma_{ij} \partial \sigma_{kl}} &= p_a^{-2} F_s \left[ n(n-1) \alpha (I_1/p_a)^{n-2} - 2\gamma \right] \delta_{ij} \delta_{kl} + \\ &+ p_a^{-1} m F_s^{\frac{m-1}{m}} \left[ n \alpha (I_1/p_a)^{n-1} - 2\gamma (I_1/p_a) \right] \cdot \left[ 3/2 S_r I_{2d}^{-1} (\delta_{ij} S_{kl} + S_{ij} \delta_{kl}) - (\delta_{ij} A_{kl} + A_{ij} \delta_{kl}) \right] + \\ &+ 3/4 m F_s^{\frac{m-1}{m}} F_b I_{2d}^{-1} \left\{ S_r I_{2d}^{-1} \left[ 5 - 3(m-1) F_s^{-\frac{1}{m}} S_r \right] S_{ij} S_{kl} + 2 \left( F_s^{-\frac{1}{m}} S_r - 1 \right) (S_{ij} A_{kl} + A_{ij} S_{kl}) \right\} - \\ &- m(m-1) F_s^{\frac{m-2}{m}} F_b A_{ij} A_{kl} + \left( p_a^{-2} - 3/2 m F_s^{\frac{m-1}{m}} F_b S_r I_{2d}^{-1} \right) (\delta_{ik} \delta_{jl} - \frac{1}{3} \delta_{ij} \delta_{kl}) + \\ &+ \frac{3\sqrt{3}}{2} m F_s^{\frac{m-1}{m}} F_b \beta I_{2d}^{-\frac{3}{2}} \left[ \delta_{ik} S_{jl} + S_{ik} \delta_{jl} - 2/3 (S_{ij} \delta_{kl} + \delta_{ij} S_{kl}) \right] \end{aligned} \quad (21c)$$

$$\frac{\partial^2 f}{\partial \xi^2 \partial \sigma_{ij}} = -a_1 \eta \xi^{-(\eta+1)} \left[ p_a^{-1} n (I_1/p_a)^{n-1} F_s \delta_{ij} + (I_1/p_a)^n m F_s^{\frac{m-1}{m}} (3/2 S_r I_{2d}^{-1} S_{ij} - A_{ij}) \right] \quad (21d)$$

$$\frac{\partial^2 f}{\partial \xi^2} = a_1 \eta (\eta+1) \xi^{-(\eta+2)} (I_1/p_a)^n F_s \quad (21e)$$

gde je uvedena sledeća oznaka:

Where the following parameter is introduced:

$$A_{ij} = \frac{3\sqrt{3}}{2} \beta I_{2d}^{-\frac{3}{2}} (S_{ik} S_{kj} - \frac{2}{3} I_{2d} \delta_{ij}) \quad (21f)$$

Pretpostavili smo da nema drugih napona izuzev normalnih, tako da su normalni naponi u ovom slučaju i glavni. Ako sa  $\sigma_{xx}$  označimo aksijalni napon, a sa  $\sigma_{yy}$  i  $\sigma_{zz}$  bočne napone, onda ćemo odgovarajuće veze izraziti prema ovim oznakama. Materijal je prvo opterećen hidrostatičkim pritiskom od  $\sigma_0 = 90$  [kPa], pri atmosferskom pritisku  $p_a = 101$  [kPa]. U ovom slučaju, jednačina (15) postaje

The assumption made was that only normal stresses exist in this case.  $\sigma_{xx}$  designates axial stresses and  $\sigma_{yy}$  and  $\sigma_{zz}$  designate side stresses. First, the material was loaded under hydrostatic pressure of  $\sigma_0 = 90$  [kPa], when the atmospheric pressure was  $p_a = 101$  [kPa]. In this case equation (15) becomes

$$\bar{\delta} = 2\gamma \left[ n^2 \frac{\eta}{\eta+1} + n(n-1) - 1 \right] \quad (22)$$

Materijalne konstante za pesak – Leighton Buzzard Sand (Desai, 1989) date su u Tabeli I.

Material constants for sand (Leighton Buzzard Sand) are given in Table I (Desai, 1989).

Tabela I. Parametri za HISS model  
Table I. Parameters for HISS model

$E$ [MPa]	$\nu$	$\beta$	$\gamma$	$n$	$a_1$	$\eta$	$m$
103.8	0.29	0.442	0.089	3	0.00018	0.85	-0.5

**Ilustracija # 1:** Konvencionalni trijaksijalni pritisak (CTC). Za CTC stanje komponente napona i devijatora napona date su sledećim izrazima

**Case # 1:** Conventional triaxial compression (CTC) state. For the CTC state of stress components of the stress tensor and the stress deviator are as follows

$$\sigma^{CTC} = \begin{bmatrix} \sigma_0 + \sigma_{xx} & 0 & 0 \\ 0 & \sigma_0 & 0 \\ 0 & 0 & \sigma_0 \end{bmatrix}, S^{CTC} = \frac{\sigma_{xx}}{3} \begin{bmatrix} 2 & 0 & 0 \\ 0 & -1 & 0 \\ 0 & 0 & -1 \end{bmatrix} \quad (23)$$

Uvodeći jednačinu (23) u (21) i zamenjujući u (15), dobija se sledeći izraz:

Introducing (23) into (21) and substituting this equation in the (15), leads to:

$$\delta = (1-2k)^2 n^2 \frac{p_a^{-2} a_1^2 \eta^2 \xi^{-2(\eta+1)}}{(1-\beta)} \left( \frac{3\sigma_0 + \sigma_{xx}}{p_a} \right)^{2(n-1)} + \frac{p_a^{-2} a_1 \eta (\eta+1) \xi^{-(\eta+2)}}{(1-\beta)} \left( \frac{3\sigma_0 + \sigma_{xx}}{p_a} \right)^n \cdot \left\{ \left[ \frac{2\sqrt{1-\beta}}{3} + n(n-1) \alpha \left( \frac{3\sigma_0 + \sigma_{xx}}{p_a} \right)^{n-2} - 2\gamma \right] - 4k \left[ -\frac{\sqrt{1-\beta}}{3} + n(n-1) \alpha \left( \frac{3\sigma_0 + \sigma_{xx}}{p_a} \right)^{n-2} - 2\gamma \right] + 2k^2 \left[ \frac{\sqrt{1-\beta}}{3} + 2n(n-1) \alpha \left( \frac{3\sigma_0 + \sigma_{xx}}{p_a} \right)^{n-2} - 4\gamma \right] \right\} \quad (24a)$$

gde je:

where:

$$k = \frac{\left[ (c_1^2 + 1/3c_1 - 2/9) - vc_2 \right] \cdot \left\{ \left[ 2c_1^2 + 2/3 \cdot c_1 + \frac{5-4v}{9(1+v)} \right] + (1-v)c_2 \right\}}{\left[ (c_1 + 2/3)^2 + c_2 \right] \cdot \left[ 2(c_1 - 1/3)^2 + (1-v)c_2 \right]} \quad (24b)$$

$$c_1 = \left( \frac{3\sigma_0}{\sigma_{xx}} + 1 \right) \left[ n \alpha \left( \frac{3\sigma_0 + \sigma_{xx}}{p_a} \right)^{n-2} - 2\gamma \right] \frac{1}{\sqrt{1-\beta}} \quad (24c)$$

$$c_2 = \frac{a_1 \eta p_a^2}{\xi^{(\eta+1)} E \sigma_{xx}} \left( \frac{3\sigma_0 + \sigma_{xx}}{p_a} \right)^n \cdot \sqrt{\left( \frac{3\sigma_0}{\sigma_{xx}} + 1 \right)^2 \left[ n \alpha \left( \frac{3\sigma_0 + \sigma_{xx}}{p_a} \right)^{n-2} - 2\gamma \right]^2 \frac{3}{(1-\beta)^3} + \frac{2}{3(1-\beta)}} \quad (24d)$$

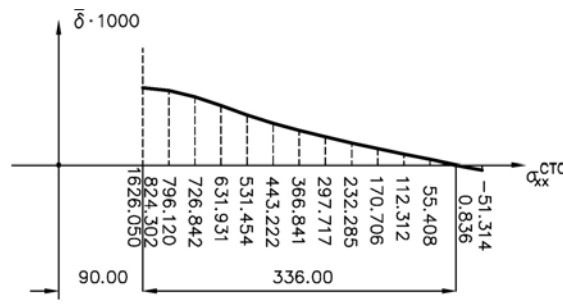
Nakon nekoliko transformacija, jednačina (24) se može prikazati u formi

After few simple transformations the equation (24) can be written in the form

$$\bar{\delta} = \left[ n^2 \frac{\eta}{\eta+1} + n(n-1) \right] \alpha \left( \frac{3\sigma_0 + \sigma_{xx}}{p_a} \right)^{n-2} - 2\gamma + \left( \frac{1+k}{1-2k} \right)^2 \frac{2\sqrt{1-\beta}}{3} = 0 \quad (25)$$

Rešenje karakteristične jednačine stabilnosti (25) prikazano je na slici 2. Najnepovoljnije ravni - u pogledu kritičnog naponskog stanja - biće one kod kojih ugao između totalnog napona i normale na ravan ima najveću vrednost.

Solution to the characteristic equation of stability of deformation (25) is shown in Fig. 2. The least favorable planes, from the critical stress point of view, are those at which the angle between the total stress and normal vector to the plane has the maximum value.

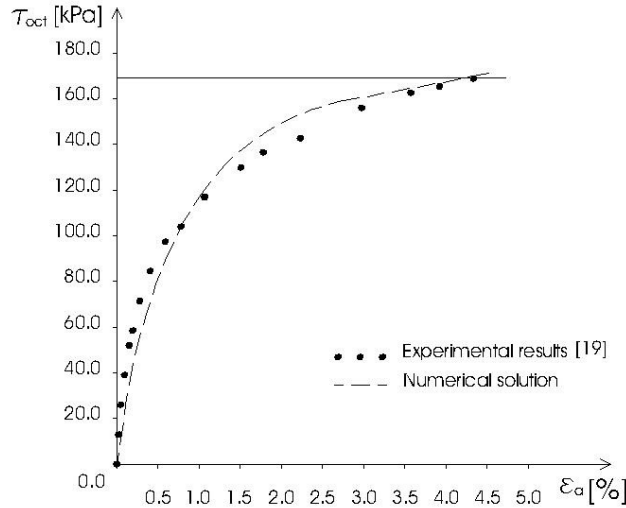


Slika 2. Konvencionalna trijaksijalna kompresija - rešenje jednačine stabilnosti  
Figure 2. Case of conventional triaxial compression - solution for stability equation

Kao što se vidi s dijagrama, nagib krive je negativan, ali je vrednost  $\bar{\delta}$  pozitivna (uslov dat izrazom (16)) i postoji ravnomernost u opadanju u tom pravcu ka vrednosti gde je krivina jednaka nuli. U tački gde je  $\bar{\delta} = 0$  (15), ta tačka površine je nazvana parabolička. Na osnovu prikazanog dijagrama, jasno se vidi da je kritična vrednost sračunata numeričkim postupkom  $\sigma_{xx}^{CTC} = 336$  [kPa]. Eksperimentalni podaci prikazani su na slici 3. (na osnovu podataka prikazanih u Referenci

As can be seen from the diagram, slope of the curve is negative but  $\bar{\delta}$  is positive (condition given by the equation  $\bar{\delta} = U^2 - T \cdot V > 0$ ) with relative equality in stress increment towards the value where y-axis approaches zero. At the point where y-axis is zero, that point is called parabolic ( $\bar{\delta} = U^2 - T \cdot V = 0$ ). As clearly stated on the diagram, critical stress value for the numerical model  $\sigma_{xx}^{CTC} = 336$  [kPa].

Experimental data is shown in Figure 3. (based on



Slika 3. Poređenje eksperimentalnih i numeričkih rezultata za CTC test.  
Figure 3. Comparing experimental and numerical results for CTC case

Iz priloženih podataka, uočava se da je kritična vrednost oktaedarskog napona smicanja  $\tau_{oct}^{CTC} = 168,90$  [kPa], odnosno koristeći izraz  $\tau_{oct} = \sqrt{2/3} \cdot I_{2d}$  može se odrediti vrednost kritičnog normalnog napona  $\sigma_{xx}^{CTC} = 358,30$  [kPa].

**Ilustracija # 2:** Test trijaksijalne kompresije (TC). Za test trijaksijalne kompresije komponente napona i komponente devijatora napona mogu se predstaviti u obliku:

$$\sigma^{TC} = \begin{bmatrix} \sigma_0 + \sigma_{xx} & 0 & 0 \\ 0 & \sigma_0 - 1/2 \sigma_{xx} & 0 \\ 0 & 0 & \sigma_0 - 1/2 \sigma_{xx} \end{bmatrix}, S^{TC} \Rightarrow \frac{\sigma_{xx}}{2} \begin{bmatrix} 2 & 0 & 0 \\ 0 & -1 & 0 \\ 0 & 0 & -1 \end{bmatrix} \quad (26)$$

Uvodeći jednačinu (26) u (21) i zamenjujući u (15), dobija se sledeći izraz:

Introducing (26) into (21) and substituting this equation in the (15), leads to:

$$\delta = (1-2k)^2 n^2 \frac{p_a^{-4} a_1^2 \eta^2 \xi^{-2(\eta+1)}}{(1-\beta)^{\frac{3}{2}}} \left( \frac{3\sigma_0}{p_a} \right)^{2(n-1)} + \frac{p_a^{-4} a_1 \eta (\eta+1) \xi^{-(\eta+2)}}{(1-\beta)^{\frac{3}{2}}} \left( \frac{3\sigma_0}{p_a} \right)^n \cdot \left\{ \left[ \frac{2\sqrt{1-\beta}}{3} + n(n-1)\alpha \left( \frac{3\sigma_0}{p_a} \right)^{n-2} - 2\gamma \right] - \left[ \frac{2\sqrt{1-\beta}}{3} + n(n-1)\alpha \left( \frac{3\sigma_0}{p_a} \right)^{n-2} - 2\gamma \right] + 2k^2 \left[ \frac{\sqrt{1-\beta}}{3} + 2n(n-1)\alpha \left( \frac{3\sigma_0}{p_a} \right)^{n-2} - 4\gamma \right] \right\} \quad (27a)$$

gde je:

where:

$$k = \frac{\left[ \frac{3}{2}(2c_1 - 1) - (1+\nu)c_2 \right] \left[ 2c_1^2 + c_1 + \frac{5-4\nu}{4(1+\nu)} + (1-\nu)c_2 \right]}{\left[ 3(c_1 + 1) + 2(1+\nu)c_2 \right] \left[ 2c_1^2 - 2c_1 + \frac{1}{2} + (1-\nu)c_2 \right]} \quad (27b)$$

$$c_1 = \frac{3\sigma_0}{\sigma_{xx}} \left[ n\alpha \left( \frac{3\sigma_0}{p_a} \right)^{n-2} - 2\gamma \right] \frac{1}{\sqrt{1-\beta}} \quad (27c)$$

$$c_2 = \frac{a_1 \eta p_a^2}{\xi^{(\eta+1)} E \sigma_{xx}} \left( \frac{3\sigma_0}{p_a} \right)^n \sqrt{\left( \frac{3\sigma_0}{\sigma_{xx}} \right)^2 \left[ n \alpha \left( \frac{3\sigma_0}{p_a} \right)^{n-2} - 2\gamma \right]^2 \frac{3}{(1-\beta)^3} + \frac{3}{4(1-\beta)}} \quad (27d)$$

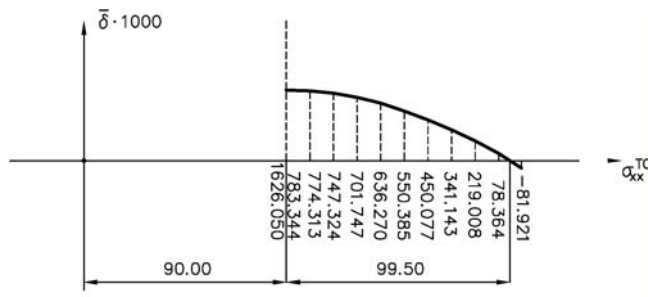
Nakon transformacija, jednačina (27) može se prikazati u formi

After few simple transformations the equation (27) can be written in the form

$$\bar{\delta} = \left[ n^2 \frac{\eta}{\eta+1} + n(n-1) \right] \alpha \left( \frac{3\sigma_0}{p_a} \right)^{n-2} - 2\gamma + \left( \frac{1+k}{1-2k} \right)^2 \frac{2\sqrt{1-\beta}}{3} = 0 \quad (28)$$

Rešenje karakteristične jednačine stabilnosti (28) prikazano je na slici 4.

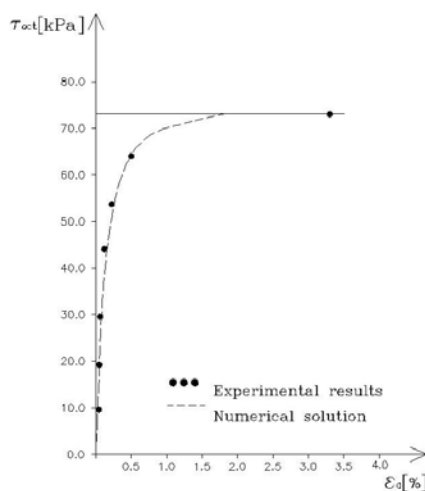
Solution to the characteristic equation of stability of deformation (28) is shown in Fig. 4.



Slika 4. Primer trijaksijale kompresije - Rešenje jednačine stabilnosti  
Figure 4. Case of triaxial compression - solution for stability equation

U tački gde je  $\delta = 0$  (15), na osnovu prikazanog dijagrama, kritična vrednost aksijalnog napona sračunata numeričkim postupkom jeste  $\sigma_{xx}^{TC} = 99,50$  [kPa]. Eksperimentalni podaci prikazani su na slici 5. (na osnovu podataka prikazanih u ref. [Desai, 1989]). Iz priloženih podataka se vidi da je kritična vrednost oktaedarskog napona smicanja  $\tau_{oct}^{TC} = 73,10$  [kPa], odnosno, korišćenjem izraza  $\tau_{oct} = \sqrt{2/3 \cdot I_{2d}}$ , može se odrediti vrednost kritičnog normalnog napona  $\sigma_{xx}^{TC} = 103,36$  [kPa].

At the point where  $\delta = 0$  (15) (for zero y-axis) as clearly shown on the diagram, critical stress value calculated using the numerical model is  $\sigma_{xx}^{TC} = 99.50$  [kPa]. Experimental data is shown in Figure 5 (based on published results from reference Desai 1989). From these results follows that critical value for the octahedral shear stress was  $\tau_{oct}^{TC} = 73.10$  [kPa], which leads to critical normal stress of  $\sigma_{xx}^{TC} = 103.36$  [kPa].



Slika 5. Poređenje eksperimentalnih i numeričkih rezultata za TC test  
Figure 5. Comparing experimental and numerical results for TC case



**Ilustracija # 3:** Test trijaksijalne ekstenzije (TE). Za stanje TE komponentalni naponi i devijator napona dati su sledećim izrazima

$$\sigma^{TE} = \begin{bmatrix} \sigma_0 - \sigma_{xx} & 0 & 0 \\ 0 & \sigma_0 + \sigma_{xx}/2 & 0 \\ 0 & 0 & \sigma_0 + \sigma_{xx}/2 \end{bmatrix}, S^{TE} = \frac{\sigma_{xx}}{2} \begin{bmatrix} -2 & 0 & 0 \\ 0 & 1 & 0 \\ 0 & 0 & 1 \end{bmatrix} \quad (29)$$

Uvođenjem jednačine (29) u (21) i zamenom u jednačinu (15), dobija se:

$$\delta = (1-2k)^2 n^2 \frac{p_a^{-2} a_1 \eta^2 \xi^{-2(\eta+1)}}{(1+\beta)} \left( \frac{3\sigma_0 - \sigma_{xx}}{p_a} \right)^{2(n-1)} + \frac{p_a^{-2} a_1 \eta (\eta+1) \xi^{-(\eta+2)}}{(1+\beta)} \left( \frac{3\sigma_0 - \sigma_{xx}}{p_a} \right)^n \cdot \left\{ \left[ \frac{2\sqrt{1+\beta}}{3} + n(n-1)\alpha \left( \frac{3\sigma_0 - \sigma_{xx}}{p_a} \right)^{n-2} - 2\gamma \right] - 4k \left[ -\frac{\sqrt{1+\beta}}{3} + n(n-1)\alpha \left( \frac{3\sigma_0 - \sigma_{xx}}{p_a} \right)^{n-2} - 2\gamma \right] + 2k^2 \left[ \frac{\sqrt{1+\beta}}{3} + 2n(n-1)\alpha \left( \frac{3\sigma_0 - \sigma_{xx}}{p_a} \right)^{n-2} - 4\gamma \right] \right\} \quad (30a)$$

gde je:

where:

$$k = \frac{\left[ \left( c_1^2 - \frac{1}{3}c_1 - \frac{2}{9} \right) - \nu c_2 \right] \cdot \left\{ \left[ 2c_1^2 - \frac{2}{3}c_1 + \frac{5-4\nu}{9(1+\nu)} \right] + (1-\nu)c_2 \right\}}{\left[ \left( c_1 - \frac{2}{3} \right)^2 + c_2 \right] \cdot \left[ 2 \left( c_1 + \frac{1}{3} \right)^2 + (1-\nu)c_2 \right]} \quad (30b)$$

$$c_1 = \left( \frac{3\sigma_0}{\sigma_{xx}} - 1 \right) \left[ n\alpha \left( \frac{3\sigma_0 - \sigma_{xx}}{p_a} \right)^{n-2} - 2\gamma \right] \frac{1}{\sqrt{1+\beta}} \quad (30c)$$

$$c_2 = \frac{a_1 \eta p_a^2}{\xi^{(\eta+1)} E \sigma_{xx}} \left( \frac{3\sigma_0 - \sigma_{xx}}{p_a} \right)^n \cdot \sqrt{\left( \frac{3\sigma_0}{\sigma_{xx}} - 1 \right)^2 \left[ n\alpha \left( \frac{3\sigma_0 - \sigma_{xx}}{p_a} \right)^{n-2} - 2\gamma \right]^2 \frac{3}{(1+\beta)^3} + \frac{2}{3(1+\beta)}} \quad (30d)$$

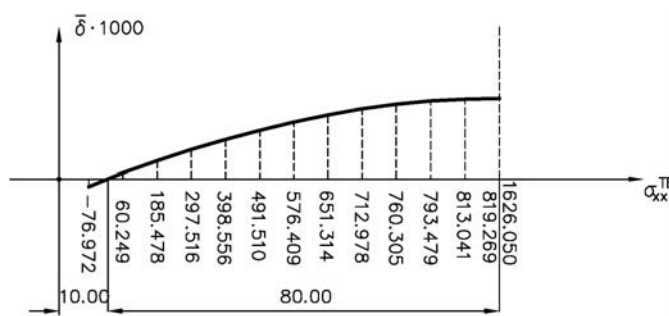
Nakon nekoliko jednostavnih transformacija, (30) može se napisati u formi:

After some simple transformation the equation (30) can be written in the form:

$$\bar{\delta} = \left[ n^2 \frac{\eta}{\eta+1} + n(n-1) \right] \alpha \left( \frac{3\sigma_0 - \sigma_{xx}}{p_a} \right)^{n-2} - 2\gamma + \left( \frac{1+k}{1-2k} \right)^2 \frac{2\sqrt{1+\beta}}{3} = 0 \quad (31)$$

Rešenje karakteristične jednačine (31) prikazano je na slici 6.

Solution to the characteristic equation of stability of deformation (31) is shown in Figure 6.



Slika 6. Primer trijaksijalne ekstenzije - Rešenje jednačine stabilnosti  
Figure 6. Case of triaxial extension - solution for stability equation.

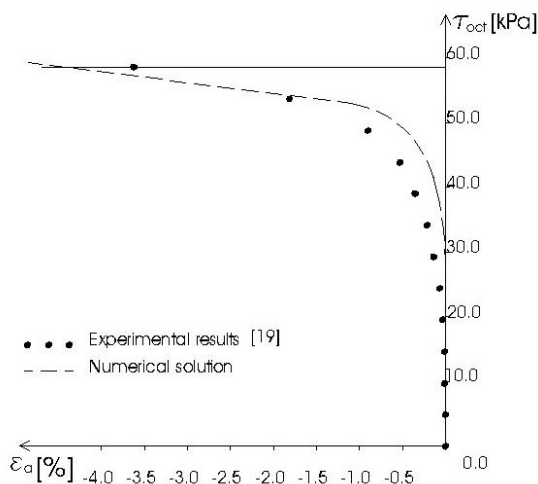
Kao što se vidi s dijagrama, nagib krive je pozitivan (uslov dat izrazom  $\delta > 0$ ).

Na osnovu prikazanog dijagrama, numerički sračunata kritična vrednost napona jeste  $\sigma_{xx}^{TE} = 80$  [kPa].

As can be seen from the diagram, slope of the curve is positive (condition  $\delta = U^2 - T \cdot V > 0$ ). As clearly stated on the diagram, critical stress value for the numerical model  $\sigma_{xx}^{TE} = 80$  [kPa]. Experimental data is

Eksperimentalni podaci prikazani su na slici 7. (Desai, 1989). Kritična vrednost oktaedarskog napona smicanja jeste  $\tau_{oct}^{TE} = 58,54$  [kPa], odnosno može se odrediti vrednost kritičnog normalnog napona  $\sigma_{xx}^{TE} = 82,80$  [kPa].

shown in Figure 7. (based on published results Desai, 1989). From these results follows that critical value for octahedral shear stress was  $\tau_{oct}^{TE} = 58,54$  [kPa], which leads to critical normal stress by substituting into equation (17a)  $\sigma_{xx}^{TE} = 82,80$  [kPa].



Slika 7. Poređenje eksperimentalnih i numeričkih rezultata za TE test  
Figure 7. Comparing experimental and numerical results for TE case.

## ANALIZA REZULTATA

Očigledno je da postoji dobro slaganje između rezultata dobijenih numeričkim postupkom i eksperimentalnih rezultata. Razlika između kritičnog napona određenih numeričkim postupkom i odgovarajućih eksperimentalnih vrednosti za TE test jeste 3.4%, za TC test je 3.7%, dok je za CTC razlika 6.2%.

Prikazan numerički kriterijum za određivanje kritične tačke pogodan je sa stanovišta praktične primene za analizu stabilnosti deformacije geomehaničkih materijala u zavisnosti od geometrije, graničnih uslova i karaktera opterećenja.

Klasični rezultati prikazani u radovima (Hill, 1950), (Rudnicki i sar., 1975) i (Rice, 1976) idu i korak dalje i definišu ugao linije nestabilnosti tečenja. Ugao linije nestabilnosti tečenja možda se može i zamisliti kao ugao analogan lokalizovanju plastične deformacije i pojavi vrata u testu zatezanja u metalnim uzorcima. Međutim, takva analogija primenjena na granularne materijale ne može se funkcionalno povezati sa uglom unutrašnjeg trenja u Mohr-Coulomb-ovom kriterijumu tečenja. U ovom radu ugao linije nestabilnosti tečenja, kao parameter od interesa, nije definisan.

## ANALYSIS OF RESULTS

Experimental and calculated numerical modulation values for critical stress are shown in Table II. It is obvious that there is good agreement between them. Percent difference between critical values predicted with numerical model and experimental results for TE test is only 3.4 %, for TC it is 3.7 % while for CTC it is 6.2 %.

Presented numerical criterion to determine critical loading point is useful from the practical point of view for the analysis of the deformation stability for geomechanical material for defined geometry, boundary conditions and loading path.

Classical results presented in work by Hill, Rudnicki and Rice, go a step further into defining the angle of instability for plastic flow. It is possible to think of this angle as analogous to the onset of localization of plastic deformation and beginning of necking in metallic samples. However, in that analogy for metal samples, angle at which macroscopic slip occurs and the beginning of plastic deformation and angle of necking and the beginning of local deformation are not functionally related. If analogy is applied to granular material, it means that angle of plastic instability is not be related to the angle of internal friction in a Mohr-Coulomb approach to plastic flow. In the presented paper, angle of plastic deformation instability for granular material was not considered to be the parameter of interest.

## ZAKLJUČAK

Prikazana je analiza uslova stabilnosti za granularni materijal. Rezultati dobijeni numeričkom analizom - korišćenjem HISS konstitutivnog modela - upoređeni su s publikovanim dijagramima za pesak (Leighton Buzzard Sand) u eksperimentalnim uslovima trijaksijalne kompresije i zatezanja. Vrednosti za kritični napon u numeričkom testu niže su za 3-6 % od vrednosti u odgovarajućem eksperimentalnom testu. Nedovoljno široka primena HISS modela možda proističe iz potrebe za relativno velikim brojem materijalnih parametara (osam), kao i zbog njihove ograničene zastupljenosti u literaturi.

## LITERATURA REFERENCES

- [1] Borst, de R., „Bifurcations in Finite Elements Models with a Non-associated Flow Law”, Int. J. Numer. Anal. Meth. Geomech., 12(1), pp 99-117 (1988).
- [2] Desai, C.S., Somasundaram, S. and G. Frantziskonis, G. „A HISS approach for constitutive modeling of geological materials”, Int. J. Num. Anal. Meth. Geom., 10(3), pp 225-257, (1987).
- [3] Desai, C.S., „Notes for Advanced School-Numerical Methods in Geomechanics Including Modelling”, Udine, Italy, July 10-14, (1989).
- [4] Drucker, D.C., „Some Implications of Work Hardening and Ideal Plasticity”, Quarterly of Applied Math., 7(4), pp 411-418 (1950).
- [5] Drucker, D.C., „A Definition of Stable Inelastic Material”, ASME Journal of Applied Mechanics, 26, pp 106-112 (1959).
- [6] Hill, R., The mathematical theory of plasticity, Clarendon Press, Oxford, England (1950).
- [7] Lelović, V.S., „Constitutive Equations for Sand and Their Application in Numerical Analysis of Strip Foundation Behavior”, PhD thesis, Civil Engin. Faculty, Universite Belgrade, (2012).

## REZIME

### KRITERIJUM STABILNOSTI DEFORMACIJE ELASTOPLASTIČNIH MATERIJALA

Selimir V. LELOVIĆ

Određivanje kritične tačke moguće je svesti na određivanje onog stanja pri kome dolazi do promene znaka drugog izvoda funkcije tečenja. U ovom radu određeno je kritično opterećenje geomehantičkog materijala numeričkim postupkom, korišćenjem inkrementalno iterativnog algoritma za različite putanje napona. Konstitutivne jednačine za hijerarhijski model (*hierarchical single surface model* - HISS) primenjene su da bi se opisalo ponašanje granularnog materijala u toku deformacije. Rezultati dobijeni numeričkom analizom upoređeni su sa eksperimentalnim rezultatima za pesak (Leighton Buzzard Sand).

**Ključne reči:** stabilnost, gubitak eliptičnosti, kriva površi tečenja, kritično opterećenje, numerička metoda

## CONCLUSION

Criterion for stability of deformation in geomechanical materials is presented. Results obtained using HISS model for numerical analysis were compared with experimental results for particular sand material (Leighton Buzzard Sand) under triaxial compression and extension. Values for critical stress were 3-6 % lower in the numerical prediction compared with experimental data. That small difference in critical values may be considered as a good agreement. However, the main drawback of the HISS model may be its requirement for eight material parameters and limited availability of those parameters in the published literature.

- [8] Mandel, J., „Conditions de Stabilite et Postulat de Drucker”, Proc. IUTAM Symp. Rheology and Soil Mechanics, Grenoble (Ed. Kravtchenko, J. and Sirieys, P.M.), pp 57-58, (1964).
- [9] Molenkamp, F., „Comparison of frictional material models with respect to shear band initiation”, Geotechnique, 35, pp 127-143 (1985).
- [10] Mroz, Z., „Nonassociated flow laws in plasticity”, J. de Mechanique, 2(1), pp 21-42 (1963)
- [11] Rice, J.R., „The Localization of Plastic Deformation”, Proc. 14th Int. Cong. Theoretical and Appl. Mech., Delft (Ed. W.T. Koiter), 1, pp 207-220, Delft, North-Holland, Amsterdam (1976).
- [12] Rudnicki, J.W., and Rice, J.R., „Conditions for the Localization of Deformation in Pressure-Sensitive Dilatant Materials”, J.Mech.Phys.Solids, 23, pp 371-394 (1975).
- [13] Vardoulakis, I., „Shear band Inclination and Shear Modulus of Sand in Biaxial Tests”, Int. J. Numer. Anal. Meth. Geomech., 4(2), pp 103-121 (1980).

## SUMMARY

### CONDITIONS FOR STABILITY OF DEFORMATION IN ELASTO-PLASTIC MATERIALS

Selimir V. LELOVIC

It is possible to look at the critical point determination as a sign change in the second derivative of the yield function. Numerical method in determining critical stress in geomechanical material using an iterative algorithm for different loading paths is presented. The constitutive relationships of the hierarchical single surface (HISS) model were used to describe the granular material during deformation. Critical stresses under applied triaxial compression and extension obtained numerically were compared with published experimental results for Leighton Buzzard Sand

**Key words:** stability, loss of ellipticity, curvature of yield surface, critical loading, numerical solution



# UNAKRSNO LAMELIRANI DRVENI ELEMENTI U SAVREMENIM DRVENIM KONSTRUKCIJAMA ZGRADA – primena i proračun

## CROSS LAMINATED TIMBER ELEMENTS IN CONTEMPORARY TIMBER STRUCTURES OF BUILDINGS – application and design

Ljiljana KOZARIĆ  
Aleksandar PROKIĆ  
Miroslav BEŠEVIĆ

STRUČNI RAD  
PROFESSIONAL PAPER  
UDK: 624.011.1  
doi: 10.5937/grmk1504051K

### 1 UVOD

Drvo je jedan od najstarijih građevinskih materijala i pored kamena je dugi niz godina bio osnovni materijal za građenje. Njegove karakteristike omogućavaju visok stepen prefabrikacije, brzu montažu na terenu i trenutnu useljivost. Zbog velike požarne otpornosti u požaru ne gubi nosiva svojstva, odnosno mehaničke karakteristike ne menjaju se bitno prilikom visokih temperatura. Drvene konstrukcije su pet puta lakše od armiranobetonskih, pa mogu lakše preuzeti seizmičke sile i predstavljaju dobar izbor u trusnim područjima. Objekti izgrađeni od drveta imaju visoku energetska efikasnost.

Poslednjih decenija, drvo se sve više primenjuje u izgradnji modernih arhitektonskih građevina (npr. sportskih objekata, stambenih zgrada, mostova) zahvaljujući boljem poznavanju drveta kao materijala, primeni savremenih drvenih konstrukcija i upotrebi kvalitetnih spojnih sredstava. Konstruktivni elementi savremenih drvenih konstrukcija bazirani su prvenstveno na savremenim proizvodima od drveta kao što su lepljeno lamelirano i unakrsno lamelirano drvo.

---

Ljiljana Kozarić, dipl. inž. građ., Univerzitet u Novom Sadu, Građevinski fakultet Subotica, Kozaračka 2a, Subotica, Srbija, tel.: 024 554 300, e-mail: [kozaric@gf.uns.ac.rs](mailto:kozaric@gf.uns.ac.rs)  
Prof.dr Aleksandar Prokić, dipl. inž. građ., Univerzitet u Novom Sadu, Građevinski fakultet Subotica, Kozaračka 2a, Subotica, Srbija, tel.: 024 554 300  
e-mail: [aprokic@eunet.rs](mailto:aprokic@eunet.rs)  
Prof.dr Miroslav Bešević, dipl. inž. građ., Univerzitet u Novom Sadu, Građevinski fakultet Subotica, Kozaračka 2a, Subotica, Srbija, tel.: 024 554 300  
e-mail [miroslav.besevic@gmail.com](mailto:miroslav.besevic@gmail.com)

### 1 INTRODUCTION

Wood is one of the oldest building materials and along with stone it is the basic building material. Its characteristics allow for a high degree of prefabrication, quick assembly, and immediate utilization. Wood has great fire resistance, and during the fire retains its characteristics, i.e. its mechanical properties do not change significantly due to high temperatures. Timber constructions are five times lighter than reinforced concrete, thus they are better capable of weathering seismic forces and stand out as material of choice for earthquake prone areas. Timber constructions have high energy efficiency.

Within last few decades, wood has been increasingly used in modern architectural buildings (sports' arenas, residential buildings and bridges) thanks to better understanding of wood as a material, utilization of modern timber construction and high quality connections. Construction elements for contemporary timber constructions are primarily based upon contemporary products such as glued laminated timber and cross laminated timber.

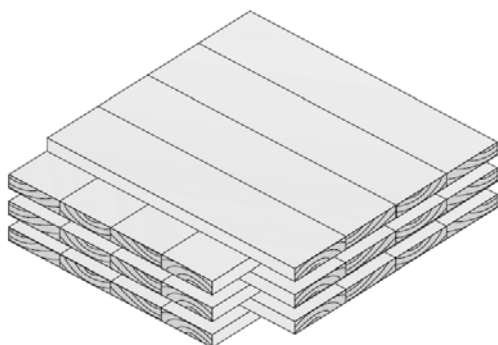
---

Ljiljana Kozarić, dipl.inž. građ., University of Novi Sad, Faculty of Civil Engineering, Subotica, Kozaračka 2a, Serbia, tel: 024 554 300, e-mail: [kozaric@gf.uns.ac.rs](mailto:kozaric@gf.uns.ac.rs)  
Prof.dr Aleksandar Prokić, dipl.inž. građ., University of Novi Sad, Faculty of Civil Engineering, Subotica, Kozaračka 2a, Serbia, tel: 024 554 300, e-mail: [aprokic@eunet.rs](mailto:aprokic@eunet.rs)  
Prof.dr Miroslav Bešević, dipl.inž. građ., University of Novi Sad, Faculty of Civil Engineering, Subotica, Kozaračka 2a, Serbia, tel: 024 554 300  
e-mail: [miroslav.besevic@gmail.com](mailto:miroslav.besevic@gmail.com)

Cilj rada jeste da se stručna javnost u Srbiji upozna s primenom unakrsno lameliranih drvenih panela u konstrukcijama, kao i s načinom proračuna pojedinih konstruktivnih elemenata.

## 2 UNAKRSNO LAMELIRANO DRVO – CLT

Unakrsno lamelirano drvo je moderan proizvod, visoke tehnologije koji je u mnogome unapredio fizičke osobine monolitnog drveta. CLT se proizvodi od kontrolisano sušenih drvenih elemenata podjednake širine - lamela, kojima su uklonjeni nedostaci (npr. čvorovi, smola). Izdvajanjem tih nedostataka i slojevitim, unakrsnim lepljenjem, dobija se materijal koji ima mehaničke karakteristike ujednačenije od mehaničkih karakteristika monolitnog drveta - slika 1.



Slika 1. Unakrsno lamelirano drvo [1]  
Figure 1. Cross laminated timber [1]

Kao kod šperploča, slojevi mekog drveta postavljaju se tako da vlakna drveta budu međusobno pod pravim uglom. Unakrsno slaganje drveta pruža stabilnost, kao i kod obične šperploče, ali veća debljina slojeva stvara panele koji su dovoljno jaki da budu korišćeni kao konstruktivni elementi, bez potrebe za ojačanjem konstrukcije upotrebom opeke ili betona - slika 2.

Objective of this paper is to introduce possibilities of application of cross laminated timber panels in structures in Serbia, as well as the way the individual structural elements can be calculated.

## 2 CROSS LAMINATED TIMBER – CLT

Cross laminated timber (CLT) is a sophisticated modern product that greatly improved the physical properties of traditional wood as building material. CLT is made of controlled dried wooden elements – laminates of uniform width, free of defects (knots, resin etc.). By removing all of the defects and cross-gluing the laminates it is possible to produce the material that has more uniform mechanical properties than the traditional wood, Figure 1.

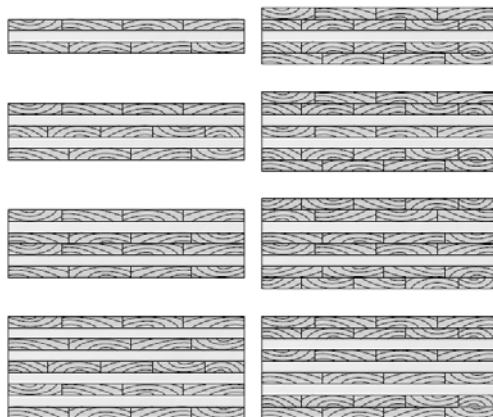
Just like with plywood, the layers of soft wood are positioned in such manner that the wooden grain of adjacent layers are mutually perpendicular. As with plywood, perpendicularly positioned elements create stability; however, greater layer thickness creates panels that are strong enough to be used as a primary structural elements without the need for brick or concrete as reinforcement, Figure 2.



Slika 2. CLT konstrukcija [2]  
Figure 2. CLT construction [2]

Poprečni preseki CLT panela sadrže najmanje tri unakrsno zalepljene lamele, a najčešće pet ili sedam. Slojevi s lamelama postavljeni su naizmenično pod pravim uglom, ali se pojedini slojevi mogu i duplirati, stvarajući tako panele s većom nosivošću u potrebnom pravcu - slika 3. Visina lamela u CLT panelima varira od 16 mm do 51 mm, a širina od 60 mm do 240 mm.

Spoljne lamele u zidnim CLT panelima postavljaju se uspravno, paralelno sa silom gravitacije, radi maksimalnog iskorišćenja vertikalne nosivosti panela. Kod podnih i krovnih CLT panela, spoljne lamele postavljaju se paralelno s pravcem dominantnog opterećenja. Spoljašnje površine panela - zbog estetskih zahteva, te zbog zahteva vatrootpornosti i zvučne izolacije - mogu se obložiti gips-kartonskim pločama ili nekom drugom pogodnom oblogom.



Slika 3. Poprečni preseki CLT panela [3]  
Figure 3. CLT Panel cross sections [3]

U Evropi, CLT paneli najčešće se proizvode od četinarara klase čvrstoće C24, vlažnosti  $12\pm 2\%$  - [4]. Dimenzije panela zavise od raspoložive tehnologije proizvođača, ali i od načina transporta.

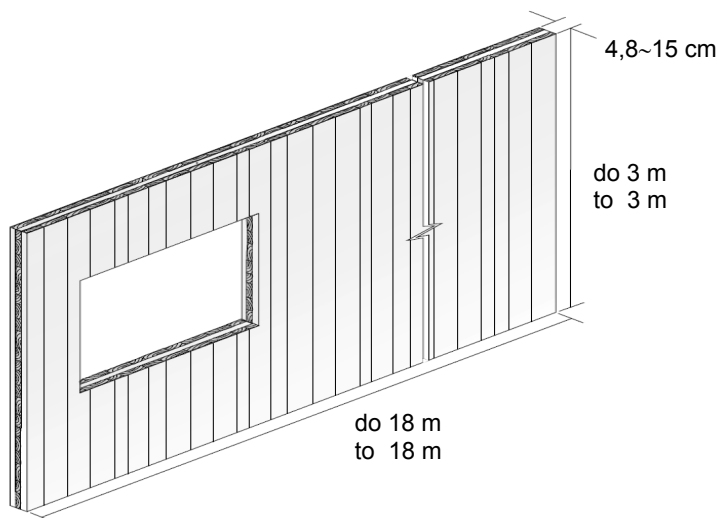
Zidni CLT paneli isporučuju se na gradilište s već formiranim otvorima po projektu. Tipičan zidni CLT panel prikazan je na slici 4.

A CLT cross section contains a minimum of three cross-glued laminates, but most often five or seven. Alternate layers are mutually perpendicular; however, it is possible to double certain layers so that greater strength can be achieved in a desired direction, Figure 3. Laminate height within a CLT varies from 16 to 51 mm while width varies between 60mm and 240mm.

Outside laminates within a CLT wall are positioned vertically, parallel with the gravitational forces so that vertical potential of the panel can be maximized, while in CLT panels for floor and roof applications are placed parallel with the direction of dominant forces. To meet aesthetic, fireproof, and insulation requirements, the exposed surfaces of the panels can be covered with gypsum or similar appropriate finish.

In Europe, CLT is most often manufactured from conifers grade C24, and moisture content  $12\pm 2\%$ , [4]. Panel dimensions are dictated by manufacturer technology and mode of transportation.

Wall CLT panels are delivered to a construction site where the wall openings have already been formed according to design. A typical CLT wall panel is shown in Figure 4.



Slika 4. Zidni CLT paneli [3]  
Figure 4. Typical Wall CLT panel [3]

Podne i krovne konstrukcije dobijaju se horizontalnim ili kosim slaganjem osnovnih panela. Tipične dimenzije osnovnog podnog i krovnog panela prikazane su na slici 5.

Među najveće evropske proizvođače CLT panela svrstavaju se: KLH (Austrija, UK, Švedska), Binderholz (Austrija), Martinsons (Švedska), Moelven (Norveška), Stora Enso (Austrija), Thoma Holz GmbH (Austrija), FinnForest Merk (Nemačka, UK), HMS (Nemačka).

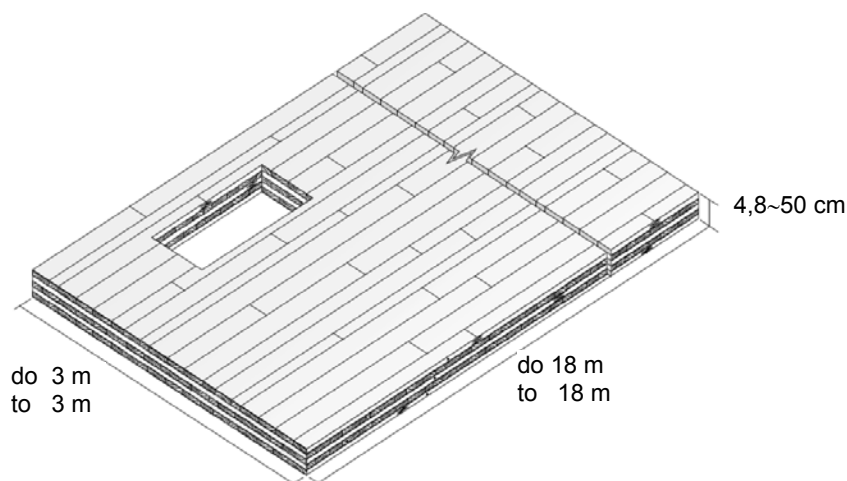
Svi navedeni proizvođači koriste isti proces proizvodnje, glavna razlika je u dimenzijama CLT panela i u izboru lepka.

Osnovne fizičko-mehaničke karakteristike CLT panela s daskama od četinaru klase čvrstoće C24 (minimalno 90%) i C16 (maksimalno 10%) date su u Tabeli 1.

Floor and roof construction are manufactured by arranging the basic panels in horizontal or angular pattern. Typical dimensions of basic floor or roof panel are depicted in Figure 5. Some of the biggest European CLT panels manufacturers are: KLH (Austria, UK, Sweden), Binderholz (Austria), Martinsons (Sweden), Moelven (Norway), Stora Enso (Austria), Thoma Holz GmbH (Austria), FinnForest Merk (Germany, UK) and HMS (Germany).

All of the above listed manufacturers use the same manufacturing process, while the main differences are panels' dimensions, and the choice of glue.

Basic physical and mechanical properties of CLT panels with planks made out of conifers grade C24 (minimum 90%) and C16 (maximum 10%) are listed in Table 1.



Slika 5. Podni i krovni CLT paneli [3]  
Figure 5. Floor and Roof CLT panel [3]

Tabela 1. Osnovne fizičko-mehaničke karakteristike CLT panela [5]  
Table 1. Basic physical and mechanical properties of CLT panels [5]

Karakteristične čvrstoće [N/mm <sup>2</sup> ] / Characteristic strength [N/mm <sup>2</sup> ]		
Savijanje / Bending	$f_{m,k}$	24
Zatezanje paralelno s vlaknima / Tension along the grain	$f_{t,0,k}$	16,5
Zatezanje upravno na vlakna / Tension across the grain	$f_{t,90,k}$	0,12
Pritisak paralelno s vlaknima / Compression along the grain	$f_{c,0,k}$	24–30
Pritisak upravno na vlakna / Compression across the grain	$f_{c,90,k}$	2,7
Karakteristične krutosti [N/mm <sup>2</sup> ] / Characteristic stiffness [N/mm <sup>2</sup> ]		
Srednja vrednost modula E paralelno s vlaknima Median value of modulus of elasticity E along the grain	$E_{0,mean}$	12000
Srednja vrednost modula E upravno s vlaknima Median value of modulus of elasticity E across the grain	$E_{90,mean}$	370
Zapreminska masa [kg/m <sup>3</sup> ] / Specific weight [kg/m <sup>3</sup> ]	$\rho$	480–500
Koeficijent toplotne provodljivosti [W/(mK)] Thermal conductivity coefficient [W/(mK)]	$\lambda$	0,13
Dopušteni ugib / Allowable deflection	$u_{max}$	$l/250$



U svetu, CLT konstrukcije doživele su veliki uspon iz sledećih razloga: neuporedivo su čvršće i imaju bolje statičke osobine od monolitnog drveta, nemaju sklonost ka uvijanju, pojava napuklina svedena je na minimum, velika požarna otpornost, visoka otpornost na potres.

Upotrebom CLT panela smanjuje se vreme izgradnje, jer se drveni elementi isporučuju kao prefabrikovani zidovi ili moduli, koji se zatim brzo uklapaju na gradilištu. Izgradnja CLT konstrukcije je oko 30% brža u poređenju sa odgovarajućom betonskom konstrukcijom. Takođe, drvo je „suv“ građevinski materijal, njemu ne treba vreme da se osuši ili očvrsne, kao što je to slučaj s betonom ili opekom. Za CLT panele koristi se mekano drvo koje raste brzo i kog ima u izobilju, pa je i cena CLT konstrukcija niža od 5 do 10% od odgovarajućih betonskih ili čeličnih [6].

Drvo je obnovljiv izvor, što je velika prednost, kao i to što u toku rasta vezuje velike količine ugljen-dioksida. Za proizvodnju tone betona potrebno je pet puta, za čelik 24 puta, dok je za tonu aluminijuma potrebno 126 puta više energije nego za proizvodnju materijala od drveta. Drvo je i mnogo bolji izolator i to pet puta bolji od betona i čak 350 puta bolji nego što je to čelik [7].

### 3 PRIMERI IZVEDENIH CLT KONSTRUKCIJA

#### 3.1 Stambena zgrada Forte u Melburnu

Zgrada Forte trenutno je najviša stambena zgrada izgrađena od drveta na svetu. Projektovala ju je i izgradila kompanija Lend Lease 2013. godine. Visoka je 32,17 metara. U prizemlju su poslovni prostori, a na spratovima ima 23 stana - slika 6.



Worldwide, CLT became greatly popular for the following reasons: CLT is much stronger with far more superior mechanical properties than traditional wood, no bending tendency, minimal fractures appearance, high resistance to fire, and resilience to earthquakes.

Since CLT is delivered to construction site in prefabricated or modular form it takes on average 30% less time to complete CLT than a comparable concrete or brick and mortar project. Contributing to the speed of completion is also the fact that unlike concrete, timber is “dry” building material that does not require either the time to dry, or the time to cure and achieve its final strength. Fast growing easily accessible softwood keeps the price of CLT 5 to 10% lower than the competing concrete or steel construction [6].

Timber's great advantage is that it is a renewable resource, and in the process of growth trees absorb great amount of carbon dioxide. To produce one ton of concrete, steel or aluminium it takes 5, 24 and 126 times more energy respectively than for the production of timber. Timber is 5 times better insulator than concrete and up to 350 times better than steel [7].

### 3 EXAMPLES OF CLT APPLICATIONS

#### 3.1 Apartment building Forte in Melbourne, Australia

Forte is currently the tallest residential timber building in the world. The design and construction has been done in 2013 by Lend Lease. The apartment building is 32,17m tall. At the ground floor there are commercial spaces, and 23 apartments in the above floors, Figure 6.



Slika 6. Zgrada Forte u Melburnu  
Figure 6. Forte Residential Building in Melbourne, Australia

Osnovni konstruktivni elementi su drveni zidni paneli i podne ploče. Za izgradnju je bilo potrebno 759 CLT panela, odnosno 485 tona drvene građe. Zgrada Forte je prva stambena zgrada sertifikovana s pet zvezda programa Green Star As Built u Australiji.

Drvena građa u ovom objektu skladišti 761 tonu ugljenika, a odabirom CLT konstrukcije količina ugljen-dioksida u atmosferi se smanjila ukupno za oko 1 451 tonu, jer bi se pri izgradnji sličnog objekta od betona ili čelika, u atmosferu ispuštao dodatni ugljen-dioksid. Ta

Basic design elements are wooden wall and floor panels. It took 759 CLT panels, or 485 tons of wooden material for construction. Forte residential building is the first Five Star Green Star as built rating in Australia. The wooden material in this building stores 761 ton of carbon, and by choosing CLT over concrete or steel the total amount of carbon dioxide released in the atmosphere has been reduced by 1,451 tons. This amount represents the equivalent of the carbon dioxide released by 345 cars during one year [8].

količina ugljen-dioksida predstavlja 345 automobila manje na ulici u toku jedne godine [8].

### 3.2 Stambena zgrada Stadthaus u Londonu

Zgrada Stadthaus sagrađena je 2008. godine u Londonu i pune dve godine bila je najviša drvena stambena zgrada na svetu. Ovu devetospratnicu projektovala je kompanija Waugh Thistleton Architects. Podovi, plafoni, kućište lifta i stepeništa izrađeni su u potpunosti od drveta - slika 7.



Slika 7. Zgrada Stadthaus u Londonu  
Figure 7. Stadthaus Residential Building in London, UK

Korisna površina stambene zgrade jeste 2.352 m<sup>2</sup> i za izgradnju bilo je potrebno 950 m<sup>3</sup> CLT panela. Zidni paneli bili su debljine 128 mm, a podni - 146 mm. Za izgradnju jednog sprata bilo je potrebno tri dana. U poređenju s betonskom konstrukcijom, projektanti su izborom CLT konstrukcije uštedeli dvadeset dve nedelje gradnje, što predstavlja uštedu u vremenu od oko 30%.

Drvo ugrađeno u Stadthaus čuva oko 186 tona ugljenika, dok bi se za čelik i beton koji se koriste u konvencionalnom građevinarstvu, za sličnu građevinu, u atmosferu isпустиo oko 137 tona ugljen-dioksida u procesu proizvodnje. Dakle, ovakav način gradnje smanjio bi količinu ugljen-dioksida u atmosferi za oko 323 tone [9].

### 3.3 Srednja škola u Noriču UK

Objekat se nalazi u Noriču i trenutno je najveća CLT konstrukcija u Ujedinjenom kraljevstvu. Sagrađena je krajem 2009. godine. Glavni arhitekta bio je Sheppard Robson. Korisna površina objekta iznosi 9.500 m<sup>2</sup>, a za izgradnju bilo je potrebno 3.065 m<sup>3</sup> CLT panela. Kompletna konstrukcija ovog trospratnog objekta izgrađena je za šesnaest nedelja. Fiskulturnu salu u sklopu škole od 600 m<sup>2</sup> (slika 8) montirala su četiri radnika za četiri dana. Za montažu jednog zidnog CLT panela dimenzije 3 m x 6 m debljine 15 cm, bilo je potrebno samo tri sata.

### 3.2 Stadthaus Residential Building in London, UK

Stadthaus Residential building was built in 2008 and for full two year was the world's tallest timber residential building. This nine story building has been designed by Waugh Thistleton Architects. Floors, ceilings, elevator shaft and stair flights were built completely out of timber, Figure 7.

Buildings used area is 2,352 m<sup>2</sup> and it took 950 m<sup>3</sup> of CLT panels for construction. Wall panels' thickness varies from 128 mm to 146 mm. It took three days for completion of one story. Compared to a concrete building construction, the CLT method is 22 weeks faster, which amounts to total time reduction of about 30%.

The amount of wood in Stadthaus stores 186 tons of carbon, while for construction of conventional steel or concrete building of this size 137 tons of carbon dioxide would have been released in the atmosphere. As a result, CLT method reduces the total carbon dioxide footprint for 323 tons [9].

### 3.3 High School in Norwich, UK

The School is located in Norwich and currently is the largest CLT construction in the United Kingdom. It was built in 2009. The lead architect was Sheppard Robson. Building's used area is 9,500 m<sup>2</sup>, and it took 3,065 m<sup>3</sup> of CLT panels for its completion. The construction of this three story building was completed in 16 weeks. The 600 m<sup>2</sup> gymnasium within the school building was assembled by 4 workers in 4 days, Figure 8. It takes only 3 hours for the installation of one 3 m by 6 m wall CLT panel.



*Slika 8. Srednja škola u Noriču UK*  
*Figure 8. High School in Norwich, UK*

Zidovi i podovi su CLT paneli, dok su gredni nosači izvedeni od lepljenog-lameliranog drveta - slika 6. Prosečan raspon međuspratnih CLT ploča iznosi 7,5 metara, sa osnovnom frekvencijom oscilovanja od 8 Hz - slika 9.

CLT panels were used for the walls and floors, while the girders were built from glued laminated timber, Figure 9. The average span of the floor CLT panels is 7,5 meters with base frequency of 8 Hz, Figure 17.



*Slika 9. Izgradnja srednje škole u Noriču UK*  
*Figure 9. Construction of High School in Norwich, UK*

#### 4 DIMENZIONISANJE ELEMENATA CLT KONSTRUKCIJA

Proizvođači CLT panela u Evropi nemaju jedinstveni analitički pristup prilikom dimenzionisanja elemenata CLT konstrukcija. Za dimenzionisanje međuspratnih i krovnih konstrukcija od CLT panela najčešće se koriste [1] [10]: Gamma metod (Evrokod 5), K-metod (Teorija kompozita), Kreuzinger-ova analogija i Uprošćen postupak proračuna.

Zidni CLT paneli dimenzionišu se kao pritisnuti štapovi složenog preseka, spojeni mehaničkim spojnim sredstvima (Evrokod 5).

#### 4 DESIGNING THE ELEMENTS FOR CLT CONSTRUCTION

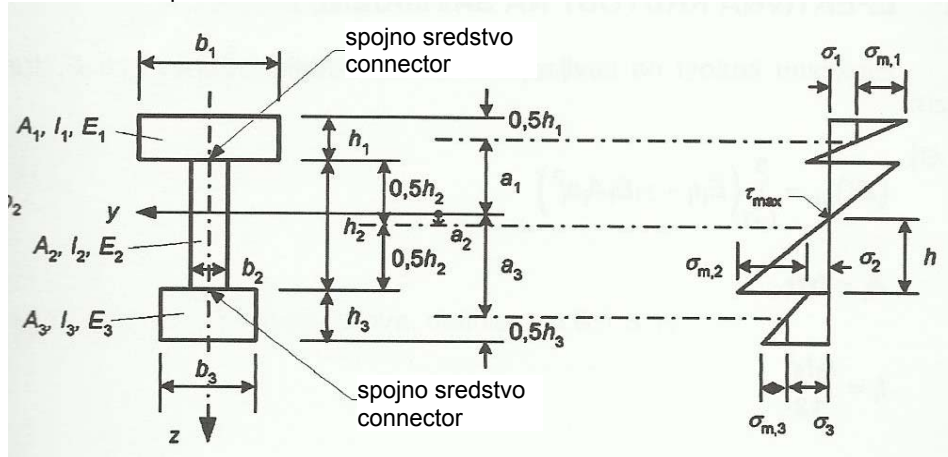
CLT manufacturers in Europe do not have unified analytical approach for the design of elements for CLT construction. The following methods are most frequently used for the floor and roof CLT design, [1] [10]: Gamma Method (Eurocode 5), K – Method (Composite theory), Kreuzinger Analogy and Simplified Design Methods.

CLT wall panels are calculated as mechanically joined compressed columns with complex cross section (Eurocode 5).

#### 4.1 Gamma metod

Gamma metod zasnovan je na Aneksu B Evrokoda 5 (EN 1995-1-1:2004) [11] koji je razvijen za gredne nosače složenog poprečnog preseka, spojene mehaničkim spojnim sredstvima krutosti  $k$  postavljenim na jednakim rastojanjima  $s$ . Prilikom proračuna CLT panela, uzimaju se u obzir samo podužne lamele to jest lamele u pravcu delovanja opterećenja. One se modeliraju kao gredni nosači koji su povezani „imaginarnim“ mehaničkim spojnim sredstvima čija je krutost jednaka modulu smicanja upravno na vlakna poprečnih lamela. Smicanje podužnih lamela zanemaruje se ako je odnos raspona i visine lamele  $\geq 30$ .

Ovaj metod proračuna prikladan je za slobodno oslonjene međuspratne i krovne CLT panele sa 3 ili 5 lamela.



Legenda / Legend:

- (1) razmak / span  $s_1$  modul pomerljivosti / displacement modulus  $K_1$  opterećenje / load  $F_1$   
 (2) razmak / span  $s_2$  modul pomerljivosti / displacement modulus  $K_2$  opterećenje / load  $F_2$

Slika 10. Model CLT panela sa 5 lamela [11]  
 Figure 10. CLT Panel with 5 laminates [11]

Efektivna krutost na savijanje računa se prema izrazu

Effective stiffness can be calculated based on the following expression:

$$(EI)_{ef} = \sum_{i=1}^3 (E_i I_i + \gamma_i E_i A_i a_i^2) \quad (1)$$

gde su simboli definisani na slici 10, a  $\gamma$  predstavlja meru efikasnosti veze i ima vrednost od 0 do 1. Kad nema spojnog sredstva u vezi  $\gamma = 0$  a kod potpuno krute veze (potpunog sprezanja)  $\gamma = 1$ . Kod CLT panela  $\gamma = 0,85 \div 0,99$ .

where the symbols have been defined in Figure 10, and  $\gamma$  represent the effectiveness of the connection with its value ranging from 0 to 1. For the connection with no connectors,  $\gamma = 0$ , while for fully fixed connection (coupling)  $\gamma = 1$ . For CLT panels  $\gamma = 0,85 \div 0,99$

U Evrokodu 5  $\gamma$  definisana je kao

Eurocode 5 defines  $\gamma$  as:

$$\gamma_i = \left[ 1 + \frac{\pi^2 E_i A_i s_i}{K_i I_i^2} \right]^{-1} \quad (2)$$

za  $i=1$  i  $i=3$

for  $i=1$  and  $i=3$

Uzimajući u obzir da je krutost „imaginarnih“ mehaničkih spojnih sredstava jednaka modulu smicanja upravno na vlakna poprečnih lamela

If taken into consideration that the stiffness of “imaginary” mechanical connectors is equal to the shear modulus along the grain of lateral laminates then:

$$\frac{s_i}{K_i} = \frac{\bar{h}_i}{G_R \cdot b} \quad (3)$$

gde je  $b$  širina panela (obično 1 m)  
 $\bar{h}_i$  visina poprečne lamele

where  $b$  is width of a panel (usually 1 m)  
 $\bar{h}_i$  is height of the lateral laminate

$G_R$  modul smicanja upravno na vlakna poprečnih lamela

$G_R$  is shear modulus along the grain of lateral laminates

za CLT panele dobija se da je

Expression for CLT panels is given as:

$$\gamma_i = \left[ 1 + \frac{\pi^2 E_i A_i}{l^2} \cdot \frac{\bar{h}_i}{G_R \cdot b} \right]^{-1} \quad (4)$$

za  $i=1$  i  $i=3$

for  $i=1$  and  $i=3$

Normalni napon računa se kao

Normal stress can be calculated as

$$\sigma_{i \max} = \sigma_{i \text{ global}} + \sigma_{i \text{ local}} \quad (5)$$

gde je

where

$$\sigma_{i \text{ global}} = \frac{\gamma_i E_i a_i M}{(EI)_{ef}} \quad (6)$$

$$\sigma_{i \text{ local}} = \frac{0,5 E_i h_i M}{(EI)_{ef}}$$

#### 4.2 K - metod (Blass&Fellmoser)

Prilikom proračuna ovom metodom, u obzir se uzima krutost svih lamela. Modul elastičnosti poprečnih lamela računa se kao

#### 4.3 K - method (Blass&Fellmoser)

This design method includes the stiffness of all laminates. Modulus of elasticity of lateral laminates can be calculated as:

$$E_{90} = E_0 / 30 \quad (7)$$

Princip proračuna sličan je proračunu šperploča. Efektivne vrednosti napona i krutosti dobijaju se pomoću koeficijenta  $k_i$  - Tabela 2.

The method is similar to the design method for plywood. The values for stress and stiffness can be calculated by using the coefficient  $k_i$ , Table 2.

Tabela 2. Efektivne vrednosti napona i krutosti CLT panela [12]  
Table 2. Normal Stress and Effective Stiffness Values [12]

Opterećenje Load	Pravac vlakana Grain direction	Efektivni napon Normal Stress	Efektivna krutost Effective Stiffness
Opterećenje normalno na ravan panela Load perpendicular to a panel			
Savijanje Bending	Paralelno s vlaknima Along the grain	$f_{m,0,ef} = f_{m,0} \cdot k_1$	$E_{m,0,ef} = E_0 \cdot k_1$
	Upravno na vlakna Across the grain	$f_{m,90,ef} = f_{m,0} \cdot k_2 \cdot a_m / a_{m-2}$	$E_{m,90,ef} = E_0 \cdot k_2$

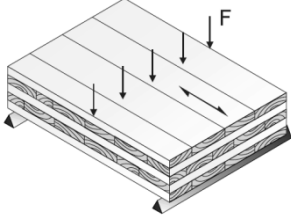
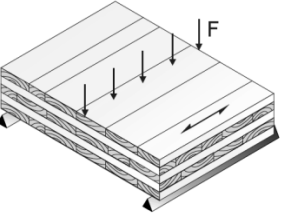
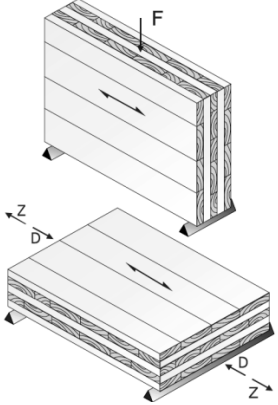
Opterećenje u ravni panela Load in the plane of a panel			
Savijanje Bending	Paralelno s vlaknima Along the grain	$f_{m,0,ef} = f_{m,0} \cdot k_3$	$E_{m,0,ef} = E_0 \cdot k_3$
	Upravno na vlakna Across the grain	$f_{m,90,ef} = f_{m,0} \cdot k_4$	$E_{m,90,ef} = E_0 \cdot k_4$
Zatezanje Tension	Paralelno s vlaknima Along the grain	$f_{t,0,ef} = f_{t,0} \cdot k_3$	$E_{t,0,ef} = E_0 \cdot k_3$
	Upravno na vlakna Across the grain	$f_{t,90,ef} = f_{t,0} \cdot k_4$	$E_{t,90,ef} = E_0 \cdot k_4$
Pritisak Compression	Paralelno s vlaknima Along the grain	$f_{c,0,ef} = f_{c,0} \cdot k_3$	$E_{c,0,ef} = E_0 \cdot k_3$
	Upravno na vlakna Across the grain	$f_{c,90,ef} = f_{c,0} \cdot k_4$	$E_{c,90,ef} = E_0 \cdot k_4$

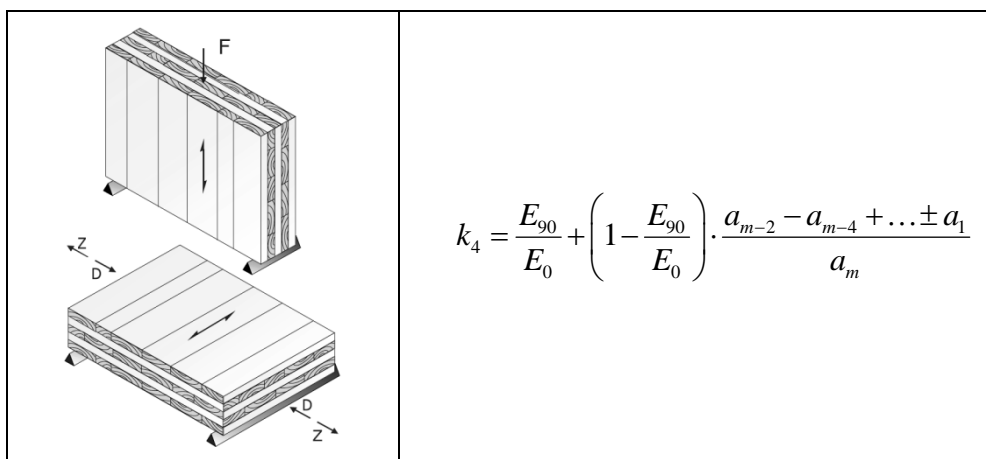
Koeficijenti  $k_i$  definisani su u zavisnosti od opterećenja - Tabela 3.

Depending on the load coefficients  $k_i$  are defined in Table 3.

Tabela 3. Vrednosti koeficijenata  $k_i$  [12][3]

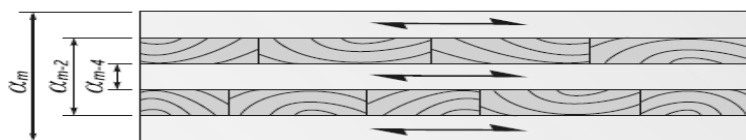
Table 3. Coefficients  $k_i$  Values [12][3]

Opterećenje / Load	$k_i$
	$k_1 = 1 - \left( 1 - \frac{E_{90}}{E_0} \right) \cdot \frac{a_{m-2}^3 - a_{m-4}^3 + \dots \pm a_1^3}{a_m^3}$
	$k_2 = \frac{E_{90}}{E_0} + \left( 1 - \frac{E_{90}}{E_0} \right) \cdot \frac{a_{m-2}^3 - a_{m-4}^3 + \dots \pm a_1^3}{a_m^3}$
	$k_3 = 1 - \left( 1 - \frac{E_{90}}{E_0} \right) \cdot \frac{a_{m-2} - a_{m-4} + \dots \pm a_1}{a_m}$



Način određivanja rastojanja  $a$  CLT panela s pet lamela ( $m = 5$ ) prikazan je na slici 11.

Figure 11. Depicts the method to determine spans  $a$  CLT panels with 5 laminates ( $m = 5$ ).



Slika 11. CLT panel sa 5 lamela [3]  
Figure 11. CLT Panel with 5 laminates [3]

Efektivna krutost na savijanje od opterećenja upravno na ravan panela jeste:

- paralelno s vlaknima

Effective bending stiffness perpendicular to the panel can be calculated as:

- along the grain

$$(EI)_{ef} = E_0 \cdot \frac{b \cdot a_m^3}{12} \cdot k_1 \quad (8)$$

- upravno na vlakna

- across the grain

$$(EI)_{ef} = E_0 \cdot \frac{b \cdot a_m^3}{12} \cdot k_2 \quad (9)$$

gde  $b$  predstavlja širinu panela opterećenog upravno na svoju ravan.

where  $b$  represents the width of the panel perpendicular to its own plane.

Normalni napon savijanja od opterećenja upravno na ravan panela jeste:

Normal bending stress from the load perpendicular to the plane of the panel can be calculated as:

- paralelno s vlaknima

- along the grain

$$\sigma_m = \frac{M}{(EI)_{ef}} \cdot E_0 \cdot \frac{a_m}{2} \quad (10)$$

- upravno na vlakna

- across the grain

$$\sigma_m = \frac{M}{(EI)_{ef}} \cdot E_0 \cdot \frac{a_{m-2}}{2} \quad (11)$$

### 4.3 Kreuzinger-ova analogija

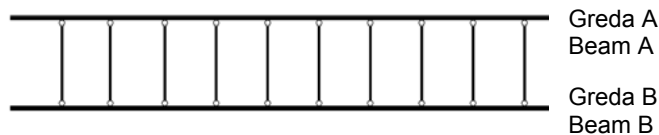
Kreuzinger pri proračunu uzima različite module elastičnosti i module smicanja podužnih i poprečnih lamela. Smicanje podužnih lamela se ne zanemaruje. Modul elastičnosti poprečnih lamela računa se po izrazu (7). Kreuzinger-ova analogija nije ograničena brojem lamela u panelu.

Ovom analogijom, CLT panel deli se u dve virtualne grede A i B - slika 12.

### 4.3 Kreuzinger Analogy

Design according to Kreuzinger considers different modules of elasticity and shear for longitudinal and lateral laminates. Longitudinal shear of laminates is also considered. Modulus of elasticity of lateral laminates can be calculated by using expression (7). Number of laminates is not a limiting factor in Kreuzinger Analogy.

This method divides the CLT panel into two virtual beams A and B as in Figure 12.



Slika 12. Kreuzinger-ova analogija [1]  
Figure 12. Kreuzinger Analogy [1]

Efektivna krutost

Effective stiffness

$$(EI)_{ef} = (EI)_A + (EI)_B = \sum_{i=1}^n E_i \cdot b_i \frac{h_i^3}{12} + \sum_{i=1}^n E_i \cdot A_i \cdot Z_i^2 \quad (12)$$

gde je  $b_i$  širina panela (obično 1 m)

where  $b_i$  is width of a panel (usually 1 m)

$h_i$  visina lamele

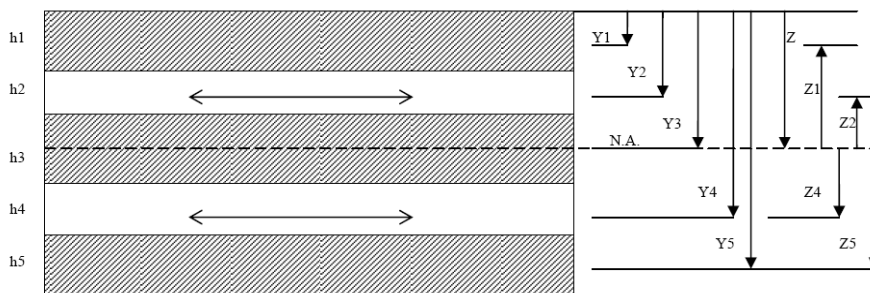
$h_i$  is height of the laminate

$Z_i$  rastojanje od težišta lamele do neutralne ose

$Z_i$  is the distance from the centroid of the laminate to the neutral axis, Figure 13.

- slika 13.

Figure 13.



Slika 13. Rastojanja  $z_i$  kod CLT panela sa 5 lamela [10]

Figure 13. Distance  $z_i$  with CLT panels with 5 laminates [10]

### 4.4 Proračun zidnih CLT panela

Zidni CLT paneli dimenzionišu se kao pritisnuti štapovi složenog preseka, spojeni mehničkim spojnim sredstvima. Postupak proračuna izložen je u Aneksu C Evrokoda 5 (EN 1995-1-1:2004) [11].

Metod proračuna zasnovan je na sledećim pretpostavkama:

- elementi su sistema proste grede, dužine  $l$
- elementi složenog preseka idu kontinualno duž štapa.

Efektivnu vitkost treba uzeti prema izrazu

### 4.4 Design Method for CLT Wall Panels

CLT wall panels are calculated as mechanically joined compressed columns with complex cross section. Design method is presented in annex C of Eurocode 5 (EN 1995-1-1:2004) [11].

The method is based upon following assumptions:

- The elements are simple beams with length  $l$ ,
- The elements with the complex cross section run longitudinally with the member.

Effective slenderness shall be calculated using the following expression:

$$\lambda_{ef} = l \sqrt{\frac{A_{tot}}{I_{ef}}} \quad (13)$$



gde je  $A_{tot}$  ukupna površina poprečnog preseka panela  
 $l$  visina panela (dužina izvijanja)  
 $I_{ef}$  efektivni momenat inercije

where  $A_{tot}$  the total area of the cross section of the panel  
 $l$  the height of the panel (bending length)  
 $I_{ef}$  the effective moment of inertia

Efektivni momenat inercije dobija se pomoću sledećeg izraza

Effective moment of inertia shall be calculated based on the following expression:

$$I_{ef} = \frac{(EI)_{ef}}{E_{mean}} \quad (14)$$

gde je

$(EI)_{ef}$  efektivna krutost  
 $E_{mean}$  srednja vrednost modula elastičnosti vertikalnih lamela

Efektivna vitkost  $\lambda_{ef}$  uvrštava se u izraz 6.21 Evrokoda 5, a proračun nosivosti CLT panela vrši se po poglavlju 6 Evrokoda 5.

where

$(EI)_{ef}$  effective stiffness  
 $E_{mean}$  median value of modulus of elasticity of the vertical laminates

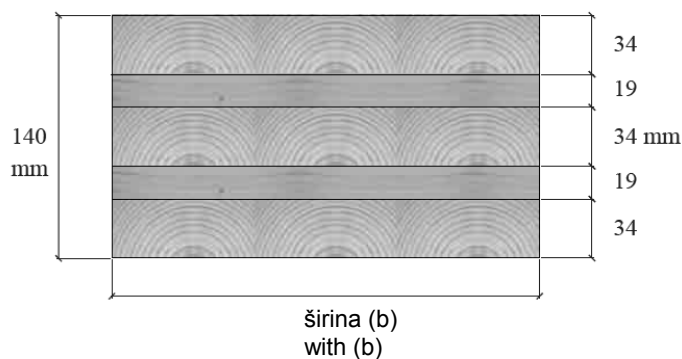
Effective slenderness  $\lambda_{ef}$  is used in expression 6.21 of Eurocode 5 while bearing capacity of a CLT panel shall be calculated following chapter 6 of Eurocode 5.

## 5 PRIMER

Sračunati efektivnu krutost  $(EI)_{ef}$  slobodno oslonjenog podnog CLT panela dužine 4,5 metara, a širine 1 metar. Poprečni presek panela prikazan je na slici 14. Ukupna visina panela je 14 centimetara. Opterećenje deluje upravno na ravan panela paralelno s vlaknima spoljnih lamela [3].

## 5 EXAMPLE

Calculate the effective stiffness  $(EI)_{ef}$  of the simply supported CLT floor panel 4,5m long and 1m wide. Panel's cross section is depicted on Figure 14. The total height of the panel is 14 centimetres. The load is acting perpendicularly to the panel and along the grain of the exterior laminates [3].



Slika 14. Geometrijske karakteristike panela  
 Figure 14. Geometric characteristics of the panel

Fizičko-mehaničke karakteristike podužnih lamela:

Physical and mechanical properties of the longitudinal laminates:

$$E_0 = 11000 \text{ MPa}$$

$$E_{90} \approx \frac{E_0}{30} = \frac{11000}{30} = 367 \approx 370 \text{ MPa}$$

$$G_0 \approx \frac{E_0}{16} = \frac{11000}{16} = 688 \approx 690 \text{ MPa}$$

$$G_R \approx \frac{G_0}{10} = \frac{690}{10} = 69 \text{ MPa}$$

Fizičko-mehaničke karakteristike poprečnih lamela:

Physical and mechanical properties of the lateral laminates:

$$E_0 = 9000 \text{ MPa}$$

$$E_{90} \approx \frac{E_0}{30} = \frac{9000}{30} = 300 \text{ MPa}$$

$$G_0 \approx \frac{E_0}{16} = \frac{9000}{16} = 563 \approx 560 \text{ MPa}$$

$$G_R \approx \frac{G_0}{10} = \frac{560}{10} = 56 \text{ MPa}$$

Odnos raspona i visine lamele CLT panela jeste

Ratio of the span to the height of the panel is:

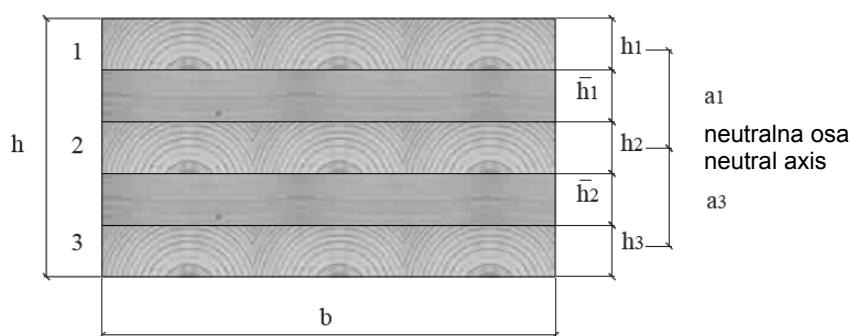
$$\frac{l}{h} = \frac{450}{14} = 32 > 30$$

pa se smicanje podužnih lamela zanemaruje.

Thus the shear of the longitudinal laminates can be neglected.

### 5.1 Gamma metod

### 5.1 Gamma method



Slika 15. Geometrijske karakteristike panela (Gamma metod)  
Figure 15. Geometric characteristics of the panel (Gamma method)

$$h_1 = h_2 = h_3 = 34 \text{ mm} \quad \bar{h}_1 = \bar{h}_2 = 19 \text{ mm} \quad h = 140 \text{ mm}$$

$$E_1 = E_2 = E_3 = 11000 \text{ MPa}$$

$$G_R = 56 \text{ MPa}$$

Efektivna krutost računa se po jednačini (1)

The effective stiffness shall be calculated by using the expression (1):

$$(EI)_{ef} = \sum_{i=1}^3 (E_i I_i + \gamma_i E_i A_i a_i^2)$$

Ako su

If

$$\gamma_1 = \gamma_3 = \gamma \quad i / \text{ and } \quad \gamma_2 = 1$$

dobijamo

then

$$(EI)_{ef} = (E_1 I_1 + \gamma_1 E_1 A_1 a_1^2) + (E_2 I_2) + (E_3 I_3 + \gamma_3 E_3 A_3 a_3^2)$$

gde je

where

$$A_1 = A_3 = A$$

$$E_1 = E_2 = E_3 = E$$

$$I_1 = I_2 = I_3 = I = \frac{bh_1^3}{12}$$

$$a_2 = 0$$

$$a_1 = a_3 = a = \frac{h_1}{2} + \bar{h}_1 + \frac{h_2}{2} = \frac{h_2}{2} + \bar{h}_2 + \frac{h_3}{2}$$

pa se za efektivnu krutost dobija

Then the effective stiffness is:

$$(EI)_{ef} = EI \left[ 3 + \frac{2\gamma Aa^2}{I} \right]$$

Ako je

If

$$\gamma = \frac{1}{\left[ 1 + \frac{\pi^2 EA}{l^2} \cdot \frac{\bar{h}}{G_R \cdot b} \right]} = \frac{1}{1 + \frac{\pi^2 11000 \cdot (1000 \cdot 34)}{4500^2} \cdot \frac{19}{56 \cdot 1000}} = 0,9418$$

$$A = bh = 1000 \cdot 34 = 34000 \text{ mm}^2$$

$$a = a_1 = a_3 = \frac{h_1}{2} + \bar{h}_1 + \frac{h_2}{2} = \frac{h_2}{2} + \bar{h}_2 + \frac{h_3}{2} = \frac{34}{2} + 19 + \frac{34}{2} = 53 \text{ mm}$$

$$I = \frac{bh_1^3}{12} = \frac{1000 \cdot 34^3}{12} = 3,275 \times 10^6 \text{ mm}^4$$

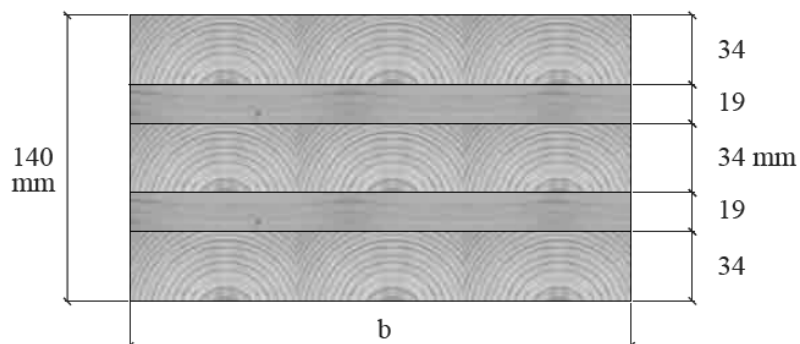
dobijamo

Then

$$(EI)_{ef} = 11000 \cdot 3,275 \times 10^6 \left[ 3 + \frac{2 \cdot 0,9418 \cdot 34000 \cdot 53^2}{3,275 \times 10^6} \right] = 2087 \times 10^9 \text{ Nmm}^2$$

## 5.2 K - metod (Blass&Fellmoser)

## 5.2 K - method (Blass&Fellmoser)



Slika 16. Geometrijske karakteristike panela (K-metod)  
Figure 16. Geometric characteristics of the panel (K- method)

$$E_0 = 11000 \text{ MPa}$$

$$E_{90} = 300 \text{ MPa}$$

Iz Tabele 3 dobijamo

From Table 3 we get:

$$a_m = a_5 = 140 \text{ mm}$$

$$a_{m-2} = a_3 = 19 + 34 + 19 = 72 \text{ mm}$$

$$a_{m-4} = a_1 = 34 \text{ mm}$$

$$k_1 = 1 - \left(1 - \frac{E_{90}}{E_0}\right) \cdot \frac{a_3^3 - a_1^3}{a_5^3} = 1 - \left(1 - \frac{300}{11000}\right) \cdot \left(\frac{72^3 - 34^3}{140^3}\right) = 0,8816$$

a iz Tabele 2

And from Table 2

$$E_{m,0,ef} = E_0 \cdot k_1 = 11000 \cdot 0,8816 = 9698 \text{ MPa}$$

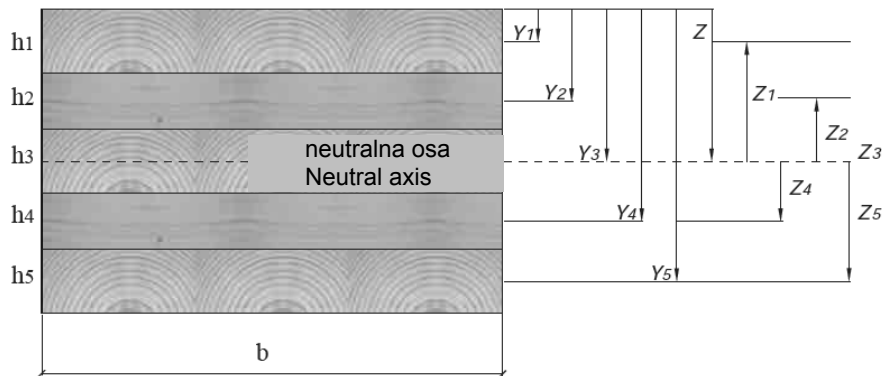
pa je efektivna krutost CLT panela širine  $b = 1000 \text{ mm}$

Finally the effective stiffness of the CLT panel with width  $b = 1000 \text{ mm}$

$$(EI)_{ef} = 9698 \cdot \frac{1000 \cdot 140^3}{12} = 2218 \times 10^9 \text{ Nmm}^2$$

### 5.3 Kreuzinger-ova analogija

### 5.3 Kreuzinger Analogy



Slika 17. Geometrijske karakteristike panela (Kreuzinger-ova analogija)  
Figure 17. Geometric characteristics of the panel (Kreuzinger Analogy)

$h_1 = 34 \text{ mm}$	$E_0 = 11000 \text{ MPa}$	$E_{90} = 370 \text{ MPa} (\approx 11000 / 30)$
$h_2 = 19 \text{ mm}$	$E_0 = 9000 \text{ MPa}$	$E_{90} = 300 \text{ MPa} (\approx 9000 / 30)$
$h_3 = 34 \text{ mm}$	$E_0 = 11000 \text{ MPa}$	$E_{90} = 370 \text{ MPa} (\approx 11000 / 30)$
$h_4 = 19 \text{ mm}$	$E_0 = 9000 \text{ MPa}$	$E_{90} = 300 \text{ MPa} (\approx 9000 / 30)$
$h_5 = 34 \text{ mm}$	$E_0 = 11000 \text{ MPa}$	$E_{90} = 370 \text{ MPa} (\approx 11000 / 30)$

$$h = h_1 + h_2 + h_3 + h_4 + h_5 = 140 \text{ mm}$$

$$b = 1000 \text{ mm}$$

Efektivna krutost dobija se iz jednačine (12)

The effective stiffness shall be calculated by using the expression (12)

$$(EI)_{ef} = (EI)_A + (EI)_B = \sum_{i=1}^n E_i \cdot b_i \frac{h_i^3}{12} + \sum_{i=1}^n E_i \cdot A_i \cdot Z_i^2$$

Položaj neutralne ose  $Z$

The location of the neutral axis  $Z$  is:

$$Z = \frac{\sum_{i=1}^n (E_i A_i) \cdot Y_i}{\sum_{i=1}^n (E_i A_i)}$$

$$E_1 A_1 = E_1 \cdot b \cdot h_1 = 11000 \cdot 1000 \cdot 34 = 3,74 \times 10^8 \text{ N}$$

$$E_2 A_2 = E_2 \cdot b \cdot h_2 = 300 \cdot 1000 \cdot 19 = 5,7 \times 10^6 \text{ N}$$

$$E_3 A_3 = E_3 \cdot b \cdot h_3 = 11000 \cdot 1000 \cdot 34 = 3,74 \times 10^8 \text{ N}$$

$$E_4 A_4 = E_4 \cdot b \cdot h_4 = 300 \cdot 1000 \cdot 19 = 5,7 \times 10^6 \text{ N}$$

$$E_5 A_5 = E_5 \cdot b \cdot h_5 = 11000 \cdot 1000 \cdot 34 = 3,74 \times 10^8 \text{ N}$$

$$\sum_{i=1}^5 (E_i A_i) = 11,334 \times 10^8 \text{ N}$$

$$Y_1 = \frac{h_1}{2} = \frac{34}{2} = 17 \text{ mm}$$

$$Y_2 = h_1 + \frac{h_2}{2} = 34 + \frac{19}{2} = 43,5 \text{ mm}$$

$$Y_3 = h_1 + h_2 + \frac{h_3}{2} = 34 + 19 + \frac{34}{2} = 70 \text{ mm}$$

$$Y_4 = h_1 + h_2 + h_3 + \frac{h_4}{2} = 34 + 19 + 34 + \frac{19}{2} = 96,5 \text{ mm}$$

$$Y_5 = h_1 + h_2 + h_3 + h_4 + \frac{h_5}{2} = 34 + 19 + 34 + 19 + \frac{34}{2} = 123 \text{ mm}$$

$$E_1 A_1 Y_1 = 3,74 \times 10^8 \cdot 17 = 6,358 \times 10^9 \text{ Nmm}$$

$$E_2 A_2 Y_2 = 5,7 \times 10^6 \cdot 43,5 = 2,48 \times 10^8 \text{ Nmm}$$

$$E_3 A_3 Y_3 = 3,74 \times 10^8 \cdot 70 = 2,618 \times 10^{10} \text{ Nmm}$$

$$E_4 A_4 Y_4 = 5,7 \times 10^6 \cdot 96,5 = 5,501 \times 10^8 \text{ Nmm}$$

$$E_5 A_5 Y_5 = 3,74 \times 10^8 \cdot 123 = 4,6 \times 10^{10} \text{ Nmm}$$

$$\sum_{i=1}^5 (E_i A_i) \cdot Y_i = 7,934 \times 10^{10} \text{ Nmm}$$

pa je

then

$$Z = \frac{\sum_{i=1}^5 (E_i A_i) \cdot Y_i}{\sum_{i=1}^5 (E_i A_i)} = \frac{7,934 \times 10^{10}}{11,334 \times 10^8} = 70 \text{ mm}$$

$$Z_1 = Z - \frac{h_1}{2} = 70 - \frac{34}{2} = 53 \text{ mm}$$

$$Z_2 = Z - h_1 - \frac{h_2}{2} = 70 - 34 - \frac{19}{2} = 26,5 \text{ mm}$$

$$Z_3 = Z - h_1 - h_2 - \frac{h_3}{2} = 70 - 34 - 19 - \frac{34}{2} = 0 \text{ mm}$$

$$Z_4 = -Z_2 = -26,5 \text{ mm}$$

$$Z_5 = -Z_1 = -53 \text{ mm}$$

Proračun krutosti virtuelne grede A

Stiffness calculation for the virtual beam A

$$(EI)_A = \sum_{i=1}^n E_i \cdot b_i \frac{h_i^3}{12}$$

$$E_1 b \frac{h_1^3}{12} = 11000 \cdot 1000 \frac{34^3}{12} = 3,603 \times 10^{10} \text{ Nmm}^2$$

$$E_2 b \frac{h_2^3}{12} = 300 \cdot 1000 \frac{19^3}{12} = 1,715 \times 10^8 \text{ Nmm}^2$$

$$E_3 b \frac{h_3^3}{12} = 11000 \cdot 1000 \frac{34^3}{12} = 3,603 \times 10^{10} \text{ Nmm}^2$$

$$E_4 b \frac{h_4^3}{12} = 300 \cdot 1000 \frac{19^3}{12} = 1,715 \times 10^8 \text{ Nmm}^2$$

$$E_5 b \frac{h_5^3}{12} = 11000 \cdot 1000 \frac{34^3}{12} = 3,603 \times 10^{10} \text{ Nmm}^2$$

$$(EI)_A = 1,084 \times 10^{11} \text{ Nmm}^2$$

Proračun krutosti virtualne grede B

Stiffness calculation for the virtual beam B

$$(EI)_B = \sum_{i=1}^n E_i \cdot A_i \cdot Z_i^2$$

$$E_1 \cdot A_1 \cdot Z_1^2 = 11000 \cdot 1000 \cdot 34 \cdot 53^2 = 1,051 \times 10^{12} \text{ Nmm}^2$$

$$E_2 \cdot A_2 \cdot Z_2^2 = 300 \cdot 1000 \cdot 19 \cdot 26,5^2 = 4,003 \times 10^9 \text{ Nmm}^2$$

$$E_3 \cdot A_3 \cdot Z_3^2 = 11000 \cdot 1000 \cdot 34 \cdot 0 = 0 \text{ Nmm}^2$$

$$E_4 \cdot A_4 \cdot Z_4^2 = 300 \cdot 1000 \cdot 19 \cdot (-26,5)^2 = 4,003 \times 10^9 \text{ Nmm}^2$$

$$E_5 \cdot A_5 \cdot Z_5^2 = 11000 \cdot 1000 \cdot 34 \cdot (-53)^2 = 1,051 \times 10^{12} \text{ Nmm}^2$$

$$(EI)_B = 2,110 \times 10^{12} \text{ Nmm}^2$$

Efektivna krutost je

Effective stiffness is:

$$(EI)_{ef} = (EI)_A + (EI)_B = 1,084 \times 10^{11} + 2,110 \times 10^{12} = 2218 \times 10^9 \text{ Nmm}^2$$

## 6 ZAKLJUČAK

Primenom CLT u konstrukcijama postiže se zdrav i prirodan ambijent. CLT konstrukcije su čvršće i imaju bolje statičke osobine od monolitnog drveta, nemaju sklonost ka uvijanju, a pojava napuklina svedena je na minimum. Karakteriše ih velika požarna otpornost, kao i visoka otpornost na potres. Izgradnja CLT konstrukcije brža je oko 30% nego kada se koristi odgovarajuća betonska konstrukcija, jer se drveni elementi isporučuju kao prefabrikovani, koji se zatim brzo uklapaju na gradilištu. Za CLT panele koristi se mekano drvo koje raste brzo i kog ima u izobilju, pa je i cena CLT konstrukcija niža od 5 do 10% od odgovarajućih betonskih ili čeličnih. Drvo je i mnogo bolji izolator - pet puta bolji od betona i čak 350 puta bolji od čelika.

U radu su prikazane analitičke metode proračuna koje se najčešće koriste prilikom dimenzionisanja CLT konstrukcija. Gamma metod daje jednostavan postupak proračuna, ali vrednost efektivne krutosti panela u prikazanom primeru manja je za oko 6% u poređenju s druge dve metode. Efektivne krutosti panela sračunate K-metodom i Kreuzinger-ovom analogijom imaju istu vrednost, ali je postupak proračuna K-metodom znatno kraći i jednostavniji.

Usvajanjem predloženog međunarodnog standarda EN 16351 Timber structures - Cross laminated timber - Requirements u svim državama Evrope postigao bi se jedinstveni analitički pristup prilikom dimenzionisanja. U

## 6 CONCLUSION

Use of CLT creates healthy and natural ambiance. Compared against traditional wood, CLT construction are stronger, have better mechanical properties, no bending tendency, and minimal fractures appearance. CLT constructions are characterized by high fire resistance, and resilience to earthquakes. Since the elements are delivered prefabricated and can be assembled quickly on the construction site, CLT constructions can be completed roughly 30% faster than comparable concrete projects. Fast growing easily accessible softwood keeps the price of CLT 5 to 10% lower than the competing concrete or steel construction. Timber is 5 times better insulator than concrete and up to 350 times better than steel.

This work presents the most frequently used analytical design methods. Even though Gamma method is a simple design procedure for CLT constructions, result in the shown example for effective stiffness of the panel is about 6% lower compared to other two methods. When calculated using both K-method, and Kreuzinger analogy, panels' effective stiffness values yield same results; however, K-method design procedure is considerably shorter and simpler.

By adopting the international standard EN 16351 Timber Structures – Cross laminated timber – Requirements across all European countries the unified design approach could be achieved. In Serbia the

Srbiji, prevod ovog standarda obuhvaćen je planom rada Instituta za standardizaciju Srbije, a njegovo prihvatanje očekuje se krajem 2015. godine.

## 7 LITERATURA REFERENCES

- [1] Sylvain Gagnon, M. Mohammad: *Structural Performance and Design of CLT Building*, CLT Symposium and Workshop, Moncton, NB, October 12, 2011.
- [2] Ian Smith, Andrea Frangi: *Use of Timber in Tall Multi-Storey Buildings*, International Association for Bridge and Structural Engineering (IABSE), Zurich, Switzerland, 2014.
- [3] *Handbook cross-laminated timber*, FPInnovations and Binational Softwood Lumber Council, 2011.
- [4] Gerhard Shickhofer: *CLT - European Experience*, Presentation in the frame of the CLT Forum 2013 in Tokyo.
- [5] European technical approval ETA-06/0138 Validity from 01.07.2011 to 30.06.2016, extends ETA-06/0138 with validity from 27.07.2006 to 26.07.2011.
- [6] Ben Toosi: *Cross Laminated Timber, The Market Opportunities in North America*, FPInnovations, Canada, May 12<sup>th</sup> 2011.

## REZIME

### UNAKRSNO LAMELIRANI DRVENI ELEMENTI U SAVREMENIM DRVENIM KONSTRUKCIJAMA ZGRADA - primena i proračun

Ljiljana KOZARIĆ  
Aleksandar PROKIĆ  
Miroslav BEŠEVIĆ

U radu se analizira unakrsno lamelirano drvo (CLT), moderan građevinski materijal koji se proizvodi od osušenih drvenih elemenata - lamela. Lamele u CLT panelima su podjednake širine i postavljene su tako da vlakna drveta u lamelama po slojevima budu međusobno pod pravim uglom.

Prikazane su osnovne fizičko-mehaničke karakteristike CLT panela, kao i analitički modeli koji se najčešće koriste prilikom projektovanja CLT podnih i zidnih elemenata u konstrukcijama. Navedene su prednosti i nedostaci ovog novog konstruktivnog sistema, u skladu sa savremenim svetskim zahtevima pri projektovanju modernih, ekološki prihvatljivih konstrukcija.

**Cljučne reči:** unakrsno lamelirano drvo, savremene drvene konstrukcije

proposal of the standard has been made the part of the agenda of the Institute for Standardization and its adoption could be finalized by the end of 2015.

- [7] <http://www.drvotehnika.info/clanci/drvo-kao-gradjevinski-materijal-zgrada-od-drveta>, 15.03.2015
- [8] <http://www.woodsolutions.com.au/Inspiration-Case-Study/forte-living>, 17.03.2015.
- [9] <http://www.drvotehnika.info/clanci/drvo-kao-gradjevinski-materijal-zgrada-od-drveta>, 15.03.2015.
- [10] Sylvain Gagnon: *Structural Design of CLT in Canada*, Québec City, May, 2010.
- [11] Evrokod 5 - Proračun drvenih konstrukcija - Deo 1-1: Opšta pravila i pravila za zgrade, EN 1995-1-1:2004, Beograd, 2009.
- [12] Hans Joachim Blass, Peter Fellmoser: *Design of solid wood panels with cross layers*, Proceedings, 8. World Conference on Timber Engineering, Lahti, Finland, 2004.

## SUMMARY

### CROSS LAMINATED TIMBER ELEMENTS IN CONTEMPORARY TIMBER STRUCTURES OF BUILDINGS - application and design

Ljiljana KOZARIĆ  
Aleksandar PROKIĆ  
Miroslav BEŠEVIĆ

This work analyses cross laminated timber (CLT), contemporary building material produced of dried wooden elements - laminates. Laminates in CLT panels are equally wide and timber fibers are rectangularly plated within layers.

Paper shows basic physical - mechanical characteristics of CLT panels and analytic models that are most commonly used in designing of CLT floor and wall construction elements. Advantages and disadvantages of this new construction system are stated according to contemporary requirements in designing environmentally and ecologically acceptable constructions.

**Key words:** cross laminated timber, contemporary timber structures

## UPUTSTVO AUTORIMA\*

### Prihvatanje radova i vrste priloga

U časopisu Materijali i konstrukcije štampaće se neobjavljeni radovi ili članci i konferencijska saopštenja sa određenim dopunama ili bez dopuna, prema odluci Redakcionog odbora, a samo izuzetno uz dozvolu prethodnog izdavača prihvatice se i objavljeni rad. Vrste priloga autora i saradnika koji će se štampati su: originalni naučni radovi, prethodna saopštenja, pregledni radovi, stručni radovi, konferencijska saopštenja (radovi sa naučno-stručnih skupova), kao i ostali prilozi kao što su: prikazi objekata i iskustava - primeri, diskusije povodom objavljenih radova i pisma uredništvu, prikazi knjiga i zbornika radova, kao i obaveštenja o naučno-stručnim skupovima.

*Originalni naučni rad* je primarni izvor naučnih informacija i novih ideja i saznanja kao rezultat izvornih istraživanja uz primenu adekvatnih naučnih metoda. Dobijeni rezultati se izlažu kratko, jasno i objektivno, ali tako da poznavalac problema može proceniti rezultate eksperimentalnih ili teorijsko numeričkih analiza i tok razmišljanja, tako da se istraživanje može ponoviti i pri tome dobiti iste ili rezultate u okvirima dopuštenih odstupanja, kako se to u radu navodi.

*Prethodno saopštenje* sadrži prva kratka obaveštenja o rezultatima istraživanja ali bez detaljnih objašnjenja, tj. kraće je od originalnog naučnog rada. U ovu kategoriju spadaju i diskusije o objavljenim radovima ako one sadrže naučne doprinose.

*Pregledni rad* je naučni rad koji prikazuje stanje nauke u određenoj oblasti kao plod analize, kritike i komentara i zaključaka publikovanih radova o kojima se daju svi neophodni podaci pregledno i kritički uključujući i sopstvene radove. Navode se sve bibliografske jedinice korišćene u obradi tematike, kao i radovi koji mogu doprineti rezultatima daljih istraživanja. Ukoliko su bibliografski podaci metodski sistematizovani, ali ne i analizirani i raspravljani, takvi pregledni radovi se klasifikuju kao stručni pregledni radovi.

*Stručni rad* predstavlja koristan prilog u kome se iznose poznate spoznaje koje doprinose širenju znanja i prilagođavanja rezultata izvornih istraživanja potrebama teorije i prakse. On sadrži i rezultate razvojnih istraživanja.

*Konferencijsko saopštenje* ili rad saopšten na naučno-stručnom skupu koji mogu biti objavljeni u izvornom obliku ili ih autor, u dogovoru sa redakcijom, bitno preradi i proširi. To mogu biti naučni radovi, naročito ako su saopštenja po pozivu Organizatora skupa ili sadrže originalne rezultate prvi put objavljene, pa ih je korisno uz određene dopune učiniti dostupnim široj stručnoj javnosti. Štampaće se i stručni radovi za koje Redakcioni odbor oceni da su od šireg interesa.

*Ostali prilozi* su prikazi objekata, tj. njihove konstrukcije i iskustava-primeri u građenju i primeni različitih materijala, diskusije povodom objavljenih radova i pisma uredništvu, prikazi knjiga i zbornika radova, kao i obaveštenja o naučno-stručnim skupovima.

Autori uz rukopis predlažu kategorizaciju članka. Svi radovi pre objavljivanja se recenziraju, a o prihvatanju za publikovanje o njihovoj kategoriji konačnu odluku donosi Redakcioni odbor.

Da bi se ubrzao postupak prihvatanja radova za publikovanje, potrebno je da autori uvažavaju Uputstva za pripremu radova koja su navedena u daljem tekstu.

### Uputstva za pripremu rukopisa

Rukopis otkucati jednostrano na listovima A-4 sa marginama od 31 mm (gore i dole) a 20 mm (levo i desno), u Wordu fontom Arial sa 12 pt. Potrebno je uz jednu kopiju svih delova rada i priloga, dostaviti i elektronsku verziju na navedene E-mail adrese, ili na CD-u. Autor je obavezan da čuva jednu kopiju rukopisa kod sebe zbog eventualnog oštećenja ili gubitka rukopisa.

**Od broja 1/2010. prema odluci Upravnog odbora Društva i Redakcionog odbora, radovi sa pozitivnim recenzijama i prihvaćeni za štampu, publikovaće se na srpskom i engleskom jeziku.**

Svaka stranica treba da bude numerisana, a optimalni obim članka na jednom jeziku je oko 16 stranica (30000 slovnih mesta) uključujući slike, fotografije, tabele i popis literature. Za radove većeg obima potrebna je saglasnost Redakcionog odbora.

Naslov rada treba sa što manje reči (poželjno osam, a najviše do jedanaeset) da opiše sadržaj članka. U naslovu ne koristiti skraćenice ni formule. U radu se iza naslova daju ime i prezime autora, a titule i zvanja, kao i ime institucije u podnožnoj napomeni. Autor za kontakt daje telefone, faks i adresu elektronske pošte, a za ostale autore poštansku adresu.

Uz sažetak (rezime) od oko 150 do 200 reči, na srpskom i engleskom jeziku daju se ključne reči (do deset). To je jezgrovit prikaz celog članka i čitaocima omogućuje uvid u njegove bitne elemente.

Rukopis se deli na poglavlja i potpoglavlja uz numeraciju, po hijerarhiji, arapskim brojevima. Svaki rad ima uvod, sadržinu rada sa rezultatima, analizom i zaključcima. Na kraju rada se daje popis literature.

Kod svih dimenzionalnih veličina obavezna je primena međunarodnih SI mernih jedinica.

Formule i jednačine treba pisati pažljivo vodeći računa o indeksima i eksponentima. Autori uz izraze u tekstu definišu simbole redom kako se pojavljuju, ali se može dati i posebna lista simbola u prilogu.

Prilozi (tabele, grafikoni, sheme i fotografije) rade se u crno-belom tehničkom, u formatu koji obezbeđuje da pri smanjenju na razmere za štampu, po širini jedan do dva stupca (8cm ili 16.5cm), a po visini najviše 24.5cm, ostanu jasni i čitljivi, tj. da veličine slova i brojeva budu najmanje 1.5mm. Originalni crteži treba da budu kvalitetni i u potpunosti pripremljeni za presnimavanje. Mogu biti i dobre, oštre i kontrastne fotokopije. Koristiti fotografije, u crno-belom tehničkom, na kvalitetnoj hartiji sa oštrim konturama, koje omogućuju jasnu reprodukciju. Skraćenice u prilogima koristiti samo izuzetno uz obaveznu legendu. Prilozi se posebno označavaju arapskim brojevima, prema redosledu navođenja u tekstu. Objašnjenje tabela daje se u tekstu.

Potrebno je dati spisak svih skraćenica korišćenih u tekstu.

U popisu literature na kraju rada daju se samo oni radovi koji se pominju u tekstu. Citirane radove treba prikazati po azbučnom redu prezimena prvog autora. Literaturu u tekstu označiti arapskim brojevima u uglastim zagradama, kako se navodi i u Popisu citirane literature, napr [1]. Svaki citat u tekstu mora se naći u Popisu citirane literature i obrnuto svaki podatak iz Popisa se mora navesti u tekstu.

U Popisu literature se navode prezime i inicijali imena autora, zatim potpuni naslov citiranog članka, iza toga sledi ime časopisa, godina izdavanja i početna i završna stranica (od - do). Za knjige iza naslova upisuje se ime urednika (ako ih ima), broj izdanja, prva i poslednja stranicapoglavlja ili dela knjige, ime izdavača i mesto objavljivanja, ako je navedeno više gradova navodi se samo prvi po redu. Kada autor citirane podatke ne uzima iz izvornog rada, već ih je pronašao u drugom delu, uz citat se dodaje «citirano prema...». Neobjavljeni članci mogu se pominjati u tekstu kao «usmeno saopštenje».

Autori su odgovorni za izneseni sadržaj i moraju sami obezbediti eventualno potrebne saglasnosti za objavljivanje nekih podataka i priloga koji se koriste u radu.

Ukoliko rad bude prihvaćen za štampu, autori su dužni da, po uputstvu Redakcije, unesu sve ispravke i dopune u tekstu i prilogima.

Za detaljnija tehnička uputstva za pripremu rukopisa autori se mogu obratiti Redakcionom odboru časopisa.

Rukopisi i prilozi objavljenih radova se ne vraćaju. Sva eventualna objašnjenja i uputstva mogu se dobiti od Redakcionog odbora.

Radovi se mogu slati i na e-mail: folic@uns.ac.rs ili miram@uns.ac.rs i dimk@ptt.rs

Već sajt Društva i časopisa: www.dimk.rs

\* Uputstvo autorima je modifikovano i treba ga u pripremi radova slediti.



Izdavanje časopisa "Građevinski materijali i konstrukcije" finansijski su pomogli:



**INŽENJERSKA KOMORA SRBIJE**



**REPUBLIKA SRBIJA  
MINISTARSTVO PROSVETE, NAUKE I  
TEHNOLOŠKOG RAZVOJA**



**UNIVERZITET U BEOGRADU  
GRAĐEVINSKI FAKULTET**



**DEPARTMAN ZA GRAĐEVINARSTVO I  
GEODEZIJU  
FAKULTET TEHNIČKIH NAUKA NOVI SAD**



**INSTITUT IMS AD, BEOGRAD**



**UNIVERZITET CRNE GORE  
GRAĐEVINSKI FAKULTET - PODGORICA**